For Reference

NOT TO BE TAKEN FROM THIS ROOM

Ex libris
Universitatis
Albertaensis

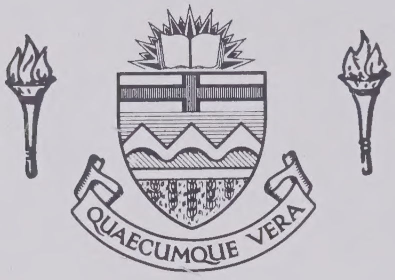

THE UNIVERSITY OF ALBERTA

RELEASE FORM

NAME OF AUTHOR: LIVIU VANCEA

TITLE OF THESIS: CARBON-13 NMR STUDIES OF STEREOCHEMICALLY NONRIGID SIX-COORDINATE METAL CARBONYL DERIVATIVES

DEGREE FOR WHICH THESIS WAS PRESENTED: Ph. D.

YEAR THIS DEGREE GRANTED: 1976

Permission is hereby granted to THE UNIVERSITY OF ALBERTA LIBRARY to reproduce single copies of this thesis and to lend or sell such copies for private, scholarly or scientific research purposes only.

The author reserves other publication rights, and neither the thesis nor extensive extracts from it may be printed or otherwise reproduced without the author's written permission.

THE UNIVERSITY OF ALBERTA

CARBON-13 NMR STUDIES OF STEREOCHEMICALLY NONRIGID SIX-COORDINATE METAL CARBONYL DERIVATIVES

by

LIVIU VANCEA ©

A THESIS

SUBMITTED TO THE FACULTY OF GRADUATE STUDIES AND RESEARCH

IN PARTIAL FULFILMENT OF THE REQUIREMENTS FOR THE DEGREE

OF

DOCTOR OF PHILOSOPHY

DEPARTMENT OF CHEMISTRY

EDMONTON, ALBERTA

SPRING, 1976

Digitized by the Internet Archive
in 2021 with funding from
University of Alberta Libraries

https://archive.org/details/Vancea1976

THE UNIVERSITY OF ALBERTA

FACULTY OF GRADUATE STUDIES AND RESEARCH

The undersigned certify that they have read, and recommend to the Faculty of Graduate Studies and Research, for acceptance, a thesis entitled

"CARBON-13 NMR STUDIES OF STEREOCHEMICALLY NONRIGID
SIX-COORDINATE METAL CARBONYL DERIVATIVES"

submitted by LIVIU VANCEA in partial fulfilment of the requirements for the degree of Doctor of Philosophy in Chemistry.

ABSTRACT

Carbon-13 nmr spectra of an extensive series of $M(CO)_4(ER_3)_2$ and $M(CO)_4(SiMe_{3-n}Cl_n)_2$ derivatives (M = Fe, Ru, Os; E = Si, Ge, Sn, Pb; R = organic group; n = 1-3) have been recorded. These compounds may exist in solution as cis, trans, or as a mixture of cis and trans isomers. ^{13}C nmr spectra have been used to distinguish among these possibilities.

Spin-spin coupling or selective enrichment with ^{13}CO in cis derivatives led to the assignment of the ^{13}CO resonance at higher field as the equatorial carbonyl group. Most cis isomers conformed to this generalization although exceptions have been found for some iron complexes.

Variable temperature ^{13}C nmr has demonstrated the stereochemically nonrigid behavior of a number of cis derivatives, which show axial-equatorial carbonyl averaging *via* the trans isomer. The barrier for this process is lowest for iron derivatives.

Preservation of ligand atom-ligand atom and ligand atom-metal atom spin-spin coupling in the high temperature limiting spectrum of a number of iron derivatives established the intramolecular nature of the carbonyl rearrangement process.

The chelates $M(CO)_4SiMe_2CH_2CH_2SiMe_2$ (M = Fe, Ru, and Os) were prepared from $HSiMe_2CH_2CH_2SiMe_2H$ and the

corresponding binary carbonyls. These compounds showed no axial-equatorial carbonyl averaging.

^{13}C nmr of *cis*-$M(CO)_4X_2$ and $M'(CO)_5X$ derivatives (M = Fe, Ru, Os; M' = Mn, Re; X = H and I) have proven the stereochemically nonrigid behavior of *cis*-$Fe(CO)_4H_2$ and the rigid behavior of the rest.

A possible explanation for the dynamic behavior of these six-coordinate complexes is presented.

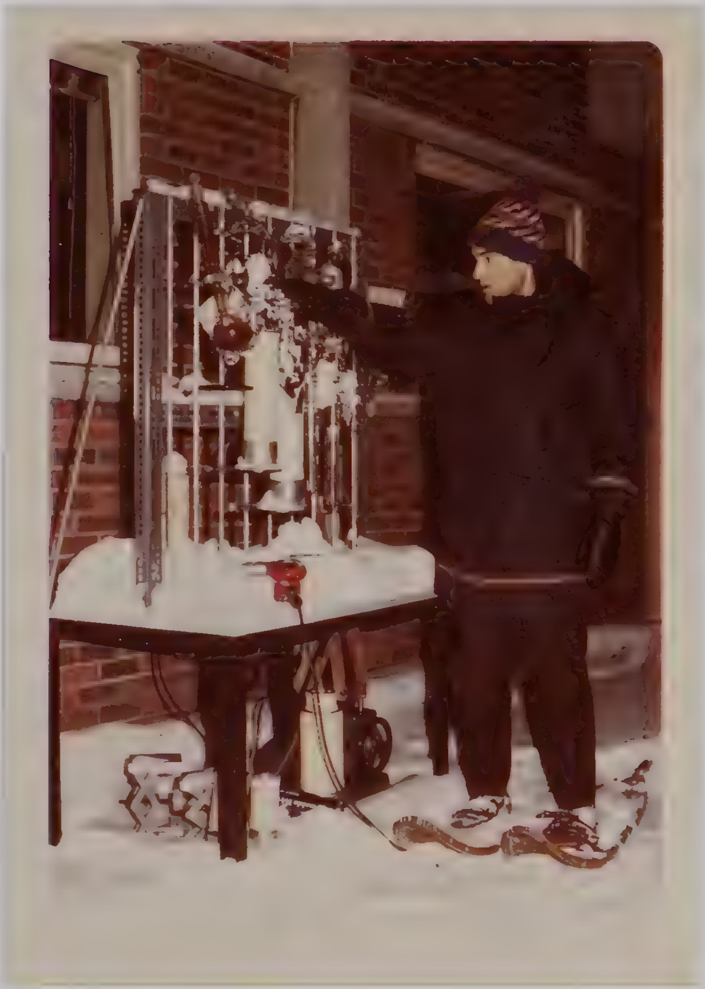

Polar Night Synthesis, cf. p. 147.

ACKNOWLEDGMENTS

I would like to express my sincere gratitude to Professor W. A. G. Graham for his guidance, patience, and enthusiasm throughout the course of this research.

I am also thankful to Dr. R. K. Pomeroy for preparing some of the compounds listed in Chapter II, and for helpful discussions, and to Dr. A. C. Sarapu for introducing me to computers.

It is a great pleasure to acknowledge Dr. T. T. Nakashima, the head of the NMR laboratory, for providing excellent facilities for this work and for many helpful discussions, and Professor D. L. Rabenstein for assistance with line-shape analyses.

My sincere thanks are extended to Professor I. Haiduc, of Babeş-Bolyai University, Cluj-Napoca, Romania, for his interest throughout my carrier, and to Mrs. Angela Sălăgeanu-Nana, my English teacher.

At last, but not least, I am grateful to my parents for their understanding and constant encouragement.

TABLE OF CONTENTS

CHAPTER PAGE

I. INTRODUCTION 1

1. Bonding and Stability of Transition Metal Carbonyl Derivatives 3

2. Structure of Iron, Ruthenium, and Osmium Carbonyl Derivatives 5

3. Stereochemical Nonrigidity 11

3.1. Dynamic Nuclear Magnetic Resonance Spectroscopy 12

3.2. Stereochemical Nonrigidity and the Iron, Ruthenium, and Osmium Carbonyl Derivatives 14

II. CARBON-13 NMR STUDIES OF SIX-COORDINATE IRON, RUTHENIUM, AND OSMIUM CARBONYL DERIVATIVES WITH GROUP IV ELEMENTS. CARBON-13 CHEMICAL SHIFTS 20

1. Introduction 20

2. Results and Discussion 21

2.1. Assignment of Axial and Equatorial Resonances 25

2.2. Carbon-13 Chemical Shifts 34

2.3. "Interpretation" of ^{13}C NMR Chemical Shifts of Carbon Atoms Directly Bound to Transition Metals 42

2.3.1. The State of the Art 42
2.3.2. "Interpretation" of ^{13}C NMR Chemical Shifts in $M(CO)_4(ER_3)_2$ Derivatives 46
3. Experimental Section 48
3.1. NMR Instrumentation and Technique . . . 48
3.2. Sources of Compounds 50
3.3. Enrichment with ^{13}CO 51
III. CARBON-13 NMR STUDIES OF SIX-COORDINATE IRON, RUTHENIUM, AND OSMIUM CARBONYL DERIVATIVES WITH GROUP IV ELEMENTS. CARBON-13 COUPLING CONSTANTS 55
1. Introduction 55
2. Results and Discussion 56
2.1. The Theory of ^{13}C Spin-Spin Couplings . 64
IV. DYNAMIC NUCLEAR MAGNETIC RESONANCE STUDIES OF SIX-COORDINATE IRON, RUTHENIUM, AND OSMIUM CARBONYL DERIVATIVES WITH GROUP IV ELEMENTS . . 66
1. Introduction 66
2. Results and Discussion 67
2.1. Spectroscopic Studies of $Fe(CO)_4(ER_3)_2$ in Solution 67
2.2. The Mechanism of Rearrangement of *cis*-$M(CO)_4(ER_3)_2$ Complexes 78

2.3. Trends in Activation Energies for the Rearrangement of $M(CO)_4(ER_3)_2$ Derivatives 84
3. Experimental Section 91

V. THE STRUCTURE OF $M(CO)_4(ER_3)_2$ DERIVATIVES . . . 97
1. Introduction 97
2. Discussion of the Structure of *cis*-$M(CO)_4$-$(ER_3)_2$ Derivatives 98
3. Discussion of the structure of *trans*-$M(CO)_4$-$(ER_3)_2$ Derivatives 109

VI. METAL CARBONYL DERIVATIVES OF 1,2-BIS(DIMETHYLSILYL)ETHANE 117
1. Introduction 117
2. Results and Discussion 117
2.1. NMR Spectra 120
3. Experimental Section 125

VII. CARBON-13 NMR STUDIES OF IRON, RUTHENIUM, OSMIUM, MANGANESE, AND RHENIUM CARBONYL HYDRIDES AND IODIDES 130
1. Introduction 130
2. Results and Discussion 131
2.1. Assignment of ^{13}CO Resonances 132
2.2. Carbon-13 Chemical Shifts 136

2.3. Carbon-13 Coupling Constants 140
2.4. Stereochemical Nonrigidity 143
3. Experimental Section 147

REFERENCES 152

LIST OF TABLES

TABLE PAGE

CHAPTER II

I ^{13}C Chemical Shifts in *cis*-$M(CO)_4(ER_3)_2$ Derivatives 35

II ^{13}C Chemical Shifts in *cis*-$Fe(CO)_4(SnR_3)_2$ Derivatives 37

III ^{13}C Chemical Shifts in *trans*-$M(CO)_4(ER_3)_2$ Derivatives 38

IV ^{13}C Chemical Shifts in R_3EX Derivatives 39

CHAPTER III

V Carbon-13 Coupling Constants in *cis*-$Fe(CO)_4$-$(SnR_3)_2$ Derivatives 58

VI Carbon-13 Coupling Constants in *cis*-$M(CO)_4$-$(EMe_3)_2$ Derivatives 60

VII Carbon-13 Coupling Constants in R_3EX Derivatives 63

CHAPTER IV

VIII Coalescence Temperature and Free Energies of Activation for Axial-Equatorial Averaging in *cis*-$M(CO)_4(ER_3)_2$ Derivatives 87

TABLE PAGE

CHAPTER VI

IX Infrared and ^1H NMR Data of 1,2-bis(Dimethylsilyl)ethane Derivatives 121
X ^{13}C NMR Data of 1,2-bis(Dimethylsilyl)ethane Derivatives 122
XI Elemental Analysis, Melting Points, and Molecular Weights of 1,2-bis(Dimethylsilyl)ethane Derivatives 127

CHAPTER VII

XII ^{13}C Chemical Shifts and ^{13}C-^1H Coupling Constants in *cis*-$M(CO)_4X_2$ and $M'(CO)_5X$ Derivatives 137

LIST OF FIGURES

FIGURE PAGE

CHAPTER II

1 ^{13}C nmr spectra of *cis*- and *trans*-$Os(CO)_4(SiMeCl_2)_2$ 24

2 ^{13}C nmr spectrum of *cis*-$Os(CO)_4(PbMe_3)_2$ 26

3 ^{13}C nmr spectrum of the equilibrium mixture of *cis*- and *trans*-$Os(CO)_4(SnMe_3)_2$ 28

4 ^{13}C nmr spectrum of *cis*-$Ru(CO)_4(SiCl_3)_2$ 29

5 ^{13}C nmr spectrum of *cis*-$Fe(CO)_4(SnBu_3)_2$ 31

6 ^{13}C nmr spectrum of *cis*-$Fe(CO)_4(SnPh_3)_2$ 33

CHAPTER IV

7 Variable temperature ^{13}C nmr spectra of *cis*-$Fe(CO)_4(SiMe_3)_2$ 69

8 ^{13}C nmr spectrum of *cis*-$Fe(CO)_4(SiMe_3)_2$ 71

9 Infrared spectra of $Fe(CO)_4(SiMe_3)_2$ and $Fe(CO)_4SiMe_2CH_2CH_2SiMe_2$ 73

10 Variable temperature ^{13}C nmr spectra of *cis*-$Fe(CO)_4(GeMe_3)_2$ 75

11 Variable temperature ^{13}C nmr spectra of *cis*-$Fe(CO)_4(SnMe_3)_2$ 77

12 Variable temperature ^{13}C nmr spectra of the equilibrium mixture of *cis*- and *trans*-$Os(CO)_4(SiMe_3)_2$ 82

FIGURE PAGE

CHAPTER V

13 Molecular structure of *cis*-$Fe(CO)_4(SiMe_3)_2$ 100

14 Molecular structure of *cis*-$Fe(CO)_4(SnPh_3)_2$ 103

15 Molecular structure of *cis*-$Fe(CO)_4HSiPh_3$ 105

16 Molecular structure of *cis*-$Ru(CO)_4(GeCl_3)_2$ 108

17 Molecular structure of *trans*-$Fe(CO)_4(SiCl_3)_2$ 114

18 Molecular structure of *trans*-$Ru(CO)_4(GeCl_3)_2$ 116

CHAPTER VII

19 Variable temperature ^{13}C nmr spectra of $Re(CO)_5I$ 134

20 Proton-decoupled and -coupled ^{13}C nmr spectra of *cis*-$Os(CO)_4H_2$ 141

21 Variable temperature ^{13}C nmr spectra of *cis*-$Fe(CO)_4H_2$ 145

CHAPTER I

INTRODUCTION

Transition metal carbonyl chemistry began in 1890 with the discovery of nickel tetracarbonyl.[1] However, a systematic investigation of metal carbonyl derivatives did not start until much later. Perhaps the "fabulous fifties" could be considered as a turning point. The availability of infrared, nuclear magnetic resonance and mass spectrometers as well as advances in X-ray crystallography were major factors in the development of transition metal carbonyl chemistry.

A comprehensive guide to the literature covering the years 1950-1970 has appeared.[2] It has been estimated that over 2500 new papers appear each year in the field of organotransition metal chemistry,[2] and an unknown but certainly substantial fraction would involve metal carbonyls.

A number of exhaustive reviews on metal carbonyls has been published;[3-6] however, the task of writing such a review is becoming increasingly difficult. Annual surveys and subject reviews are now appearing in such publications as the "Journal of Organometallic Chemistry" and "Advances in Organometallic Chemistry." Complete coverage of the literature would be beyond the scope of this thesis, and only selected topics, related to the work presented here, will be discussed.

The following sections of the Introduction will deal first with the bonding, stability, and structure of transition metal carbonyls, in particular those of iron, ruthenium and osmium, and secondly with the stereochemical nonrigidity of these derivatives.

1. Bonding and Stability of Transition Metal Carbonyl Derivatives

Bonding of the CO molecule to a transition metal is generally considered to involve two mechanisms: firstly, a σ-bond is created by electron donation from the carbonyl 5σ orbital to the unfilled metal orbitals, and secondly, a π-bond is created by electron donation from the filled metal d-orbitals to the unfilled 2π carbonyl orbitals. Examination of overlap populations shows that both the 5σ and 2π orbitals are antibonding in character.

Electron donation from 5σ will strengthen the carbon-oxygen bond, while electron donation to the 2π will weaken the bond. In other words, competition between the two bonding processes will determine the carbon-oxygen bond strength.[7] Since the carbon-oxygen bond strength is related to its stretching force constant, variations in force constants should reflect changes in the metal-carbon bond.

Other kinds of transition metal-carbon σ-bonds, such as those involving methyl or phenyl groups, were formerly considered the simplest and thermodynamically least stable.[8] However, the synthesis of quite a few alkyl and aryl derivatives of the transition metals that contained π-bonding ligands, such as CO, PR_3, or η^5-cyclopentadienyl led to the belief that the weak transition metal to carbon σ-bond was strengthened in these compounds.[9]

The point has recently been emphasized, however, that the instability of many metal-alkyl complexes is due to the availability of a number of low energy degradative pathways,[10] such as α- or - especially - β-elimination of metal hydride and an olefin, homolysis, or coupling of ligands at the transition metal.[11]

It was suggested[10,12] and verified by synthesis,[12,13] that alkyl derivatives of the transition metals would be stable if one or more of the following conditions were met: a) they are of the form $M\text{-}CH_2\text{-}XHR_n$, where X can form single bonds but no double bonds to carbon, e.g., silicon or a bridgehead carbon*; b) the β-carbon of the alkyl chain bears atoms or groups that cannot be readily transferred to the metal as hydrogen, e.g., $M\text{-}CH_2\text{-}CF_3$, $M\text{-}CH_2\text{-}CMe_3$; or c) the coordination sites required for the decomposition reaction to occur are blocked off by the other ligands attached to the metal. This is the role currently ascribed to π-acid type ligands such as CO, PR_3, or η^5-cyclopentadienyl.

For example, methyl derivatives of the transition metals should be stable because they cannot undergo

---

* According to Bredt's rule,[14] one cannot place a double bond at the bridgehead position. Exceptions to this rule are known, however.[15,16]

alkene elimination, and indeed, compounds such as WMe_6 have been prepared.[17] However, the essentially kinetic stability of these compounds is underlined by the explosions which have occurred when frozen samples of WMe_6, $TaMe_5$, and $ReMe_6$ were allowed to warm to room temperature.[17,18]

An impressive number of derivatives containing bonds between transition metals and silicon or heavier members of that group has been prepared.[19-21] Their stability is frequently greater than that of the carbon analogs. This has been attributed to a greater silicon-transition metal bond strength, which could in turn be ascribed to metal-silicon $d\pi$-$d\pi$ bonding. However, chemical evidence has very recently been brought forward which indicates, in one series of compounds at least, that Fe-C and Fe-Si bonds are of comparable strength.[22] Clearly, the first criterion for kinetic stability mentioned above would account for the stability of trimethylsilyl derivatives, say, in comparison with tertiary butyl.

2. Structure of Iron, Ruthenium, and Osmium Carbonyl Derivatives

The number of ligands and their mode of bonding in organotransition metal complexes may be rationalized by invoking the Effective Atomic Number (EAN) Rule, also known as the "Noble Gas Formalism."[23,24] According to this

rule, the number of valence shell electrons, which consists of the valence electrons of the metal and those donated by or shared with the ligands, would be 18.* Ligands such as carbon monoxide and tertiary phosphines are considered to be two electron donors. Groups bound to the metal *via* single covalent bonds, like hydrogen, halogens, and alkyl groups are all considered one electron donors. The nitrosyl group, bridging halogen atoms or phosphine groups donate three electrons to the metal system.

Structural studies in transition metal carbonyl chemistry have revealed four (although only three will be discussed here) ways for the attachment of the carbon monoxide ligand in a molecule:[25]

a) the terminal arrangement: the M-C-O unit is essentially linear.

b) doubly bridging arrangement: the M-C(O)-M unit is essentially planar and symmetrical. That is, the two M-C bonds are equal.

c) grossly asymmetric bridges: the M-C(O)-M unit is planar but the two M-C bonds are of different

---

* While this rule holds for the great majority of organometallic compounds, it is by no means infallible, and several notable exceptions exist, e.g., $V(CO)_6$, $(C_5H_5)_2Ni$.

length. When pairs of carbonyl bridges occur within the same molecule, they can appear either in a compensatory fashion (i.e., the direction of asymmetry of one bridge is opposite to that of the other), or in a noncompensatory fashion.

d) the triply bridging arrangement.

Considerable effort has been put into, and a vast amount of controversy has arisen from, the determination of the structure of the binary carbonyls of iron, ruthenium and osmium.

Iron pentacarbonyl, the second metal carbonyl to be discovered,[26] is one of the most thoroughly investigated. However, it was only in the last decade that the structure of this compound was solved satisfactorily and an unambiguous distinction was made between the two possible geometries, trigonal bipyramidal (D_{3h}) and square pyramidal (C_{4v}). The structure in the gas phase, as established by an electron diffraction study, is trigonal bipyramidal with an $Fe\text{-}C_{axial}$ distance of 1.806(5) Å and an $Fe\text{-}C_{equatorial}$ distance of 1.833(4) Å.[27] An X-ray diffraction study showed the same type of geometry in the solid state;[28] however, the accuracy of the structure leaves a great deal to be desired. Infrared spectroscopic evidence is consistent with a trigonal bipyramidal structure in solution on the basis that two infrared active bands are predicted for D_{3h} symmetry, and two were observed. Three

infrared active bands are predicted for C_{4v} symmetry.

The trigonal bipyramidal structure of $Fe(CO)_5$ is in accord with the X-ray diffraction studies of some pentacoordinate carbonyl derivatives such as $HFe(CO)_4^-$,[29] $Fe(CO)_4C_5H_5N$,[30] $Fe(CO)_4C_4H_4N_2$,[30] $Fe(CO)_4PPh_2H$,[31] $Fe_2(CO)_8^{2-}$,[32] $Mn(CO)_5^-$,[33] and $Mn(CO)_4NO$,[34] all of which showed an idealized or slightly distorted trigonal bipyramidal arrangement of the ligands. The latter of these compounds, $Mn(CO)_4NO$, is isoelectronic with $Fe(CO)_5$.

No structural data are available for the ruthenium and osmium pentacarbonyl derivatives, although infrared data suggest a trigonal bipyramidal geometry.[35]

Nonacarbonyldiiron, $Fe_2(CO)_9$, was the third metal carbonyl to be discovered.[36] Early X-ray diffraction work established the existence of three symmetrical carbonyl bridges and a metal-metal bond, as in 1.[37]

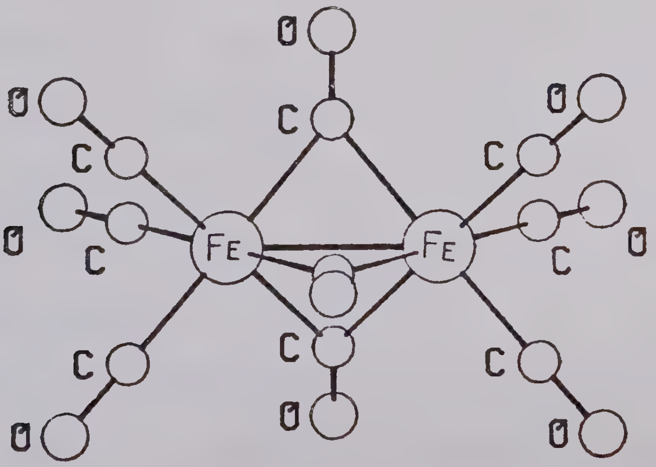

1

This was the first metal carbonyl whose structure was determined by X-ray crystallography. The rather short Fe-Fe bond of 2.46 Å prompted a more accurate determination

which came exactly 25 years after the original one.[38] The improved Fe-Fe distance is 2.523(1) Å. A notable feature of this structure is the acute angle at the bridging carbon atom of 77.6(1)°. This is, so far, the lowest angle of this type known.

The ruthenium and osmium analogs of $Fe_2(CO)_9$ were not prepared until recently.[39] The infrared spectrum of $Os_2(CO)_9$ indicates a C_{2v} structure in solution:

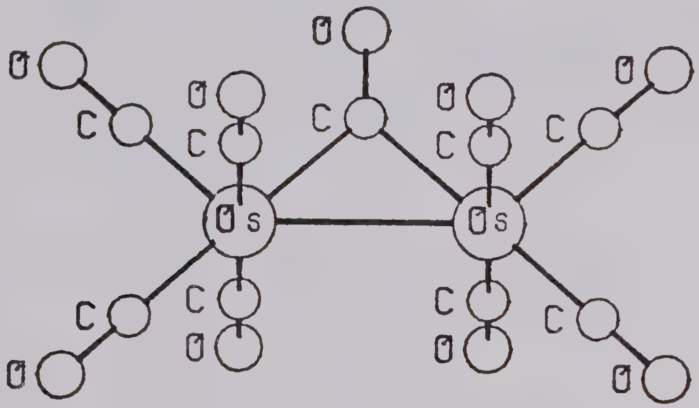

2

The molecule is isoelectronic with $Cp_2Re_2(CO)_5$, the X-ray structure of which showed a similar geometry with a bridging carbonyl group.[40] The enneacarbonyl of ruthenium, $Ru_2(CO)_9$, has not yet been isolated, but presumably has the same structure as $Os_2(CO)_9$.[39]

The structure determination of dodecacarbonyltriiron, $Fe_3(CO)_{12}$, was by far the most interesting and controversial of all transition metal complexes. Although this compound was prepared in 1906,[41] its solid state structure was not unambiguously known until 1969[42] due to a severe

disorder problem.

To a first approximation, the molecular structure of $Fe_3(CO)_{12}$ may be regarded as being derived from that of $Fe_2(CO)_9$ by replacing one bridging carbonyl group by an $Fe(CO)_4$ fragment.[42]

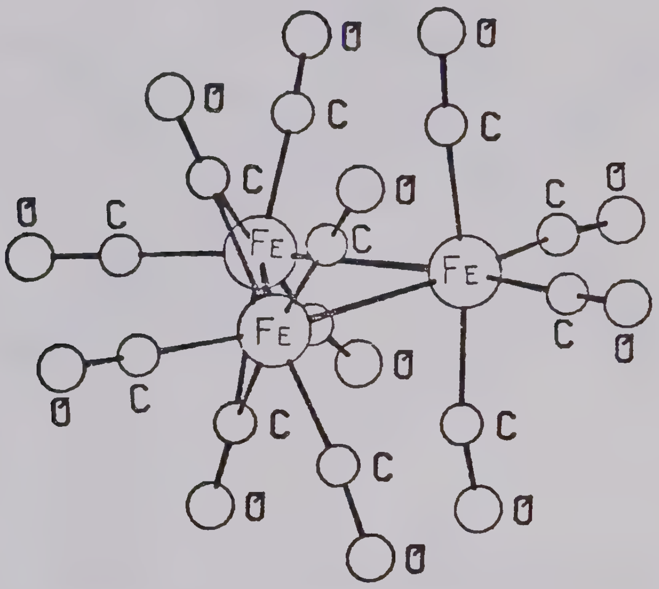

3

The two bridging CO groups were suspected,[42] but not proven, to be asymmetric. However, further refinement of the structure of $Fe_3(CO)_{12}$ has clearly demonstrated the asymmetric nature of the bridges.[43]

The solution structure of this molecule is still not fully understood, but the most recent view is that the energy of the molecule changes little on passing from a symmetrically bridged structure (C_{2v}) *via* unsymmetrically bridged intermediates (C_2) to a completely unbridged form (D_{3h}).[25,43,44]

The solid state structures of $Ru_3(CO)_{12}$[45,46] and $Os_3(CO)_{12}$[45,47] are similar and both show D_{3h} symmetry:

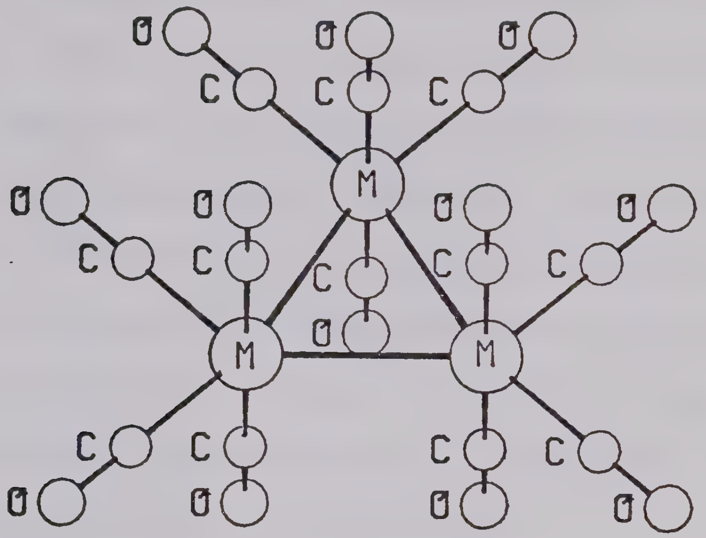

4

Infrared studies indicate that $Ru_3(CO)_{12}$ and $Os_3(CO)_{12}$ adopt the same geometry in solution.[48]

The most common derivatives of iron, ruthenium, and osmium carbonyls are of the $M(CO)_4X_2$ type, where X is a formally one-electron donor, such as alkyl or aryl group, halogen, hydrogen. Numerous structural studies of these derivatives exist. However, since this thesis is concerned with derivatives of this type, their structures will be mentioned later.

3. Stereochemical Nonrigidity

The atoms in a molecule execute more-or-less harmonic vibrations about their equilibrium positions. If these

motions are sufficiently large in amplitude as to permute nuclear positions, they lead to stereoisomerization.

The term stereochemically nonrigid applies to molecules or ions in which atom or ligand permutations occur at a rate such that they can be detected by some physical or chemical method. Fluxional molecules are a subclass of stereochemically nonrigid molecules in which all the interconverting species are chemically and structurally equivalent. When the different configurations are not chemically and structurally equivalent, the process is called isomerization or tautomerism.

The term "polytopal isomers" has been used to describe isomers having the same coordination number but different idealized coordination geometry,[49] as for example, square planar and tetrahedral. Therefore, any permutation which does not involve bond breaking implies polytopal isomers as intermediates or transition states, and is called a polytopal rearrangement.[49]

3.1 Dynamic Nuclear Magnetic Resonance Spectroscopy

The method most often - if not exclusively - used to study stereochemically nonrigid molecules is nuclear magnetic resonance. Processes with free energies of activation from 5 to 25 kcal mol^{-1} are amenable for this type of study. By proper choice of temperature, the system can be made to exchange at a rate slower than,

comparable to, or faster than the time scale of the nmr instrument. The temperature ranges where these three possibilities occur are called "slow exchange", "intermediate exchange", and "fast exchange limit", respectively.

Carbon-13 nmr has proven to be an invaluable tool in the study of stereochemically nonrigid organometallic compounds and in particular of metal carbonyl derivatives. A comparison between ^{13}C nmr and ^{1}H nmr would definitely favour the former, despite some of its drawbacks. Like the proton, carbon-13 possesses a spin of 1/2, but its low natural abundance (1.1%), a smaller gyromagnetic ratio, and long values of the relaxation time result in a very much reduced sensitivity to nmr detection (the decrease is about 5700-fold). However, the ^{13}C absorption exhibits a positive nuclear Overhauser effect and a maximum enhancement of three-fold can be obtained by decoupling the protons.[50]

Undoubtedly, the main advantage of ^{13}C nmr is that shielding constants for ^{13}C nuclei extend over a wide range (600 ppm) and have been found to be very sensitive to slight changes in electronic environment. This is particularly important in the study of stereochemically nonrigid molecules as the coalescence temperature of resonances increases with the chemical shift separation between them. Thus, exchange processes with small

activation energies which could not be studied by ^{1}H nmr are readily detectable using ^{13}C nmr.

Routine ^{13}C nmr spectroscopy has until recently been hindered by instrumental difficulties. However, as a result of the application of the pulse Fourier transform technique,[51] routine ^{13}C spectra (particularly of organic samples) can be obtained almost as easily as proton spectra. However, metal carbonyl samples frequently cannot be considered routine, and often require enrichment of the sample with ^{13}CO for satisfactory results.

Stereochemically nonrigid organometallic derivatives have received a great deal of attention over the last years, and a number of reviews on the subject have appeared.[52-57] The last one of these references is a book entitled "Dynamic Nuclear Magnetic Resonance." An anecdotal account of the earliest developments in this field is also available.[58] In addition, the ^{13}C nmr of transition metal carbonyl derivatives has also been reviewed recently.[59-61]

3.2 Stereochemical Nonrigidity and the Iron, Ruthenium and Osmium Carbonyl Derivatives

The stereochemical nonrigidity of the carbonyl derivatives of iron is unsurpassed and seldom matched by those of any other transition metal.

^{13}C nmr has been used, along with other physical methods, in attempts to decide between the two possible stereoisomers of Fe(CO)$_5$, trigonal bipyramidal and square pyramidal. For the former structure, one would expect two different ^{13}C resonances in relative intensities 2:3, while for the latter structure, a 1:4 ratio of the ^{13}C resonances is expected.

The ^{13}C spectrum of Fe(CO)$_5$ was reported by not less than ten research groups.[62-71] However, the room temperature spectrum showed only a single resonance. This resonance remained sharp down to -63°,[63] -110°,[69] -150° (63 MHz)[70] and even -170°.[71] It seems to be generally accepted that this is the result of a rapid intramolecular rearrangement.[63] The possibility of an intermolecular exchange or ligand dissociation can be rigorously excluded since $^1J(^{13}C-^{57}Fe)$ was observed in Fe(CO)$_5$.[67]

The chemical shift difference between the axial and equatorial sites in Fe(CO)$_5$ was calculated to be 17.7 ± 1.5 ppm, which corresponds to a minimum exchange rate between these sites of 1.1 x 10^{10} sec^{-1} at -20°.[72] This chemical shift separation and the rate of exchange in Fe(CO)$_5$ seem exceedingly large (see Chapter IV of this thesis).

Similarly, the ^{13}C nmr spectra of Ru(CO)$_5$[73] and Os(CO)$_5$ (Chapter VII) showed only one sharp line down

to -120° and -70°, respectively.

To date there are only a few five-coordinate transition metal complexes known for which the slow exchange nmr spectrum could be determined. These are complexes of the type ML_5 (M = Fe, L = $P(OMe)_3$),[74] MX_2L_3 (M = Ru, Os; L = PPh_3; X = Cl, Br[75]), or $ML_5^+X^-$ (M = Rh(I),[71,76-78] Co(I),[77,78] Ir(I),[77,79] Ni(II),[78] Pd(II),[78] Pt(II);[78] L = phosphite; X^- = BPh_4^-, BF_4^-, 1/2GeF_6^{2-}, 1/2SiF_6^{2-}, PF_6^-, AsF_6^-, SbF_6^-, Cl^-). In all these complexes the slow exchange spectrum shows an A_2B_3 or an A_2B_3X pattern, thus confirming their trigonal bipyramidal structure in solution. Also, detailed line-shape analysis of several Pd(II),[78] Ni(II),[78] Co(I),[78] and Rh(I)[76,78] complexes indicate the Berry rearrangement mechanism[80] as the most likely one for these species.

Although the slow exchange nmr spectrum of $Fe(CO)_5$ has not been observed (and probably never will be), this was achieved for some of its derivatives, such as $Fe(CO)_4$-(olefin)[81,82] and $Fe(CO)_4$(diene),[83-85] or the corresponding ruthenium analogs.[85-87] These compounds could be regarded as pseudo-six-coordinate and the activation energies for their rearrangement are higher than for five-coordinate species.

The ^{13}C nmr spectrum of the enneacarbonyls has not been reported yet. This is not surprising in view of the insolubility of $Fe_2(CO)_9$ in most solvents and the

instability of the heavier congeners. However, it would be interesting to see if scrambling of carbonyl groups occurs in these molecules.

For the enneacarbonyls, there are two possible structures, with one or with three bridges, which are equivalent from the EAN viewpoint:

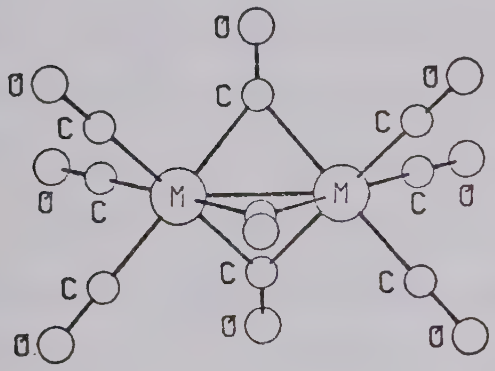

5

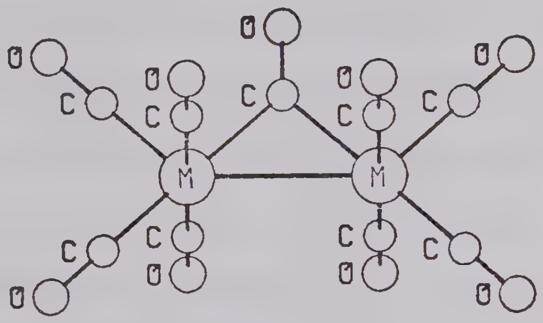

6

Repeated interconversions between these two structures would afford a pathway for scrambling of CO groups.

Similarly, for the trinuclear species, the following structures may be drawn (three other terminal carbonyls on each metal are not shown):

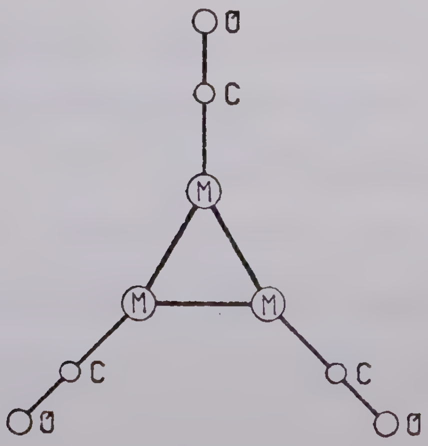

7

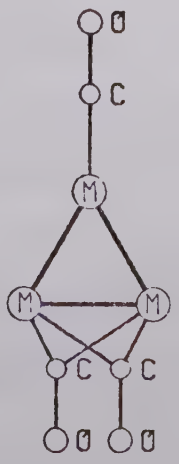

8

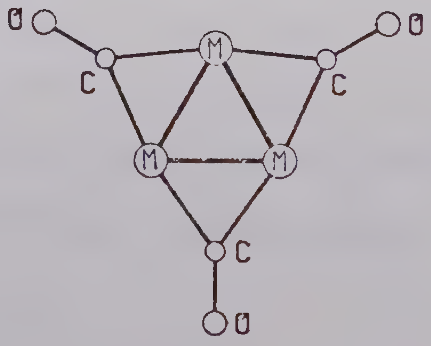

9

Structure **7** occurs in $Ru_3(CO)_{12}$ and $Os_3(CO)_{12}$, **8** was found in crystalline $Fe_3(CO)_{12}$ and **9** was proposed earlier for $Fe_3(CO)_{12}$ in solution.[42] Scrambling of CO groups may occur *via* **7** → **8** → **9** or **7** → **8** interconversions.

The ^{13}C nmr spectrum of $Fe_3(CO)_{12}$ between -10 and 50° showed one sharp resonance[69] indicating a rapid and complete scrambling of all CO groups. Later, it was proposed[43] and verified[44] that the coalescence temperature for the bridge-terminal rearrangement in this molecule is below - 150°. This means that even if the maximum chemical shift difference between bridging and terminal CO's were as little as 10 ppm, the activation energy for this process would be lower than 6 kcal mol^{-1}.[44]

Variable temperature ^{13}C nmr studies of $Os_3(CO)_{12}$ and $Ru_3(CO)_{12}$ showed coalescence (at 70°) of the axial and equatorial resonances for the former species and a single resonance for the latter species from 40° down to -50°[88] or -100°.[89] The ^{13}C nmr of $Ru_3(CO)_{12}$ was reported by others,[60] and two resonances were observed. However, this report was questioned, and one of the resonances was assigned to $H_4Ru_4(CO)_{12}$.[89]

This thesis is concerned with the ^{13}C nmr spectra and stereochemical nonrigidity of $M(CO)_4X_2$ species. In contrast to the five-coordinate derivatives, six-coordinate species have not been expected to display stereochemical

nonrigidity, and such behaviour was found only in special cases. This is because the octahedron is thought to be so much more stable than any other polytopal isomer.[53]

^{1}H nmr studies of $Os(CO)_4(SiMe_3)_2$ carried out in this laboratory indicated the stereochemical nonrigid character of this derivative.[90] The work in this thesis was undertaken to apply the powerful technique of ^{13}C nmr to compounds of this type. The following four chapters will deal with $M(CO)_4(ER_3)_2$ derivatives ($M = Fe, Ru, Os$; $E = Si, Ge, Sn, Pb$; E = organic group, halogen), and their ^{13}C chemical shifts, ^{13}C coupling constants, stereochemical nonrigidity and structure. In the last two chapters, the ^{13}C nmr spectra of $M(CO)_4SiMe_2CH_2CH_2SiMe_2$ and $M(CO)_4X_2$ derivatives ($M = Fe, Ru, Os$; $X = H, I$) will be considered.

CHAPTER II

CARBON-13 NMR STUDIES OF SIX-COORDINATE IRON, RUTHENIUM, AND OSMIUM CARBONYL DERIVATIVES WITH GROUP IV ELEMENTS.

CARBON-13 CHEMICAL SHIFTS.

1. Introduction

The first ^{13}C nmr spectrum of an inorganic compound was obtained in 1958,[62] only one year after the first natural abundance ^{13}C spectrum was reported.[91] This was the spectrum of $Fe(CO)_5$, which even to this date is not understood with certainty.[57]

Of all transition metal carbonyl derivatives, those containing iron are among the most widely studied. Ruthenium and especially osmium derivatives have been much less studied. Prior to the date when results from Chapter VI of this thesis were published,[92] there had been only two reports on the ^{13}C nmr of an osmium carbonyl derivative.[93,94]

Some of the ^{13}C nmr studies of iron, ruthenium and osmium carbonyl derivatives were reviewed in the Introduction. The rest of the papers, almost 100 now, are not pertinent to this thesis and are not mentioned here.

Recent reports from this laboratory have described the remarkable stereospecific carbon monoxide exchange

that takes place in *cis*-$Ru(CO)_4(SiCl_3)_2$[95] and the stereochemical nonrigid character of $Os(CO)_4(SiMe_3)_2$,[90] for which cis and trans isomers interconvert rapidly in a nondissociative process. It was anticipated that ^{13}C nmr spectroscopy would play a key role in the continuation of these studies.

In this chapter, the ^{13}C nmr chemical shifts of an extensive series of $M(CO)_4(ER_3)_2$ type derivatives will be discussed (M = Fe, Ru, Os; E = Si, Ge, Sn, Pb; R = Me, Et, *n*-Pr, *n*-Bu, Ph*, and Cl).[96-98]

2. Results and Discussion

Compounds of the type $M(CO)_4(ER_3)_2$ or $M(CO)_4(SiMe_{3-n}Cl_n)_2$ may exist in solution as pure cis, pure trans, or as a mixture of observable amounts of cis and trans isomers (which may or may not be in rapid equilibrium at a given temperature). All these possibilities have been observed among the compounds investigated here.

Infrared spectroscopy has commonly been used to distinguish among the possibilities, on the basis that a single carbonyl stretching band is expected for a trans

---

* Throughout this thesis, the methyl, ethyl, propyl, butyl, acetyl, and phenyl group are abbreviated as Me, Et, Pr, Bu, Ac, and Ph, respectively.

isomer, and four for the cis.[99] However, infrared spectroscopy will not reliably detect a cis-trans mixture because the single carbonyl band of the trans isomer is often coincident with one of the four cis bands (see page 112 where the interesting case of $Fe(CO)_4(SiCl_3)_2$ is discussed). A further problem arises in molecules such as $M(CO)_4(SiMe_{3-n}Cl_n)_2$ (n = 1,2) where extra bands result from various conformations of the unsymmetrical ligands.[100]

Proton nmr spectroscopy may in certain cases reveal the presence of two isomers, but even so it is generally not possible to assign the signals to the individual isomers without other evidence. On the other hand, ^{13}C nmr is broadly applicable to $M(CO)_4(ER_3)_2$ and related complexes. Two ^{13}C resonances of equal intensity are expected in the metal carbonyl region for a cis isomer, whereas a single resonance is expected for the trans isomer:

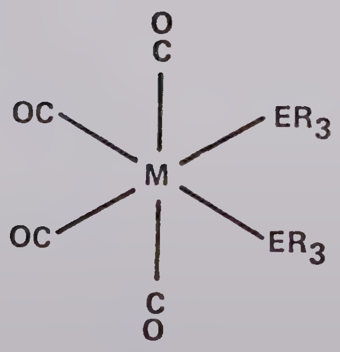

cis

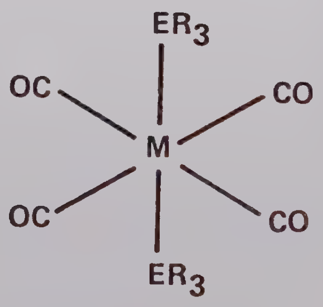

trans

As an illustration, Figure 1 shows the ^{13}C nmr spectra of *cis*- and *trans*-$Os(CO)_4(SiMeCl_2)_2$. The Si-Me resonances are at high field, close to 20 ppm, and the CO resonances lie at low field, around 170 ppm.

Assignment of peaks in cis-trans mixtures can normally be made on an intensity basis; ambiguities which might result if the intensities of the three ^{13}CO resonances were very similar (i.e., a cis : trans ratio near 2 in the mixture) could be resolved by examining the spectrum over a range of temperatures at different equilibrium ratios.

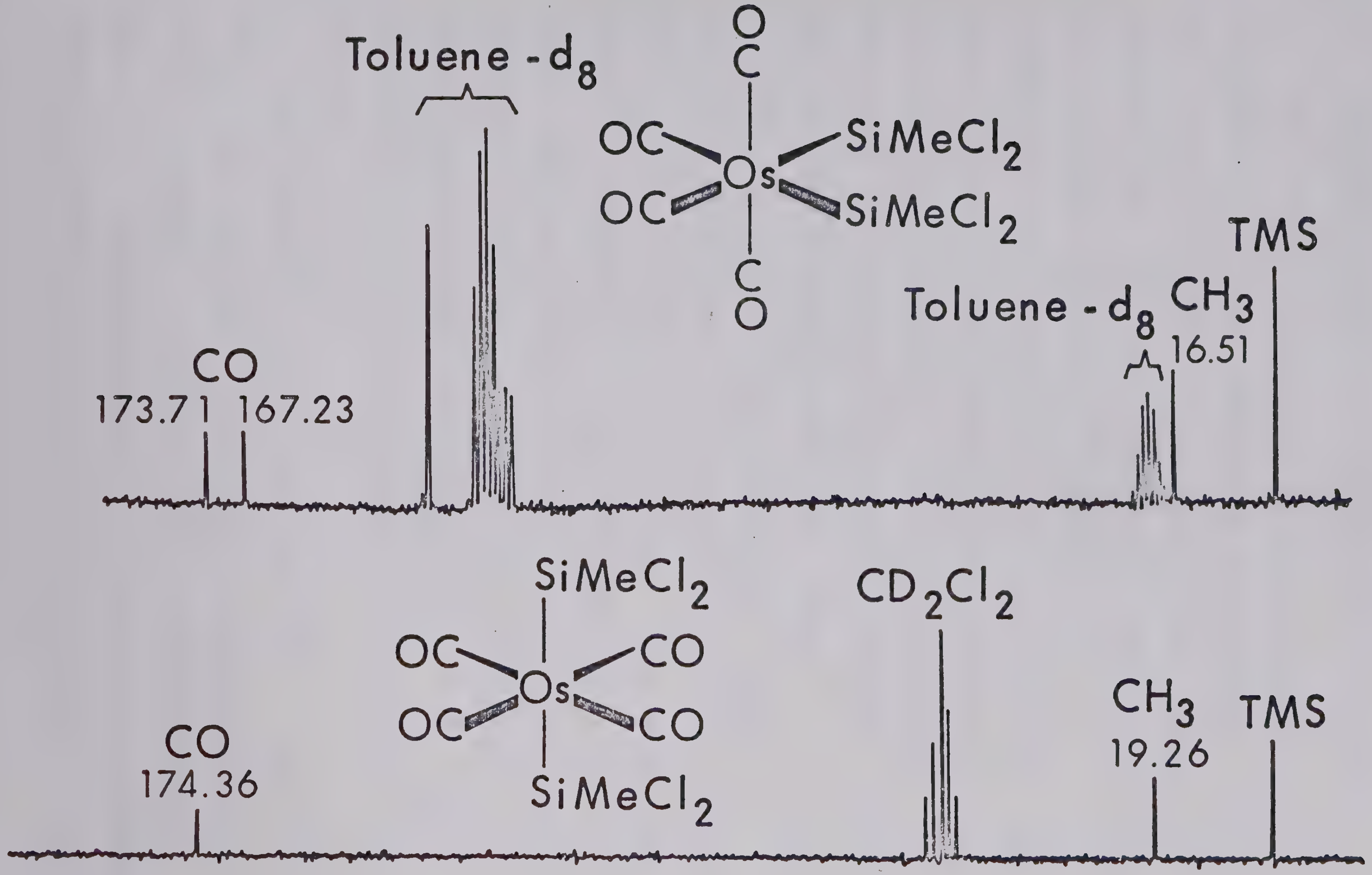

Figure 1. ^{13}C nmr spectrum of *cis*- and *trans*-$Os(CO)_4(SiMeCl_2)_2$.

2.1 Assignment of Axial and Equatorial Resonances

From the proton-coupled ^{13}C nmr spectrum of *cis*-$Os(CO)_4H_2$, it was possible to assign unambiguously the resonance at lower field (A_2X pattern) to the axial carbonyl group, and the resonance at higher field (AA'X) to the equatorial carbonyl[92] (see also page 140). Evidence is now presented that the same assignment also holds for many of the *cis*-$M(CO)_4(ER_3)_2$ derivatives discussed in this Chapter. It may hold for most, if not all of the ruthenium and osmium derivatives, although there are exceptions for some iron analogs.

When the element E has a significant proportion of an isotope of spin 1/2, coupling is observed between this element and the carbonyl carbons. The equatorial carbon is expected to show two different couplings, one due to the E atom trans to it, the other to the mutually cis E atom. The axial carbonyl carbon is expected to show a single coupling, with satellites of twice the intensity of those centered around the equatorial resonance.

This possibility exists for tin (^{117}Sn, 7.6%; ^{119}Sn, 8.6%) and lead (^{207}Pb, 22.6%) derivatives and it has been observed in this work. It is illustrated in Figure 2 for *cis*-$Os(CO)_4(PbMe_3)_2$, in which the equatorial carbonyl resonance, flanked by two satellite pairs, lies

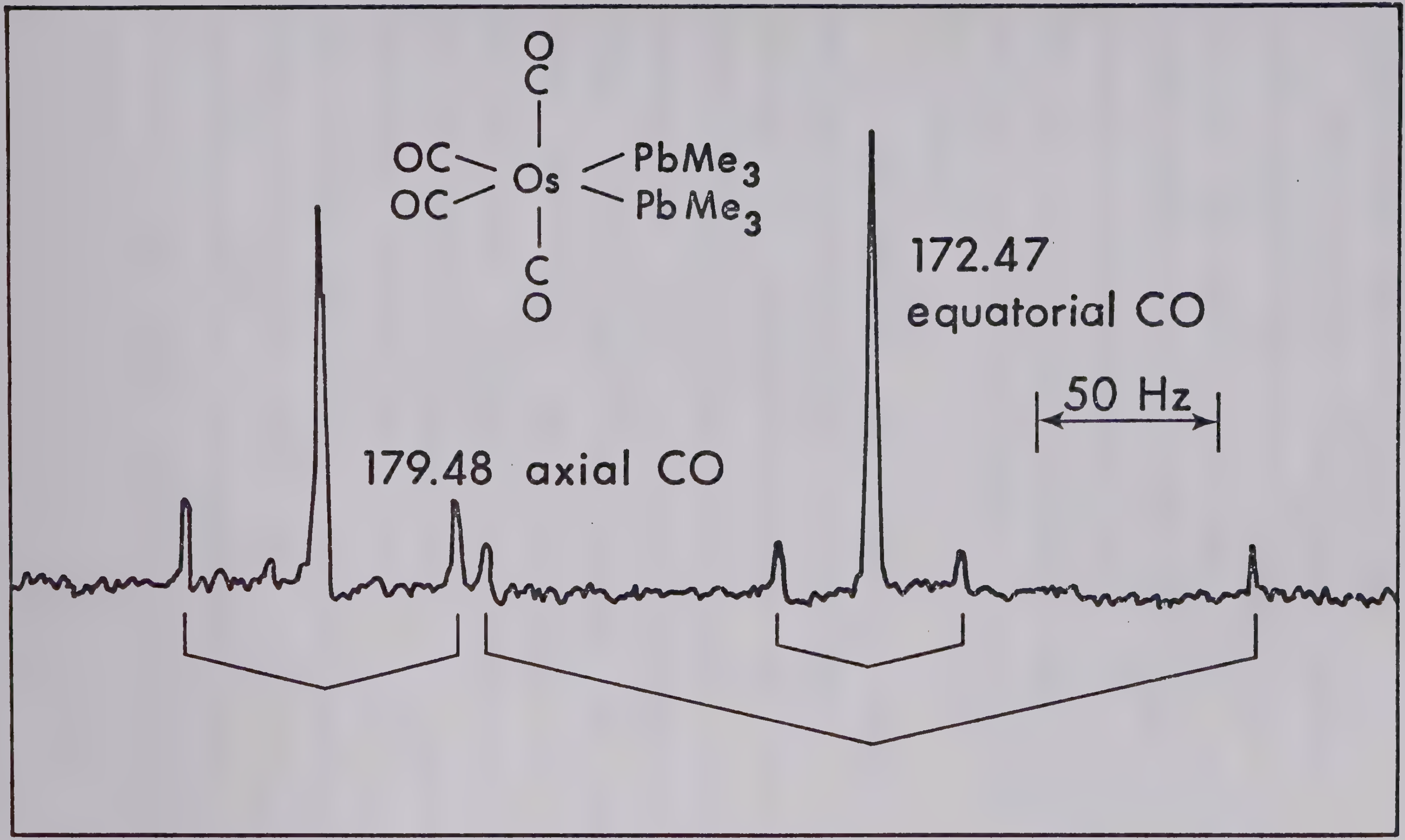

Figure 2. ^{13}C nmr spectrum (carbonyl portion) of *cis*-$Os(CO)_4(PbMe_3)_2$ in toluene-d_8 at -20°.

at higher field. The coupling constants will be discussed more fully in Chapter III.

In Figure 3 the ^{13}C nmr spectrum (carbonyl portion) of an equilibrium mixture of *cis*- and *trans*-Os$(CO)_4(SnMe_3)_2$ is shown. The sample is enriched in ^{13}CO. The peak at lowest field is assigned to the trans isomer; the two resonances of equal intensity, at high field, belong to the cis isomer. The peak at highest field, with two satellite pairs, is due to the equatorial groups of the cis isomer.

A quite different method leads to a similar assignment in the case of *cis*-Ru$(CO)_4(SiCl_3)_2$. It has been shown by a detailed infrared analysis that the equatorial carbonyl groups of this molecule undergo exchange with ^{13}CO in a completely stereospecific way.[94] Figure 4 compares the ^{13}C nmr spectrum of the molecule at natural abundance with that of the equatorially ^{13}CO enriched species. The natural abundance spectrum shows two ^{13}CO resonances of equal intensity, as expected; the equatorially enriched compound shows a single peak at the higher field resonance of the upper spectrum, thereby confirming the assignment. It should also be pointed out that the ^{13}C nmr experiment provides a striking confirmation of the stereospecificity of the exchange.[94]

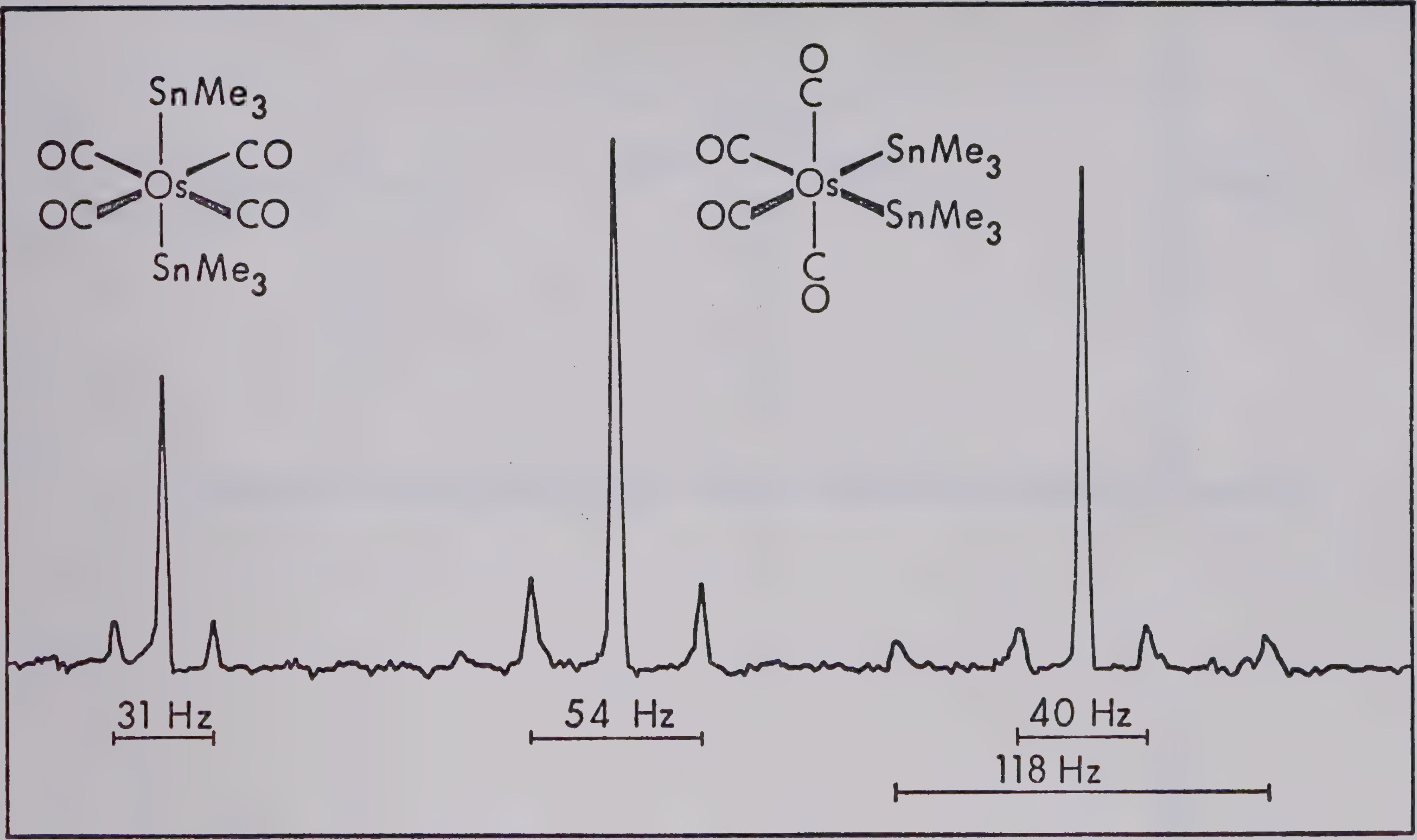

Figure 3. ^{13}C nmr spectrum (carbonyl portion) of the equilibrium mixture of *cis*- and *trans*-$Os(CO)_4(SnMe_3)_2$ in CD_2Cl_2 at -20°. The sample is enriched with ^{13}CO.

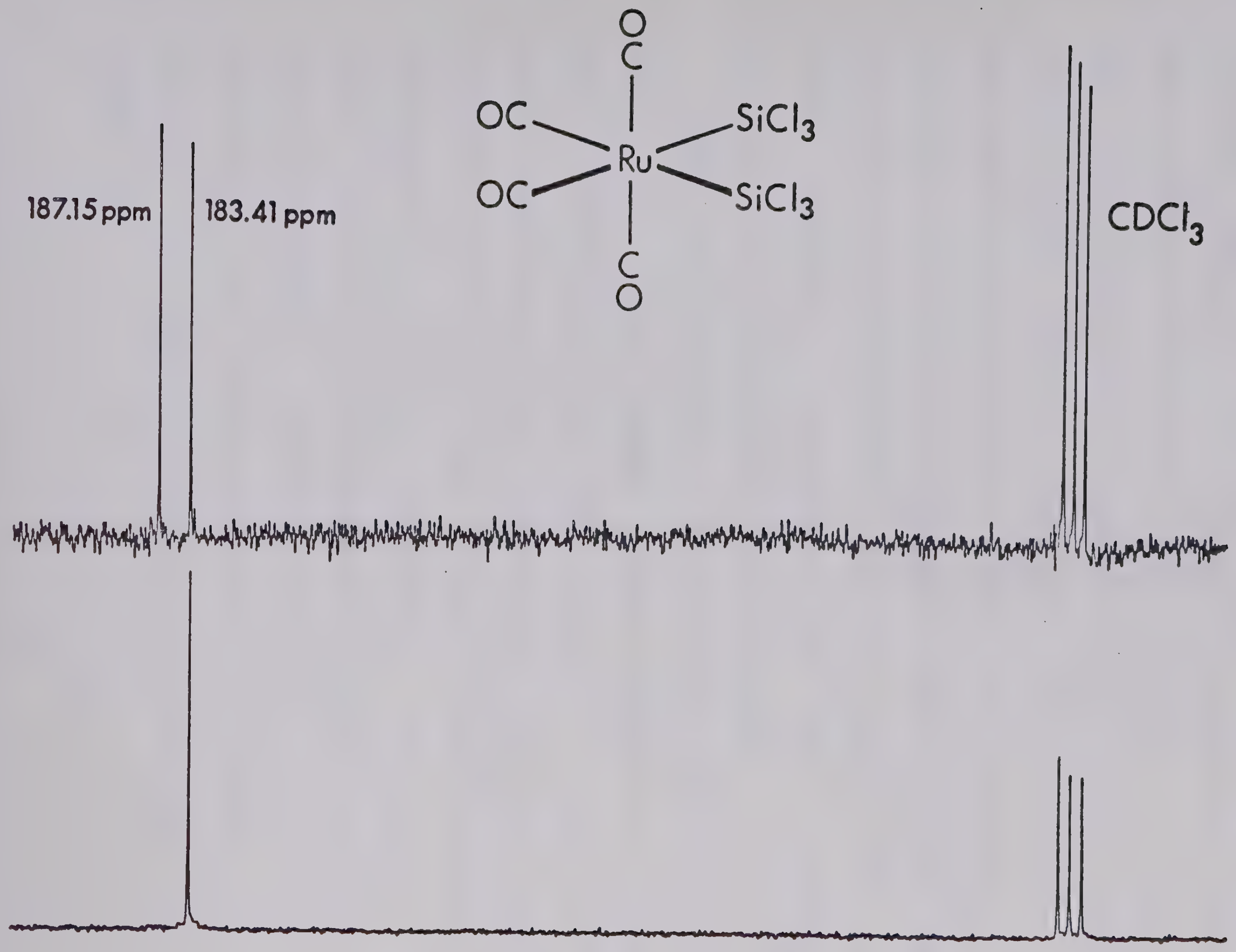

Figure 4. ^{13}C nmr spectrum of *cis*-Ru(CO)$_4$(SiCl$_3$)$_2$. Upper trace: natural abundance ^{13}CO. Lower trace: after ^{13}CO enrichment stereospecifically in the equatorial positions.

In summarizing our findings to date on the ^{13}C chemical shifts of axial and equatorial carbonyls in *cis*-$M(CO)_4(ER_3)_2$ or *cis*-$M(CO)_4X_2$* (X represents a formal one-electron donor to the zerovalent metal), we may state that *the ^{13}C resonance of the carbonyl trans to the one-electron donor ligand is at higher field.*[97] This assignment applies also to a number of pentacarbonylmanganese and pentacarbonylrhenium compounds which have been investigated[60,101,102] (see also Chapter VII), and differs from that in complexes of the type *cis*-$M(CO)_4L_2$, where L is an electron-pair donor ligand.[61]

This rule, however, is by no means infallible, and exceptions to it are known. These are compounds of the type *cis*-$Fe(CO)_4(SnR_3)_2$, where R = Me,[97] Et, Pr, Bu.[98] In all these cases, the ^{13}C resonance due to the equatorial carbonyl groups is at lower field than the resonance corresponding to the axial carbonyls. For example, Figure 5 shows the low temperature limiting spectrum of *cis*-$Fe(CO)_4(SnBu_3)_2$. At room temperature, the ^{13}C nmr spectrum of this compound shows only one carbonyl resonance. This aspect will be fully discussed in Chapter IV.

---

* These derivatives will be discussed in detail in Chapter VII.

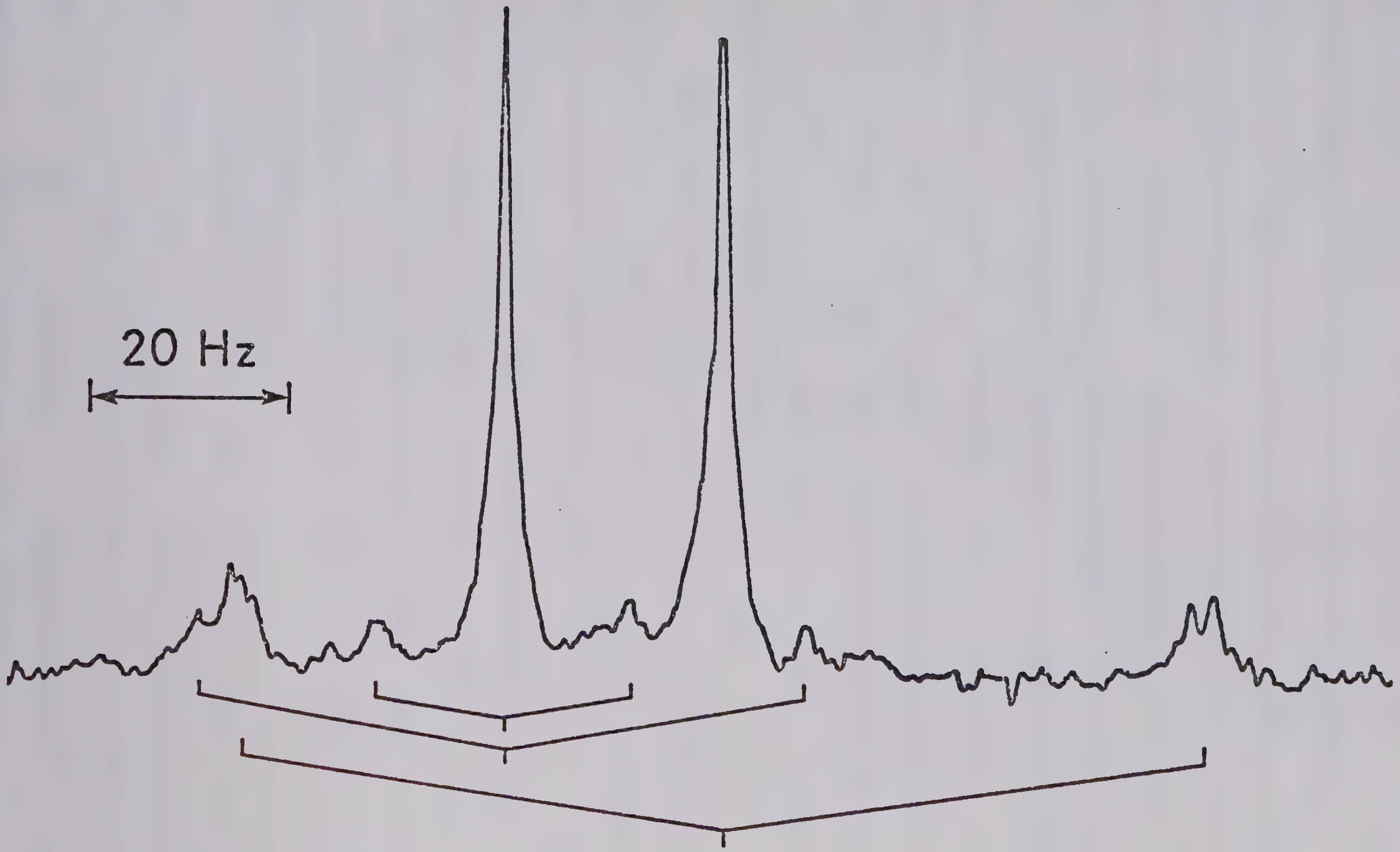

Figure 5. ^{13}C nmr spectrum (carbonyl portion) of *cis*-$Fe(CO)_4(SnBu_3)_2$ in CD_2Cl_2 at -90°. The sample is enriched with ^{13}CO.

By contrast, *cis*-$Fe(CO)_4(SnPh_3)_2$ (Figure 6) and *cis*-$Fe(CO)_4(SnCl_3)_2$ obey the above rule. The reversal of the carbonyl resonances in *cis*-$Fe(CO)_4(SnR_3)_2$ derivatives may be the consequence of a severe distortion from octahedral geometry. This point will be discussed further in Chapter V, when the structure of these complexes, as derived from X-ray crystallography, will be considered.

Because of these exceptions, assignment of ^{13}CO resonances in other *cis*-$Fe(CO)_4(ER_3)_2$ compounds, where element E does not have (or has only a small percentage of) an isotope of spin 1/2, must be regarded as uncertain. No exceptions to this rule have been found or reported for the ruthenium or osmium derivatives.

Over the last five years, several attempts to correlate ^{13}C chemical shifts with Cotton-Kraihanzel force constants[103] have been made,[60,101,104-114] and it was argued that the most shielded carbonyl of the molecule has the largest force constant.[104] This argument seems surprising since a higher force constant is considered to imply a more positive character for the carbonyl carbon atom.[115]

In complexes of the type *cis*-$M(CO)_4L_2$ or $M(CO)_5L$ the carbonyl stretching force constant of the group trans to $L(k_1)$ is always lower than that of the group cis to $L(k_2)$.[103] Thus, according to this argument,[104] the CO trans to L should always be less shielded than the cis CO, irrespective of whether L is a one- or a two-electron

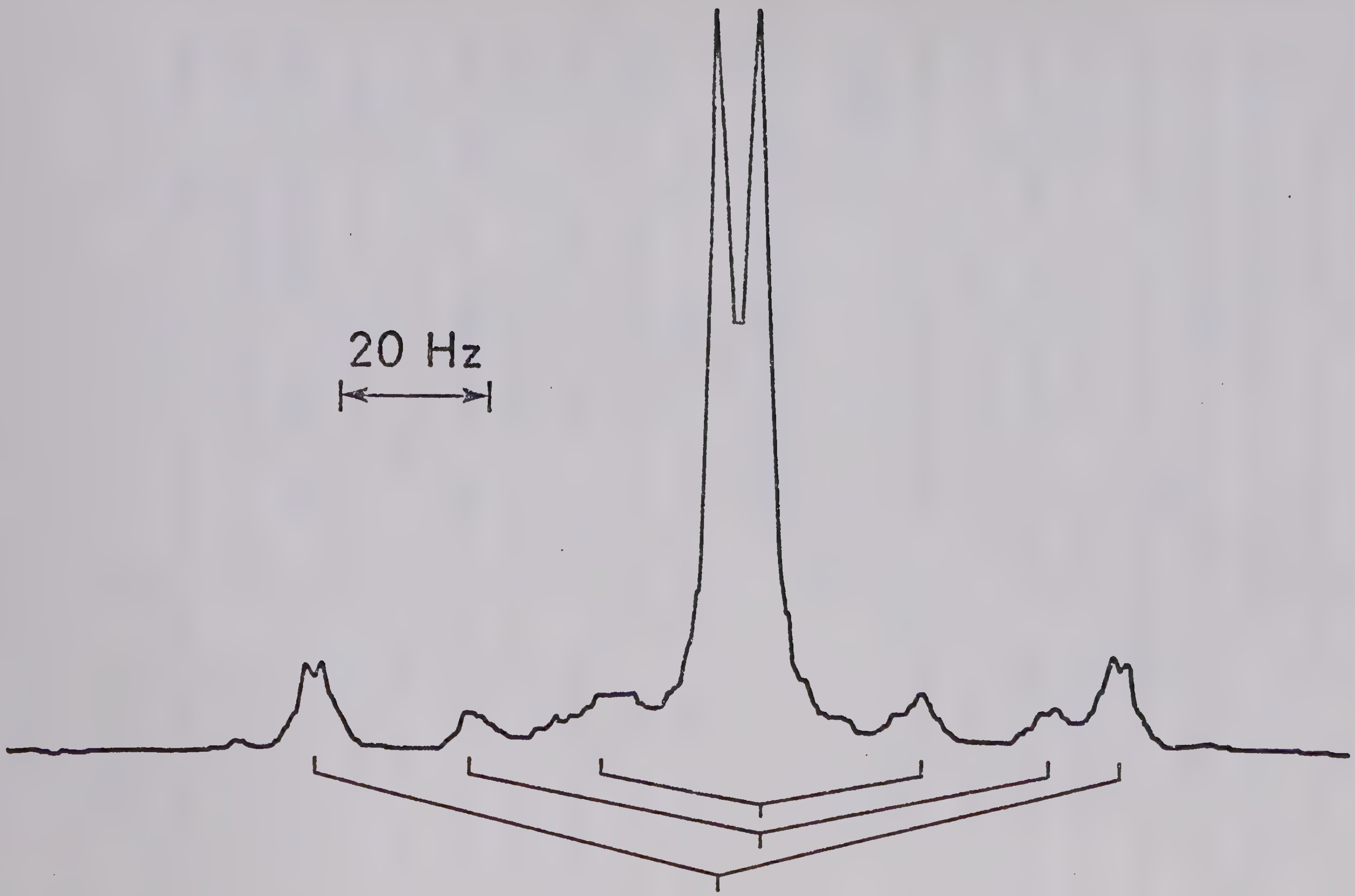

Figure 6. ^{13}C nmr spectrum (carbonyl portion) of *cis*-$Fe(CO)_4(SnPh_3)_2$ in CD_2Cl_2 at -90°. The sample is enriched with ^{13}CO.

donor. This, of course, is contradicted by the findings of this chapter.

For example, in *cis*-$Ru(CO)_4(SiCl_3)_2$, where unambiguous assignment was possible, the two force constants, as obtained by an energy-factored force field calculation and employing ^{13}CO substitution, are almost equal (k_{ax} = 17.96, k_{eq} = 17.91),[94] yet the axial and equatorial ^{13}CO resonances are separated by 3.83 ppm. All of this suggests that using force constants in assigning ^{13}CO resonances is of limited utility in these systems.

2.2 Carbon-13 Chemical Shifts

Values of chemical shifts measured for cis derivatives are presented in Table I and II, and those for the trans derivatives in Table III. In several cases, chemical shift values for the two isomers were obtainable only from low temperature spectra, and this aspect will be fully discussed in Chapter IV. Here, the trends in chemical shifts, which are apparent from Table I-III, will be discussed. Also, the ^{13}C chemical shifts of the parent stannanes (Table IV) will be compared with the values found in their transition metal complexes.

Table I

^{13}C Chemical Shifts in *cis*-$M(CO)_4(ER_3)_2$ Derivatives[a]

Compound	CO_{ax}		CO_{eq}	Me	Temp. °K
$Fe(CO)_4(SiMe_3)_2$	208.50		207.64	7.50	183[b]
		208.07		7.61	298[b]
		207.96		7.71	301
$Fe(CO)_4(SiMe_2Cl)_2$	205.70		203.27	12.09	253
		204.53		12.30	303
$Fe(CO)_4(SiMeCl_2)_2$	202.46		200.14	17.16	253
	202.46		200.04	16.89	303
$Fe(CO)_4(SiCl_3)_2$	199.44		197.34	...	303
	199.71		197.88	...	308[b]
$Fe(CO)_4(GeMe_3)_2$	208.94		207.15	6.96	223[b]
		208.07		7.34	293[b]
$Ru(CO)_4(SiMe_3)_2$	198.53		191.62	7.72	253
$Ru(CO)_4(SiMe_2Cl)_2$	194.54		188.12	12.36	303
$Ru(CO)_4(SiMeCl_2)_2$	190.60		185.42	17.37	305
$Ru(CO)_4(SiCl_3)_2$	187.46		183.63	...	293[b]

continued.....

Table I (continued)

Compound	CO_{ax}	CO_{eq}	Me	Temp. °K
$Ru(CO)_4(GeMe_3)_2$	198.04	191.30	7.02	303
$Ru(CO)_4(SnMe_3)_2$	197.39	192.27	-4.74	300
$Ru(CO)_4(PbMe_3)_2$	196.96	192.21	-0.86	303
$Os(CO)_4(SiMe_3)_2$	181.48	172.58	6.74	303
$Os(CO)_4(SiMe_2Cl)_2$	177.54	169.61	11.44	303
$Os(CO)_4(SiMeCl_2)_2$	173.71	167.23	16.51	303
$Os(CO)_4(GeMe_3)_2$	180.40	171.88	5.24	293
$Os(CO)_4(SnMe_3)_2$	179.05 179.21	172.26 172.58	-6.63 -6.69	303 293[b]
$Os(CO)_4(PbMe_3)_2$	179.32	172.31	-3.18	303

[a] Chemical shifts in ppm downfield from TMS. Solvent is toluene-d_8 except as noted.

[b] CD_2Cl_2 as solvent.

Table II

^{13}C Chemical Shifts in *cis*-$Fe(CO)_4(SnR_3)_2$ Derivatives[a]

Compound	CO_{ax}		CO_{eq}	C-1	C-2	C-3	C-4	Temp. °K
$Fe(CO)_4(SnMe_3)_2$	207.86		208.07	-3.67	-	-	-	163[b]
		207.75		-3.29	-	-	-	273[c]
		207.75		-3.24	-	-	-	293[b]
		208.07		-2.75	-	-	-	300
$Fe(CO)_4(SnEt_3)_2$	207.42		208.40	6.31	11.81	-	-	193
		207.91		7.44	11.60	-	-	303
$Fe(CO)_4(SnPr_3)_2$	207.64		208.56	17.26	21.36	19.58	-	193
		208.13		18.77	21.36	19.15	-	303
$Fe(CO)_4(SnBu_3)_2$	207.64		208.56	14.54	29.86	28.16	14.21	193
		208.13		15.77	29.99	27.78	13.70	303
$Fe(CO)_4(SnPh_3)_2$	206.72		206.45	140.69	137.08	128.93	129.35	183
		206.78		141.56	137.08	128.82	129.15	303
$Fe(CO)_4(SnCl_3)_2$	195.29		195.18	-	-	-	-	293

[a] Chemical shifts in ppm downfield from TMS. The carbon attached to tin is taken as number one. Solvent CD_2Cl_2 except as noted.

[b] CD_2Cl_2 : methylcyclohexane-d_{14} (1:1) as solvent.

[c] Toluene-d_8 solvent.

Table III

^{13}C Chemical Shifts in *trans*-$M(CO)_4(ER_3)_2$ Derivatives[a]

Compound	CO	Me	% Trans	Temp °K
$Fe(CO)_4(SiMeCl_2)_2$	203.59	18.78	8[d]	253
$Fe(CO)_4(SiCl_3)_2$	199.49 199.12	... ...	21[d] 19[d]	308[b] 303
$Ru(CO)_4(SiMeCl_2)_2$	191.14	18.94	12[c]	305
$Ru(CO)_4(SiCl_3)_2$	187.03	...	...[e]	293[b]
$Os(CO)_4(SiMe_3)_2$	186.17	8.04	63[c]	303
$Os(CO)_4(SiMe_2Cl)_2$	179.53	13.38	60[c]	303
$Os(CO)_4(SiMeCl_2)_2$	174.36	19.26	...[e]	303[b]
$Os(CO)_4(SiCl_3)_2$	170.31	...	...[f]	303[b]
$Os(CO)_4(GeMe_3)_2$	184.99	6.21	20[c]	293
$Os(CO)_4(SnMe_3)_2$	185.47 185.50	-6.75 -6.78	23[d] 20[d]	303 293[b]

[a] Shifts in ppm downfield from TMS. Solvent is toluene-d_8 except as noted. % trans refers to mole percent of that isomer present in solution at time of measurement.

[b] CD_2Cl_2 solvent.

[c] Estimated from integrated areas of methyl resonances in ^{13}C spectrum.

[d] Estimated from integrated areas of carbonyl resonances in ^{13}C spectrum.

[e] Measurements on pure trans isomer after separation from cis; rate of isomerization negligible at temperature of measurement.

[f] Pure trans isomer; cis isomer unknown.

Table IV

^{13}C Chemical Shifts in R_3EX Derivatives[a]

Compound	C-1	C-2	C-3	C-4
Me_3SnCl[b]	-0.70	-	-	-
Me_3SnCl[c]	0.0	-	-	-
Me_3SnCl[d]	-0.7	-	-	-
Et_3SnCl[b]	9.3	9.9	-	-
Pr_3SnCl	20.66	19.58	18.45	-
Bu_3SnCl	17.75	28.16	27.08	13.70
Ph_3SnCl	137.67	136.38	129.44	130.79
Ph_3SnCl[c]	137.5	136.1	129.2	130.5
Me_3PbCl	20.55			

[a] Chemical shifts in ppm downfield from TMS. The carbon attached to E is taken as number one. Solvent is CD_2Cl_2. Temperature is 303°K except as noted.

[b] Temperature is 300°K.

[c] Value taken from T. N. Mitchell, J. Organometal. Chem., **59**, 189 (1973). Solvent is $CDCl_3$.

[d] Value taken from G. Singh, J. Organometal. Chem., **99**, 251 (1975). Solvent is $CDCl_3$.

The range of ^{13}CO shifts is 209-195 ppm for iron, 199-183 for ruthenium, and 181-167 ppm for osmium derivatives. This upfield shift on descending the group is typical of metal carbonyl derivatives,[60] and was also observed for the closely related chelate complexes $M(CO)_4(Me_2SiCH_2CH_2SiMe_2)$[92] (Chapter VI).

In the *cis*-$M(CO)_4(EMe_3)_2$ derivatives, keeping the EMe_3 ligand constant, the difference between axial and equatorial ^{13}CO shifts increases as the central atom changes from Fe to Ru to Os (Table I). On the other hand, holding M constant, the axial-equatorial separation decreases as E is varied from Si to Pb. In the series *cis*-$M(CO)_4(SiMe_{3-n}Cl_n)_2$, for a given M, axial-equatorial separation decreases with an increase in n. As n is increased monotonically from 0 to 3, the remaining methyl carbon resonance undergoes a regular downfield shift, of about 5 ppm, while the axial and equatorial carbonyl resonances undergo a regular upfield shift, of about 3 ppm.

It is of interest to observe that among the cis derivatives of Table I, a change in the non-carbonyl ligand often causes a greater change in the shift of the axial carbonyl than in that of the equatorial carbonyl.

In the *cis*-$Fe(CO)_4(SnR_3)_2$ derivatives (Table II), there is practically no variation in the carbonyl chemical shifts as R is changed from Me to Bu. A small upfield shift is observed for the *cis*-$Fe(CO)_4(SnPh_3)_2$ derivative.

The carbon atoms of the organic substituent show much larger variation. Assignment of these resonances was carried out using the off-resonance decoupling technique and comparison of the carbon-tin coupling constants in these compounds with those of the parent halostannanes.

Comparing the chemical shifts of the parent stannanes with those in the iron complexes, an upfield shift of about 3 ppm for C-1 is observed upon complexation. Other carbons of R show a downfield shift of about 2 ppm for C-2 and 1 ppm for C-3 and C-4.

Table III lists the percent of trans isomer present as nmr measurements were made. These values are approximate only, having been obtained by integration of the ^{13}C nmr spectra. They do not necessarily represent equilibrium values at the temperature in question. Those compounds of Table I or Table II for which no reference is made to a trans isomer in Table III can be assumed to be completely cis, within the limits of detection of ^{13}C nmr, under the conditions stated.

The ^{13}CO resonance of the trans isomer is usually at lower field than the axial ^{13}CO resonance of the cis isomer (as shown in Figure 1 and 3). The compounds $Fe(CO)_4(SiCl_3)_2$ and $Ru(CO)_4(SiCl_3)_2$ are exceptions, in which the ^{13}CO resonance of the trans isomer is at slightly higher field than the axial cis resonance.

2.3 "Interpretation" of ^{13}C NMR Chemical Shifts of Carbon Atoms Directly Bound to Transition Metals.

2.3.1 The State of the Art

Although a great deal of interest has been devoted to the interpretation and calculation of ^{13}C chemical shifts, the end result was mainly controversy.

Traditionally, equations for calculation of ^{13}C chemical shifts (or total screening, σ) contain two terms denoted "diamagnetic" and "paramagnetic" contributions

$$\sigma = \sigma_d + \sigma_p$$

where σ_d reflects the screening due to electrons in the electronic ground state and σ_p the screening due to the mixing of ground and excited states under the influence of the magnetic field. This is an artificial distinction which has meaning only in the context of the computational technique used.[116]

Usually, if not generally, the diamagnetic contribution, σ_d, is quickly dismissed from the discussion of the changes in screening because variations in it are small.

The dominating factor governing ^{13}C chemical shifts changes in hydrocarbons is the paramagnetic term. According to Pople's LCAO-MO theory of diamagnetism,[117,118] the paramagnetic term is given by:

$$\sigma_p = - \frac{e^2 \hbar^2}{2m^2c^2(\Delta E)} \langle r_{2p}^{-3} \rangle \left\{ Q_{AA} + \sum_{B \neq A} Q_{AB} \right\}$$

where ΔE is the average excitation energy, r is the radius of the carbon 2p-orbitals, and the Q terms contain elements of the charge density and bond order matrix.

Calculations of ^{13}C chemical shifts based on Pople's formalism have met some success in that they reproduced the main features of the experimental data, but due to the approximate nature of this theory, the accuracy was rather poor (e.g., errors of about 50% were observed for aromatic hydrocarbons).[59]

^{13}C chemical shifts of the carbonyl group in organic compounds of the type 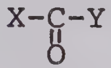 $X-\underset{\underset{O}{\|}}{C}-Y$ were found to correlate with the CO π-bond polarity.[119] This was explained using the above formula. Electron withdrawing substituents decrease the π-bond polarity, thus increasing r, and result in upfield shifts. However, these correlations became linear after certain "corrections" were applied to carbonyl shieldings. The experimental data show no simple correlation of shielding with polarity parameters of X and Y.[59]

Nevertheless, the above treatment was applied to metal carbonyls, and it appeared that carbonyl carbons are deshielded as the metal→carbonyl π back-donation increases.[60,109-112] This theory received some theoretical support.[120] An increase in the metal→carbonyl π back-donation leads to a decrease in the energy of the lowest electronic excited state.[121] This produces a decrease in

ΔE, and therefore causes a deshielding of the carbonyl resonance.

A linear relationship has been found between the Cotton - Kraihanzel (CK) force constants (k) and the 5σ and 2π carbonyl occupancies, which for the series $M(CO)_{6-n}X_n$ (M = Cr, Mn, Fe; X = Cl, Br; n = 1, 2) has the form[7]

$$k = -9.50\ (5\sigma) - 11.73\ (2\pi) + 35.81$$

Many have tried to correlate CK force constants with 2π occupancies alone, or with ^{13}C chemical shifts (page 32). Although in numerous cases linear plots of CK force constants versus ^{13}C chemical shifts were obtained for very closely related compounds, the correlation broke down when extended to ligands with different bonding characteristics or to complexes having a different transition metal.[85,101,107,109,113] For example, a plot of CK force constants versus the ^{13}CO chemical shift of $Re(CO)_5X$ derivatives (X = Me, Ac, Ph, PhCO, Br, $SiCl_3$, $SiMe_3$, $GeMe_3$, $SnMe_3$ and $PbMe_3$) showed a linear correlation for the radial carbonyls but no correlation for the axial carbonyls.[101] When X was replaced by a two-electron donor, in $[Re(CO)_5NCMe][PF_6]$, the radial carbonyl correlation broke down. Also, although the CK force constants for $Cr(CO)_6$, $Mo(CO)_6$, and $W(CO)_6$ are practically identical within experimental error (16.49, 16.52 and 16.41 mdyn/Å),[103] their ^{13}CO chemical shifts are very much different,

212.5, 202.0, and 192.1 ppm,[104] respectively. Correlations of this type and their utility is questionable.

Changes in the diamagnetic term, as given by Lamb's formula,[122]

$$\sigma_d = \frac{e^2}{3mc^2} \sum_i \langle r_i^{-1} \rangle$$

where $\langle r_i^{-1} \rangle$ is the mean inverse distance of electron i from the nucleus and the summation is over all electrons on the nucleus of interest, accounted for about one twentieth of the total ^{13}C shift changes in hydrocarbons.[59]

However, in the calculation of chemical shifts of carbons bound to a transition metal, the diamagnetic term, σ_d, as given by Flygare and Goodisman's formula,[123]

$$\sigma_d(k) = \sigma_d(\text{free atom}) + \frac{e^2}{3mc^2} \sum_\alpha \frac{Z_\alpha}{r_\alpha}$$

becomes very significant. Here Z_α is the atomic number of the α nucleus, and r_α is the distance from the kth nucleus to the αth nucleus.

Estimates of the second term in the above expression afforded values of 120, 190, and 340 ppm for a carbon bound to iron, ruthenium, and osmium, respectively.[124] These values will vary between complexes.[124] Application of Flygare and Goodisman's formula to $Cr(CO)_6$, $Mo(CO)_6$, and $W(CO)_6$ yields values of 625, 700, and 845 ppm for the total diamagnetic shielding in these complexes.[125]

Therefore, treatments of the total screening in transition metal carbonyls in terms of the paramagnetic contribution alone are almost certainly inadequate. In the coordination sphere of a transition metal simple explanations are unlikely to be valid.[124]

More elaborate methods, based on *ab-initio* molecular orbital calculations of chemical shifts, are now available.[126] Their accuracy is better (the mean standard deviation is approximately 5 ppm), but still not good enough to reflect subtle changes in molecular structure.

Nonetheless, the π back-bonding theory of chemical shifts in metal carbonyls has its value as a qualitative means of explaining ^{13}C chemical shifts, and lately has received some support.[85,125] For lack of anything better, this theory should not be abandoned, but its limitations should be realized. Perhaps at this stage some pessimism about the present state of the art of the ^{13}C shielding theory is warranted.

2.3.2 "Interpretation" of ^{13}C NMR Chemical Shifts in $M(CO)_4(ER_3)_2$ Derivatives.

Despite the foregoing limitations, the π back-bonding theory may be used to rationalize some of the data presented in Tables I - III.

One example is the observation that the ^{13}CO chemical shift of the equatorial carbonyls in *cis*-$Os(CO)_4(SiMe_3)_2$ is at 172.58 ppm, while the shift of the axial

carbonyl in the related molecule $Re(CO)_5SiMe_3$ is 182.9 ppm. In the former, the oxidation state of osmium is 2, while for rhenium it is 1. It is well established that π back-bonding decreases along an isoelectronic series such as $Cr(CO)_5Br^-$, $Mn(CO)_5Br$, and $Fe(CO)_5Br^+$ as the oxidation state of the metal increases.[7] Thus it is reasonable to suppose that there is less π back-bonding in $Os(CO)_4(SiMe_3)_2$ than in $Re(CO)_5SiMe_3$, so the carbonyl groups in the rhenium derivative are expected to resonate at lower field than in the osmium derivative. A similar trend is observed in other pairs of related rhenium and osmium derivatives, as well as in related manganese and iron compounds (see Table XII).

A second trend capable of rationalization by the π back-bonding theory is observed in the series $M(CO)_4(SiMe_{3-n}Cl_n)_2$. It is reasonable to expect that π back-bonding to the carbonyls will decrease as the electronegativity of the group IV ligand increases, that is to say as n increases; this is also borne out by the increased carbonyl stretching frequencies as n increases.[101] It is observed that the carbonyl carbons become more shielded as n increases.

However, this theory does not account for the higher field position of the carbonyl carbon trans to the one-electron donor in *cis*-$M(CO)_4(ER_3)_2$ and $M'(CO)_5ER_3$ complexes; indeed, in terms of the conventional view of

relative amounts of π back-bonding,[103] the prediction would be the reverse of the observed order.

3. Experimental Section

3.1 Nmr Instrumentation and Techniques.

Spectra were recorded in the pulse Fourier transform mode of operation on a Bruker HFX-90 - Nicolet 1085, or a modified Varian HA-100 spectrometer interfaced to a Digilab FTS/NMR-3 Data System and pulse unit. The instruments operated at 22.6 and 25.1 MHz respectively.

The Bruker instrument, with which the majority of the spectra were obtained, was equipped with a single coil; a pulse width of 6-8 μsec (90° pulse = 27 μsec) was used with a dwell time of 100 μsec and an acquisition time of 0.8 sec. Spectra were recorded using proton broad-band decoupling conditions. The number of scans was usually one thousand (1K). However, in the cases where exchange was observed or in order to determine coupling constants as many as 8- or 12K pulses were taken. The number of data points (channels) was 8K and the sweep width was 5000 Hz. This afforded a digital resolution of 0.06 ppm or 1.25 Hz.

The temperature unit of the instrument was calibrated with a thermocouple held coaxially in the spinning sample

tube partially filled with solvent. The temperature was controlled by means of a thermocouple situated just beneath the sample.

The nmr solvent and lock was either toluene-d_8 or, for the less soluble compounds, CD_2Cl_2. Tetramethylsilane (TMS) was employed as an internal standard or, where this was not possible, the peaks were referenced to the quaternary carbon of toluene-d_8 and converted to the TMS scale by taking the chemical shift of this latter peak as 137.46 ppm. Chemical shifts downfield from TMS are taken as positive.

Approximately 2 ml of a 0.7 - 1.0 M solution contained in a 10 mm (o.d.) nmr tube was used to obtain the ^{13}C nmr spectrum of the compound in question. For the less soluble compounds, a relaxation agent,[68] tris(acetylacetonato)chromium(III) (approximately 10 mg) was employed; no relaxation reagent was used in low temperature experiments.[127] In one experiment the ^{13}C nmr spectrum of $Os(CO)_4(SiMe_3)_2$ was recorded with and without $Cr(acac)_3$; no differences in the chemical shifts of the resonances were noted. The nmr tubes containing the particularly air-sensitive compounds $Fe(CO)_4(GeMe_3)_2$ and $Ru(CO)_4(SiMe_3)_2$ were sealed under vacuum before spectra were recorded. Spectra of $Fe(CO)_4(SnMe_3)_2$ in $CF_2HCl:CD_2Cl_2$ were also measured in an evacuated sealed tube.

3.2 Sources of Compounds

Reactions were carried out under an atmosphere of dry, oxygen-free argon or nitrogen. Hydrocarbon solvents were distilled from $LiAlH_4$ and saturated with argon or nitrogen prior to use. Deuterated nmr solvents were dried over $CaCl_2$ or molecular sieve (type 4A). Carbonyls of ruthenium[128] and osmium[129] were prepared by literature methods. All other starting materials were commercially available and were used as received.

Of the compounds studied here the following have appeared in the literature before: $Fe(CO)_4(SiMe_3)_2$,[103*] $Fe(CO)_4(SiMeCl_2)_2$,[131†] $Fe(CO)_4(SiCl_3)_2$,[100] $Fe(CO)_4(SnMe_3)_2$,[132†] $Fe(CO)_4(SnPh_3)_2$,[133†] $Fe(CO)_4(SnCl_3)_2$,[134] $Ru(CO)_4(SiMe_3)_2$,[135†] $Ru(CO)_4(SiMeCl_2)_2$,[136†] $Ru(CO)_4(SiCl_3)_2$,[136] $Ru(CO)_4(GeMe_3)_2$,[137†] $Ru(CO)_4(SnMe_3)_2$,[136,138†] $Ru(CO)_4(PbMe_3)_2$,[139†] $Os(CO)_4(SiMe_3)_2$,[136,140] $Os(CO)_4(SiMe_2Cl)_2$,[136] $Os(CO)_4(SiMeCl_2)_2$,[136] $Os(CO)_4(SiCl_3)_2$,[136†] $Os(CO)_4(GeMe_3)_2$,[137†] $Os(CO)_4(SnMe_3)_2$,[136,140†] $Os(CO)_4(PbMe_3)_2$.[139†]

The preparation of the new compounds, $Fe(CO)_4(SiMe_2Cl)_2$,[†] $Fe(CO)_4(GeMe_3)_2$,[†] $Fe(CO)_4(SnEt_3)_2$,[†] $Fe(CO)_4(SnPr_3)_2$,[†] $Fe(CO)_4(SnBu_3)_2$,[†] and $Ru(CO)_4(SiMe_2Cl)_2$ along

---

[*] This compound was prepared by Dr. W. Jetz.

[†] This compound was prepared by Dr. R. K. Pomeroy.

with improved syntheses of some of the above complexes will be described shortly.[98,141] Attempts to prepare $Fe(CO)_4(PbMe_3)_2$ and $Os(CO)_4(CMe_3)_2$ were unsuccessful.[97] Compounds were characterized by elemental analysis, infrared, ^1H nmr and mass spectroscopy as well as the ^{13}C nmr spectra reported here.

The $M(CO)_4(EMe_3)_2$ compounds are, with the exception of $Fe(CO)_4(SiMe_3)_2$, air-sensitive liquids at room temperature and are very soluble in the solvents used.

3.3 Enrichment with ^{13}CO, General.

Some of the compounds were enriched with ^{13}CO because of their reduced solubility at low temperature or in order to clearly observe ^{13}C-Si or Sn satellites. The following compounds were enriched with ^{13}CO: $Fe(CO)_4(SiMe_3)_2$, $Fe(CO)_4(SiCl_3)_2$, $Fe(CO)_4(SnMe_3)_2$,† $Fe(CO)_4(SnBu_3)_2$, $Fe(CO)_4(SnPh_3)_2$,† *cis*-$Fe(CO)_4(SnCl_3)_2$, *cis*-$Ru(CO)_4(SiCl_3)_2$, $Os(CO)_4(SiMe_3)_2$,† and $Os(CO)_4(SnMe_3)_2$.†

The exchange of ^{13}CO with *cis*-$Ru(CO)_4(SiCl_3)_2$ has been described before.[94] Enriched *cis*-$Fe(CO)_4(SnCl_3)_2$ was prepared from ^{13}CO enriched - $Fe(CO)_5$.[142] The enrichment of the other complexes was similar and is only described in detail for *cis*-$Fe(CO)_4(SiMe_3)_2$.

---

† This compound was enriched with ^{13}CO by Dr. R. K. Pomeroy.

The ^{13}CO used was of 91-92% isotopic purity (Monsanto Research Corporation, Miamisburg, Ohio). Enriched carbon monoxide was manipulated in a glass vacuum system of conventional design by means of a Toepler pump. The reaction vessel consisted of a roundbottom quartz flask sealed to a condenser resulting in a total volume of approximately 60 ml. The vessel could be attached to the vacuum line by means of a ball joint. The unit was also fitted with a Teflon valve so that once filled with CO it could be transferred to other areas of the laboratory. Samples for infrared analysis could be withdrawn with the aid of a 1-ml syringe through a serum cap covering a side arm on the bulb.

Irradiation with ultraviolet light was usually required to bring about exchange with ^{13}CO. The bulb was positioned 3-15 cm from a 140 watt lamp (Engelhard-Hanovia Inc., Newark, N.J.) and cold water was passed through the condenser during irradiation.

Accurate isotope combination patterns were calculated using a program written by Drs. R. S. Gay and E. H. Brooks (formerly of this department); simulated patterns for varying ^{13}C content were compared with the observed mass spectrum to estimate the degree of enrichment. Mass spectra were taken with an Associated Electrical Industries MS-9 instrument, with the inlet system at room temperature.

Infrared spectra were recorded using a Perkin-Elmer 337 grating spectrometer with scale expansion and calibration with gaseous CO.

^{13}CO Enrichment of $Fe(CO)_4(SiMe_3)_2$.

In view of the very low solubility of the compound below about -40°, moderately high degrees of enrichment were required.

Freshly sublimed $Fe(CO)_4(SiMe_3)_2$ (400 mg) and *n*-heptane (10 ml) were placed in the exchange apparatus. The flask was then attached to a vacuum system having a Toepler pump for manipulation of ^{13}CO. After degassing the solution by several freeze-thaw cycles, the flask was cooled to -78° and ^{13}CO pumped in to a pressure of 800 mm Hg.

Exchange was performed at room temperature with stirring, and was followed by infrared spectra of samples removed through the serum cap. No ^{13}CO exchange was observed in the dark over a 12 hr period. Ultraviolet irradiation at a distance of 15 cm from a 140 watt lamp (Engelhard-Hanovia Inc., Newark, N.J., Model 616 A) resulted in exchange. Irradiation was interrupted after 100 min. while the atmosphere of ^{13}CO was replaced with fresh 91% enriched material. Irradiation was continued for 270 min., and the solution was syringed from the flask.

Solvent was removed under vacuum and the product was sublimed onto a water-cooled probe. From mass spectrometry it was estimated that the degree of enrichment was 35-40%.

CHAPTER III

CARBON-13 NMR STUDIES OF SIX-COORDINATE IRON, RUTHENIUM, AND OSMIUM CARBONYL DERIVATIVES WITH GROUP IV ELEMENTS. CARBON-13 COUPLING CONSTANTS.

1. Introduction

The great majority of ^{13}C nmr spectra are determined under proton "broad-band" decoupling conditions. This, of course, increases the signal to noise ratio; however, valuable ^{13}C - ^{1}H coupling constant information is lost. In organometallic chemistry many elements contain isotopes with spin of 1/2, and coupling to the neighbouring carbons may be observed. The proton decoupling does not affect these isotopes as they resonate at a different frequency from that of ^{1}H. Observation of coupling constants *via* ^{13}C nmr is difficult because of the low natural abundance of ^{13}C. In most cases, ^{13}C-enriched samples are required to detect coupling to nuclei such as ^{117}Sn, ^{119}Sn, ^{29}Si, or ^{57}Fe.

In this chapter the ^{13}C coupling constants in $M(CO)_4(ER_3)_2$ derivatives (M = Fe, Ru, Os; E = Sn, Pb; R = Me, Et, Pr, Bu, Ph, and Cl) will be given and discussed. Data from this chapter have been used already in Chapter II to assign the axial and equatorial carbonyl resonances in *cis*-$M(CO)_4(ER_3)_2$ derivatives, and will be

further mentioned in Chapter IV in the discussion of the stereochemical nonrigidity of these derivatives. Since the coupling constants given here were determined simultaneously with the ^{13}C chemical shifts, the experimental details have been given at the end of Chapter II.

2. Results and Discussion

In a *cis*-$M(CO)_4(ER_3)_2$ derivative, element E may couple to the equatorial carbon cis and trans to it, and to the axial carbon. The intensity of the axial carbon satellites is twice that of the equatorial carbon. In a *trans*-$M(CO)_4(ER_3)_2$ derivative, there is only one coupling constant involving E and the carbonyl carbons. All these possibilities are shown below

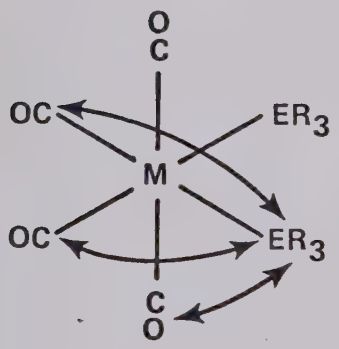

cis

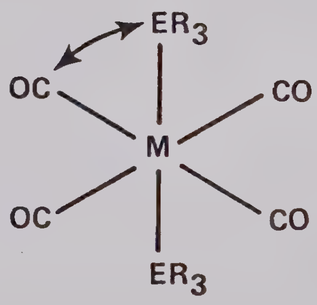

trans

and are demonstrated in the ^{13}C nmr spectrum of *cis*- and *trans*-$Os(CO)_4(SnMe_3)_2$, Figure 3 (page 28).

In addition, couplings from E to the carbons of the R group may be recognized. ^{13}C - $^{117,119}Sn$ coupling constants in *cis*-$Fe(CO)_4(SnR_3)_2$ derivatives are listed in Table V. Table VI contains ^{13}C - $^{117,119}Sn$ and ^{13}C - ^{207}Pb coupling constants in *cis*-$M(CO)_4(EMe_3)_2$ derivatives (M = Ru, Os; E = Sn and Pb). ^{13}C coupling constants in the parent stannanes and Me_3PbCl are given in Table VII.

Table V

Carbon-13 Coupling Constants in *cis*-$Fe(CO)_4(SnR_3)_2$ Derivatives[a]

	Carbonyl groups			Organic groups				
Compound	CO_{ax}-Sn	CO_{eq}-Sn_{cis}	CO_{eq}-Sn_{trans}	C-1	C-2	C-3	C-4	Temp °K
$Fe(CO)_4(SnMe_3)_2$	101	33	65	262,274	-	-	-	163[b]
	60			262,274				293[b]
$Fe(CO)_4(SnEt_3)_2$	98	26	62	-	-	-	-	193
	59			259,271	24	-	-	303
$Fe(CO)_4(SnPr_3)_2$	97	26	65	-	-	-	-	193
	59			252,263	21	67	-	303
$Fe(CO)_4(SnBu_3)_2$	93,98	25	61	-	-	-	-	193
	59			251,263	21	66	-	303
$Fe(CO)_4(SnPh_3)_2$	107,112	43	80	398,416	36	47	-	183
	66			397,416	38	50	-	303
$Fe(CO)_4(SnCl_3)_2$	224,235	37	170	-	-	-	-	303

Footnotes to Table V

[a] Values in Hertz. Values separated by commas indicate ^{117}Sn and ^{119}Sn couplings. Otherwise, the average value is given. The carbon attached to tin is taken as number one.

[b] CD_2Cl_2: methylcyclohexane-d_{14} (1:1) solvent.

Table VI

Carbon-13 Coupling Constants in *cis*-$M(CO)_4(EMe_3)_2$ Derivatives[a]

Compound	$^2J(E\text{-}CO_{ax})$	$^2J(E_{trans}\text{-}CO_{eq})$	$^2J(E_{cis}\text{-}CO_{eq})$	$^1J(E\text{-}CH_3)$	$^3J(E\text{-}CH_3)$
cis-$Ru(CO)_4(SnMe_3)_2$[b]	61	143	36	255,267	...
cis-$Os(CO)_4(SnMe_3)_2$[c]	54	118	40	266,278	...
cis-$Ru(CO)_4(PbMe_3)_2$	94	252	66	108	12
cis-$Os(CO)_4(PbMe_3)_2$	78	221	53	138	13

[a] Values in Hertz. M = Ru and Os; E = $^{117,119}Sn$ and ^{207}Pb. Temperature 253°K except as noted. Solvent toluene-d_8 except as noted.

[b] Neat liquid, 303°K.

[c] In CD_2Cl_2.

Table VII

Carbon-13 Coupling Constants in R_3EX Derivatives[a]

Compound	C-1	C-2	C-3	C-4
Me_3SnCl	364, 381	-	-	-
Me_3SnCl[b]	386	-	-	-
Me_3SnCl[c]	365, 379	-	-	-
Et_3SnCl[b]	352	26	-	-
Pr_3SnCl	326, 341	23	63	-
Bu_3SnCl	325, 341	24	65	-
Ph_3SnCl	592, 618	49	63	13
Ph_3SnCl[b]	610	49	68	12
Me_3PbCl	312	-	-	-

[a] Values in Hertz. Values separated by commas indicate ^{117}Sn and ^{119}Sn couplings. Otherwise, the average value is given. The carbon attached to E is taken as number one. Solvent is CD_2Cl_2. Temperature is 303°K.

[b] Values taken from T. N. Mitchell, J. Organometal. Chem., 59, 189 (1973). Solvent is $CDCl_3$.

[c] Values taken from G. Singh, J. Organometal. Chem., 99, 251 (1975). Solvent is $CDCl_3$.

The two-bond coupling of the group IV atom to ^{13}CO are believed to be the first reported,[97] with the exception of ^{13}C-Fe-^{29}Si coupling found for $Fe(CO)_4(SiMe_3)_2$ (Chapter IV).[96]

Coupling to ^{117}Sn and ^{119}Sn could only be resolved in the case of methyl groups directly bonded to tin, or when the coupling constant was close to or greater than 100 Hz. The ratio of the ^{117}Sn-^{13}C and ^{119}Sn-^{13}C coupling constants is equal to 0.956, the ratio of the nuclear magnetic moments of the tin isotopes.

Although $^2J(E\text{-}CO_{ax})$ was unambiguously defined by satellite intensities, $^2J(E_{trans}\text{-}CO_{eq})$ and $^2J(E_{cis}\text{-}CO_{eq})$ could not be experimentally distinguished, and it was assumed that the larger was due to trans coupling, i.e., $^2J(E_{trans}\text{-}CO_{eq})$. For the ruthenium and osmium derivatives (Table VI), the value of the trans coupling constant was much larger than the other two. However, for the *cis*-$Fe(CO)_4(SnR_3)_2$ derivatives (Table V), $^2J(E\text{-}CO_{ax})$ was the largest.

This may be the consequence of a severe distortion of *cis*-$Fe(CO)_4(SnR_3)_2$ derivatives from octahedral geometry, as has been found in the solid state structure of *cis*-$Fe(CO)_4(SiMe_3)_2$[96] and *cis*-$Fe(CO)_4(SnPh_3)_2$[98] (see Chapter V). The possibility of "through-space" spin-spin coupling[143-145] in the distorted complex cannot be ruled out.

The magnitude of the $^{117,119}Sn-^{13}CO$ coupling constants is essentially the same for the series *cis*-$Fe(CO)_4(SnR_3)_2$ (R = Me, Et, Pr, and Bu); however, a small increase is observed for *cis*-$Fe(CO)_4(SnPh_3)_2$. It is interesting to note that two of the coupling constants in *cis*-$Fe(CO)_4(SnCl_3)_2$ are twice those in the other iron-tin complexes.

In Table V the value of the $Sn-^{13}CO$ coupling constant at room temperature is also given. At this temperature, the carbonyl groups become equivalent, and only one $Sn-^{13}CO$ coupling is observed. This will be discussed further in Chapter IV.

Two $E-^{13}CH_3$ coupling constants are possible for *cis*-$M(CO)_4(EMe_3)_2$ molecules, namely the one- and three-bond types. These were observed in the lead derivatives (Table VI), where $^3J(^{207}Pb-^{13}CH_3)$ was approximately one tenth the magnitude of $^1J(^{207}Pb-^{13}CH_3)$. No three-bond couplings were observed for the tin analogs despite a careful search.

In the iron complexes, the $^{13}C-Sn$ coupling constants of the organic group are readily observed and $^2J(^{13}C-C-Sn)$ is approximately one tenth of $^1J(^{13}C-Sn)$. The three-bond $^{13}C-Sn$ coupling is larger than the two-bond coupling. No four-bond $^{13}C-Sn$ coupling was observed.

The one-bond $^{13}C-Sn$ couplings are about 100 Hz larger in the parent stannanes (Table VII); although, the two-bond and three-bond couplings are about the same as in the

iron-tin complexes. Ph_3SnCl is an exception in that $^1J(^{13}C-Sn)$ is 200 Hz larger than the value observed in *cis*-$Fe(CO)_4(SnPh_3)_2$; also, $^4J(^{13}C-Sn)$ is large enough to be clearly resolved in Ph_3SnCl.

In Tables V-VII the absolute value of the coupling constants is given; no attempt has been made to determine the sign of these coupling constants. However, it is known that in $SnMe_4$[146,147] and in $SnEt_4$,[148] the one-bond ^{13}C-Sn coupling constant is negative and the two-bond coupling is positive.

2.1 The Theory of ^{13}C Spin-Spin Couplings

The theory of spin-spin couplings, as developed by Ramsey,[149] expresses the coupling as the sum of three terms: a) the Fermi contact, b) the dipole-dipole interaction between the nuclear and electronic magnetic moments, J(dipole), and c) the interaction of the magnetic field of the nuclear dipole with the orbital magnetic moment of the electron, J(orb).

The Fermi contact term is usually considered to be dominant in the coupling between directly bonded nuclei,[150,151] although the second term can make a significant contribution to the one-bond metal-carbon coupling.

A simplified Fermi contact term for $^2J(M-C-H)$[152,153] can be written as

$$^{2}J_{M\text{-}C\text{-}H} \propto \gamma_M \gamma_H (\alpha_{MC})^2 (\alpha_{HC})^2 \left(\frac{Z_M^*}{n_M}\right)^3 \left(\frac{Z_H^*}{n_H}\right)^3 \Delta E^{-1}$$

where γ's are nuclear gyromagnetic ratios, $(\alpha_{MC})^2$ and $(\alpha_{HC})^2$ are the fractional s characters of the orbitals of M and H respectively involved in bonding to carbon, Z_M^* and Z_H^* are the effective nuclear charges of these orbitals, n is the principal quantum number of the period to which the atom belongs, and ΔE is the average energy approximation term. The $(\alpha_{HC})^2$, n_H, and Z_H^* are equal to 1.

In *cis*-$Fe(CO)_4(SnR_3)_2$, $^{2}J(Sn\text{-}^{13}CO)$ increases with the substituent electronegativity $SnCl_3 > SnPh_3 > SnR_3$ (R = Me-Bu). This may be interpreted using Bent's rule,[154] according to which the s character tends to concentrate in orbitals directed toward the groups of lowest electronegativity. This causes an increase in the Fermi contact term and consequently in the coupling constant. Similarly, this would explain the much lower ^{13}C-E coupling constants in $M(CO)_4(ER_3)_2$ complexes as compared to the parent R_3ECl derivatives (E = Sn, Pb).

CHAPTER IV

DYNAMIC NUCLEAR MAGNETIC RESONANCE STUDIES OF SIX-COORDINATE IRON, RUTHENIUM AND OSMIUM CARBONYL DERIVATIVES WITH GROUP IV ELEMENTS.

1. Introduction

Intramolecular or polytopal rearrangements in six-coordinate transition metal complexes are rare, or at least, that was the general consensus up to about 1970. This was attributed to the "pervasive stability of the octahedron with respect to all alternative six-coordinate geometric forms."[53]

In 1970, the first unequivocal demonstration of a polytopal rearrangement in six-coordinate complexes, $Fe[P(OEt)_3]_4H_2$ and $Fe[PhP(OEt)_2]_4H_2$ was presented.[155] In subsequent publications, it was amply demonstrated that ML_4H_2 complexes (M = Fe and Ru, L = phosphite, phosphine) are a rich source of stereochemically nonrigid molecules.[156,157]

The mechanism proposed for the interconversion of these species,[156] and substantiated by detailed line-shape analysis,[156,157] is known as the "tetrahedral jump", and accommodates these highly distorted structures, as proven by X-ray diffraction studies.[158,159] However, a trigonal, or Bailar, twist could not be ruled out.[157]

In 1972, a report from this laboratory provided ^1H nmr data on the first stereochemically nonrigid six-coordinate transition metal carbonyl derivative, $Os(CO)_4(SiMe_3)_2$, for which cis and trans isomers interconvert rapidly in solution above 55°.[90]

It was anticipated that ^{13}C nmr spectroscopy would play a key role in the continuation of these studies. Since axial and equatorial carbonyl groups of a cis tetracarbonyl derivative can be distinguished, any process which involves their interchange at an appropriate rate may be recognized.

This chapter presents the results of a dynamic nuclear magnetic resonance study of an extensive series of $M(CO)_4(ER_3)_2$ type derivatives (M = Fe, Ru, Os; E = Si, Ge, Sn, Pb; R = organic group or halogen).

2. Results and Discussion

2.1 Spectroscopic Studies of $Fe(CO)_4(ER_3)_2$ in Solution

At 25°, the ^{13}C nmr spectrum of $Fe(CO)_4(SiMe_3)_2$ consists of a single carbonyl resonance at 208.07 ppm and a methyl resonance at 7.61 ppm (Table I, page 35). At -90°, the spectrum shows carbonyl peaks at 208.50 (assigned[97] as axial) and 207.64 ppm (assigned as equatorial) in addition to the methyl resonance at 7.50 ppm. The pattern of coalescence as the sample is warmed from -90° is shown in Figure 7. The low temperature limiting

spectrum is reached at -80° and the coalescence temperature is -55°. Spectra are completely reversible. The compound is stereochemically nonrigid.

The half-width of the carbonyl signals at -90° was 4.0 Hz, larger than the width of 2.6 Hz observed at -20°. We attribute this to a ^{13}C-^{13}C spin-spin coupling (the sample was 35-40% ^{13}CO enriched because of solubility problems below -40°) rather than to a viscosity effect since the half-width of the TMS signal was practically unchanged to -90°. In the simulation of the spectra, a low temperature limiting half-width of 2.6 Hz was employed. Line-shape analysis of seven spectra recorded between -40° and -70° led to the following activation parameters: $\Delta H^{\dagger} = 10.4 \pm 0.6$ kcal mol^{-1}, $\Delta S^{\dagger} = -2.3 \pm 2.6$ eu.

The free energy of activation for this rearrangement process can be calculated considering the chemical shift separation of the axial and equatorial resonances in the low temperature limiting spectrum (19.5 Hz) and the coalescence temperature (see Experimental Section). The $\Delta G^{\dagger}$ value (10.7 kcal mol^{-1}) is remarkably close to the one calculated from $\Delta H^{\dagger}$ and $\Delta S^{\dagger}$ values obtained from complete line-shape analysis (10.9 kcal mol^{-1}).

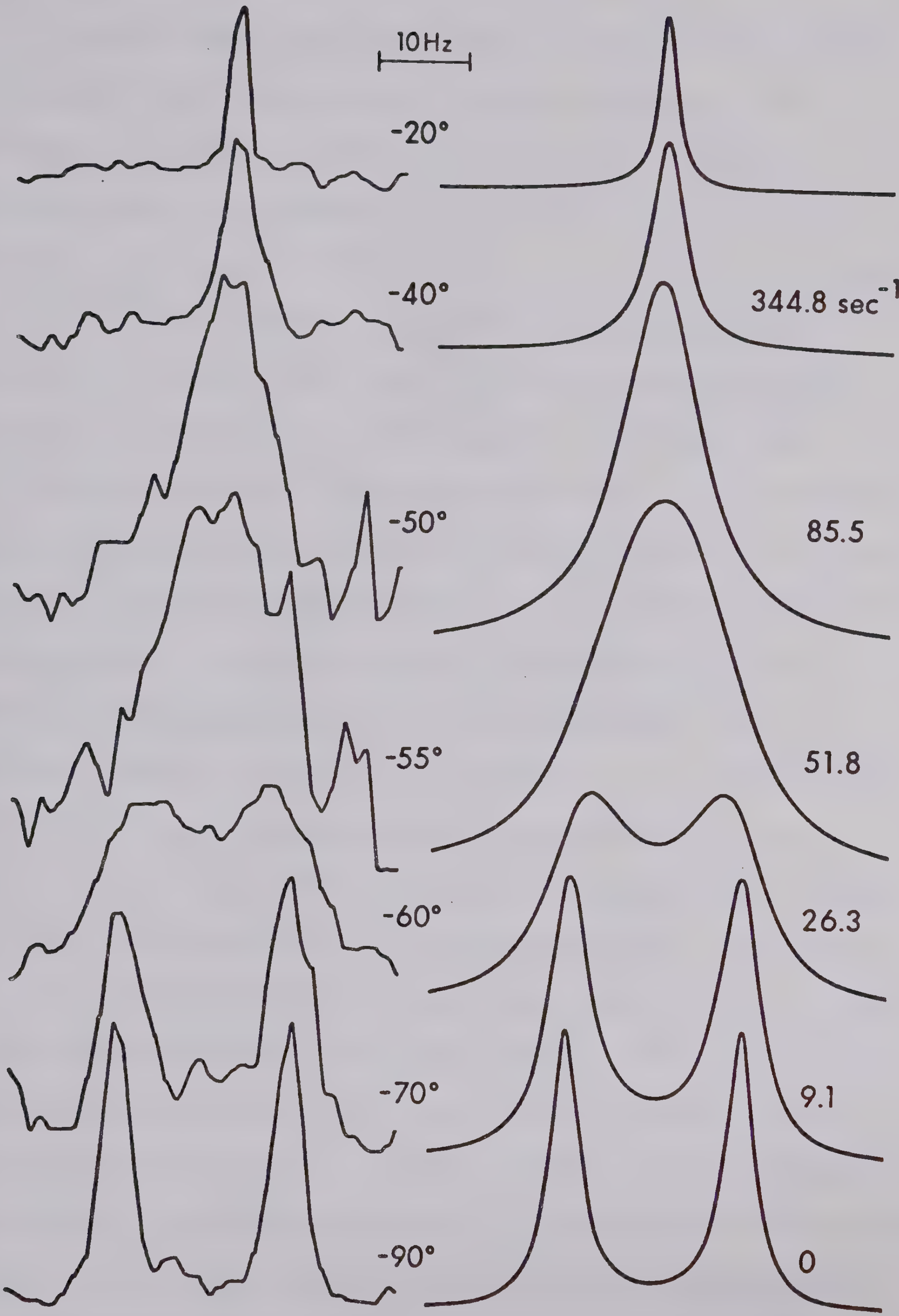

Figure 7. Variable temperature ^{13}C nmr spectra (carbonyl portion) of *cis*-$Fe(CO)_4(SiMe_3)_2$ in CD_2Cl_2 with corresponding simulated spectra at right. Sample is enriched with ^{13}CO.

A careful examination of the ^{13}C nmr spectrum above coalescence (25°) showed two satellite pairs of the carbonyl resonance at 208.07 ppm, as shown in Figure 8. The inner pair is assigned as $^{2}J(^{13}C\text{-}Fe\text{-}^{29}Si)$ = 5.3 Hz, and the outer pair as $^{1}J(^{13}C\text{-}^{57}Fe)$ = 25.1 Hz. This value of $^{1}J(^{13}C\text{-}^{57}Fe)$ compares favourably with the similar coupling in $Fe(CO)_5$ (23.4 Hz)[67] and (butadiene)$Fe(CO)_3$ (27.9 Hz).[85] Observation of ligand atom-ligand atom and ligand atom-metal atom spin-spin coupling in the high temperature spectrum of $Fe(CO)_4(SiMe_3)_2$ confirms that the carbonyl averaging process does not involve ligand-metal bond breaking. This is further substantiated by the failure of $Fe(CO)_4(SiMe_3)_2$ to exchange with ^{13}CO in solution without ultraviolet irradiation, and also by the $\Delta S^{\dagger}$ for the rearrangement, which is consistent with a process which is neither dissociative (large positive $\Delta S^{\dagger}$ expected) nor associative (large negative $\Delta S^{\dagger}$ expected).

The low temperature ^{13}C nmr spectrum of $Fe(CO)_4(SiMe_3)_2$ indicates cis geometry for this species. Evidence for this isomer comes from an X-ray study as well, which will be described in Chapter V. A likely mechanism for carbonyl interchange in *cis*-$Fe(CO)_4(SiMe_3)_2$ would involve its passage through a trans intermediate (all carbonyls equivalent) and return to the cis form. Had the low temperature limiting ^{13}C nmr spectrum shown a detectable amount of *trans*-$Fe(CO)_4(SiMe_3)_2$ in equilibrium with the cis isomer

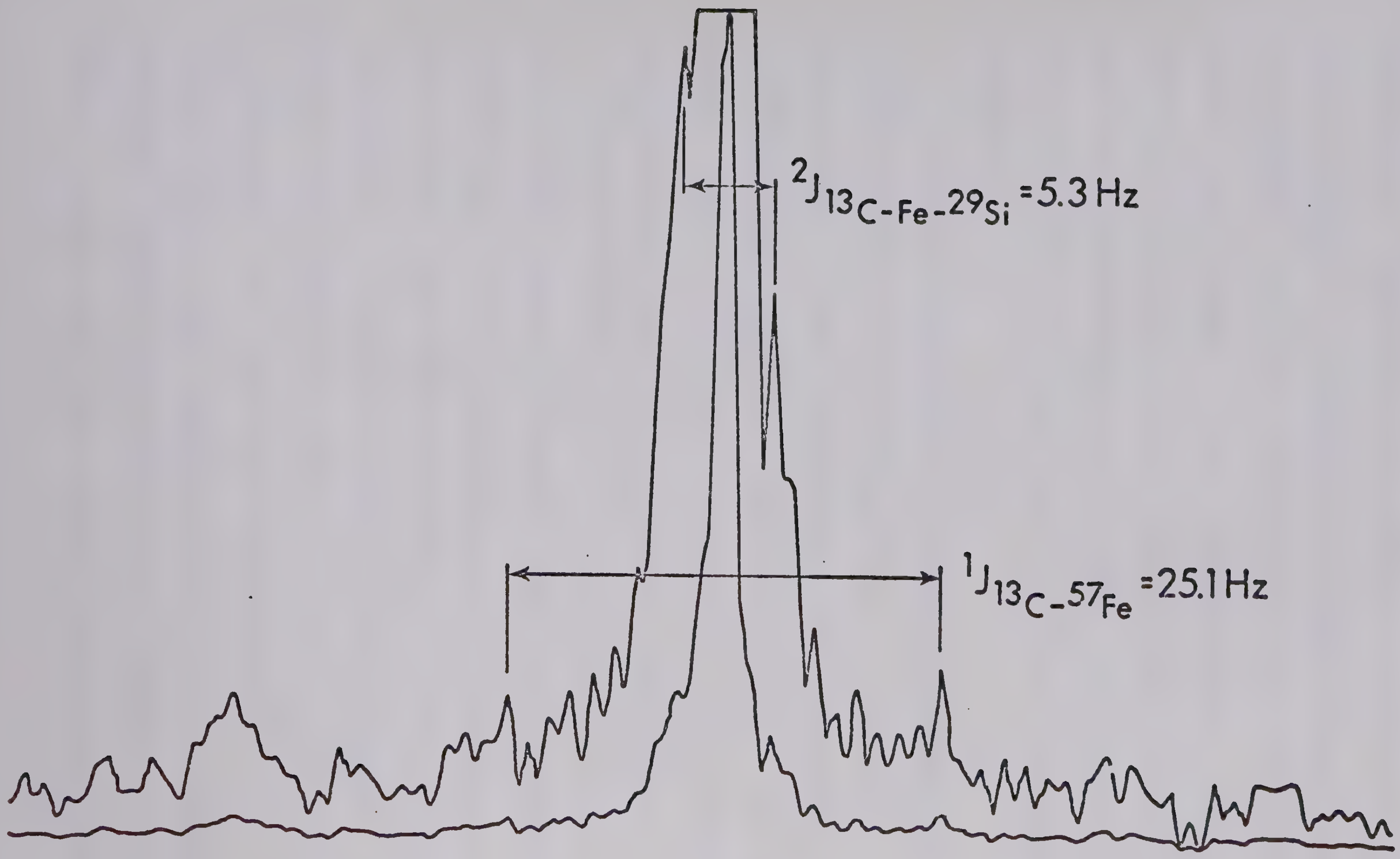

Figure 8. ^{13}C nmr spectrum (carbonyl portion) of *cis*-$Fe(CO)_4(SiMe_3)_2$ in CD_2Cl_2 at 25°. The sample is enriched with ^{13}CO.

(as is the case with the osmium analog)[90] its intermediacy in carbonyl interchange of the cis isomer would have been indicated by the coalescence of peaks of both isomers on warming. While our failure to detect any peak due to the trans isomer in the low temperature limiting spectrum means that no such positive indication is available, it is in no way inconsistent with a trans intermediate since it might merely reflect a small cis $\rightleftharpoons$ trans equilibrium constant.

A strong indication for a trans intermediate in the rearrangement of *cis*-$Fe(CO)_4(SiMe_3)_2$ comes from the variable temperature ^{13}C nmr study of the related chelate derivative, $Fe(CO)_4SiMe_2CH_2CH_2SiMe_2$. For this compound the trans form is inaccessible, and consequently the spectra showed stereochemical rigidity, on the nmr time scale, at 80°.[92]

Infrared spectra in solution provide evidence that significant amounts of trans isomer (about 20%) exist in equilibrium with its cis counterpart at room temperature. In Figure 9, the infrared spectrum of $Fe(CO)_4(SiMe_3)_2$[130] is compared with that of $Fe(CO)_4SiMe_2CH_2CH_2SiMe_2$, both spectra in *n*-heptane. For a *cis*-$M(CO)_4X_2$ derivative of C_{2v} symmetry four infrared active bands $(2A_1 + B_1 + B_2)$ are expected. This indeed was observed in the infrared spectrum of $Fe(CO)_4SiMe_2CH_2CH_2SiMe_2$ (Figure 9). It is apparent that four of the bands of *cis*-$Fe(CO)_4(SiMe_3)_2$

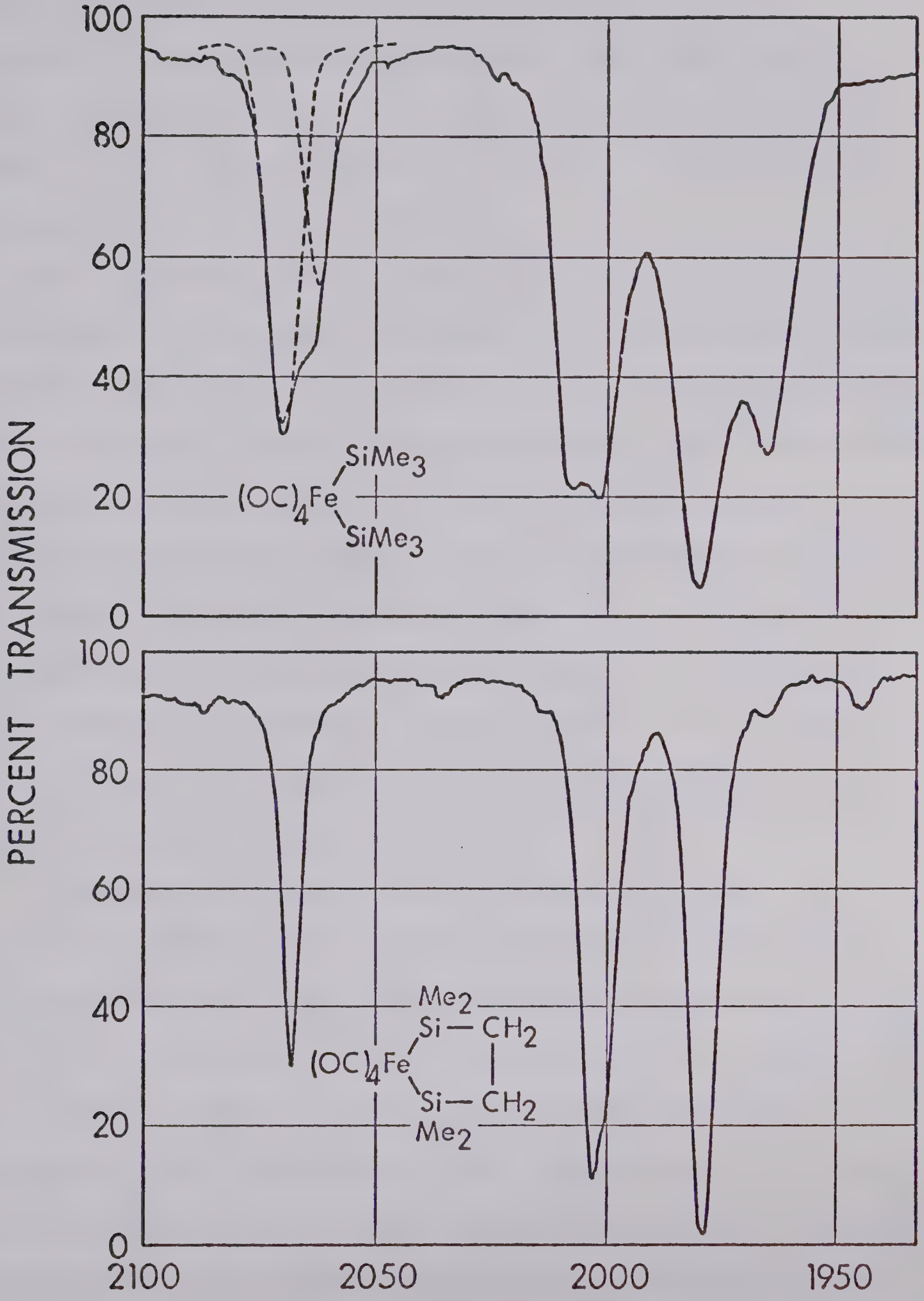

Figure 9. Infrared spectra of $Fe(CO)_4(SiMe_3)_2$ and $Fe(CO)_4SiMe_2CH_2CH_2SiMe_2$ in *n*-heptane.

(those at 2069, 2006, 2000, and 1979 cm^{-2}) are very similar to the bands of the chelate. The remaining two bands (at 2062 and 1964 cm^{-1}) are assigned to the trans isomer. The infrared spectrum of the trans isomer will be discussed further in Chapter V.

In *cis*-$Fe(CO)_4(SiMe_3)_2$ the coalesced signal at ambient temperature is the exact average of the two carbonyl signals at -90°. One way to rationalize this observation in light of the infrared results is to assume that the ^{13}CO chemical shift of the trans isomer is nearly the same as that of the mean of axial and equatorial ^{13}CO resonances of the cis isomer. However, given the error of ± 0.06 ppm in chemical shift, one could have 20% trans at room temperature, assuming a chemical shift of 208.50 (the chemical shift of the axial carbonyl in *cis*-$Fe(CO)_4(SiMe_3)_2$, see Table I), without exceeding that error limit.

The variable temperature ^{13}C nmr spectra of *cis*-$Fe(CO)_4(GeMe_3)_2$ are shown in Figure 10. Activation parameters derived from spectral simulation are $\Delta H^{\dagger}$ = 12.5 ± 0.4 kcal mol^{-1} and $\Delta S^{\dagger}$ = 0.6 ± 1.5 eu. The free energy of activation for the rearrangement process, calculated from the chemical shift separation of the axial and equatorial resonances in the low temperature limiting spectrum (40.5 Hz) and the coalescence temperature (-20°), is 12.1 kcal mol^{-1}. This value is very close to the one derived from $\Delta H^{\dagger}$ and $\Delta S^{\dagger}$ parameters obtained from complete

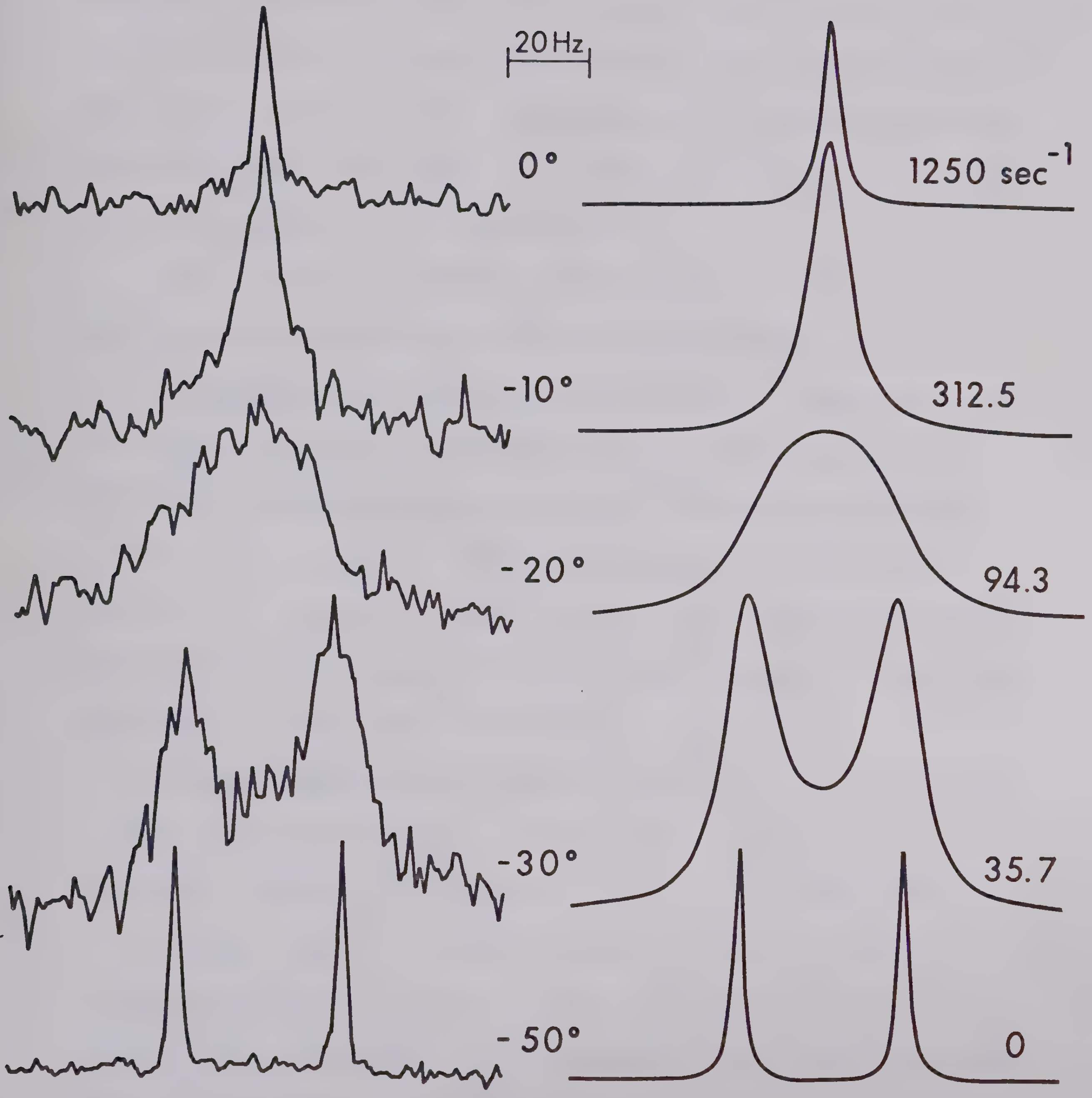

Figure 10. Variable temperature ^{13}C nmr spectra (carbonyl portion) of *cis*-$Fe(CO)_4(GeMe_3)_2$ in CD_2Cl_2 with corresponding simulated spectra at right.

line-shape analysis (12.3 kcal mol^{-1}). The infrared spectrum of $Fe(CO)_4(GeMe_3)_2$ shows four bands at room temperature, which is consistent with a cis geometry in solution. However, the infrared spectrum does not rule out the presence of the trans isomer since the band(s) expected for it may be coincident with bands assigned to the cis isomer (see page 112, where the infrared spectrum of $Fe(CO)_4(SiCl_3)_2$ is discussed).

All *cis*-$Fe(CO)_4(SnR_3)_2$ derivatives (R = Me, Et, Pr, Bu, and Ph) studied here were stereochemically nonrigid. At low temperatures, say below -50°, the ^{13}C nmr spectra of these derivatives shows two ^{13}CO resonances, due to the axial and equatorial carbonyls of the cis molecule, and the corresponding ^{13}CO-Sn satellites. The lower spectrum of Figure 11 presents the slow exchange limiting spectrum of *cis*-$Fe(CO)_4(SnMe_3)_2$; other examples were given in Figure 5 (page 31) and Figure 6 (page 33).

At low temperature broadening of the ^{13}C resonances due to the carbon atoms of the organic group in *cis*-$Fe(CO)_4(SnR_3)_2$ derivatives (R = Et, Pr, Bu) occur. For example, the half-width of the C-1 to C-4 peaks of *cis*-$Fe(CO)_4(SnBu_3)_2$ are 5.5, 4.3, 3.6 and 3.5 Hz, respectively, at -80°. It is probably that, at these low temperatures, there is restricted rotation about these bonds in these derivatives. A similar effect was noted for *cis*-$Fe(CO)_4(SnPh_3)_2$, only in this case the resonance

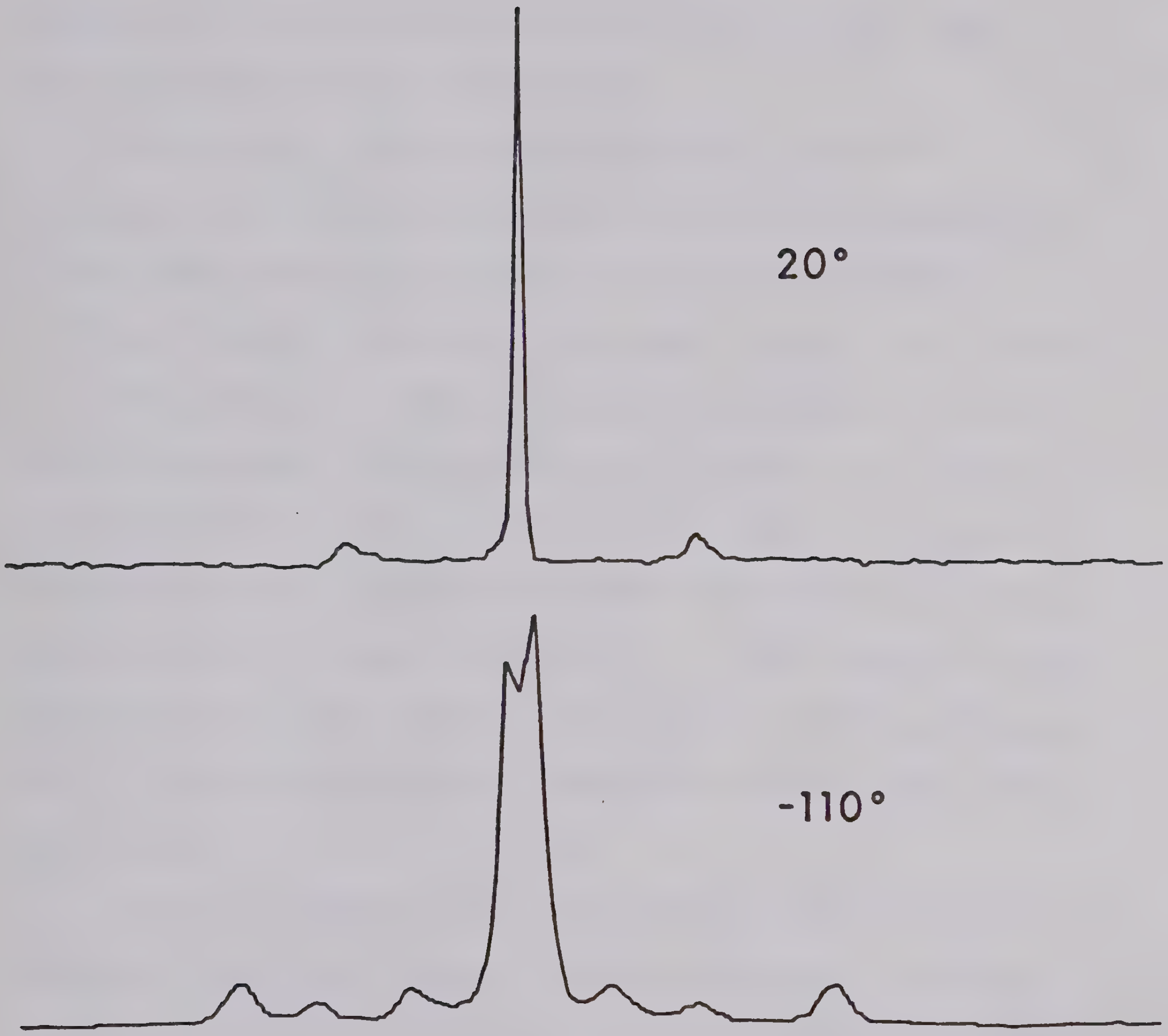

Figure 11. Variable temperature ^{13}C nmr spectra (carbonyl portion) of *cis*-$Fe(CO)_4(SnMe_3)_2$ in CD_2Cl_2 : methylcyclohexane-d_{14} (1:1). The sample is enriched with ^{13}CO.

due to C-1 remained sharp, at 2.5 Hz, whereas the C-2 and C-3 resonances broadened to 8.8 and 9.5 Hz, respectively, at -90°. The C-4 peak was obscured by the C-3 absorption. A possible explanation is a restricted rotation about the C-1, C-4 axis of the phenyl ring.

On warming, the two carbonyl peaks coalesce. Similarly the ^{13}CO-Sn couplings collapse but because of their large chemical shift separation do not appear - as a single doublet about the main peak - until 20° (Figure 11, top spectrum). The retention of coupling in the high temperature limiting spectrum of this, as well as other *cis*-$Fe(CO)_4(SnR_3)_2$ derivatives (Table V, page 58) establishes the crucial point that the averaging process occurs *without ligand dissociation*. This has been shown to be the case in a similar way for *cis*-$Fe(CO)_4(SiMe_3)_2$, and it is assumed that all compounds of this type behave similarly.

Infrared spectra of $Fe(CO)_4(SnR_3)_2$ derivatives in solution show four carbonyl stretching bands consistent with a cis geometry. In most cases the bands were broader than normal due to conformational effects.

2.2 The Mechanism of Rearrangement of *cis*-$M(CO)_4(ER_3)_2$ Complexes.

The ^{13}C nmr and infrared study of *cis*-$Fe(CO)_4(SiMe_3)_2$ presented above have suggested the intermediacy of the

trans isomer in the carbonyl rearrangement process.

Alternative axial-equatorial averaging processes which do not involve the trans form can readily be imagined. If the activation energy for any of these alternative processes is lower than that for isomerization, then averaging will occur in the cis molecule independently of the trans. A test of this possibility is afforded by several of the compounds discussed here, for which both cis and trans isomers are clearly observable in the ^{13}C nmr spectrum below coalescence. In such cases, *all three ^{13}CO peaks of the spectrum appeared to coalesce to a single peak at the same rate as the temperature was raised.* Qualitatively, there was no indication of earlier coalescence of the two peaks of the cis compound as would have been expected had an averaging mechanism of lower barrier been available in the cis isomer.

In order to show more quantitatively that the trans isomer is involved as an intermediate in the averaging process, a detailed study was made of the cis-trans isomer mixture of $Os(CO)_4(SiMe_3)_2$. This compound was chosen in view of the quality of the spectra obtainable and the fact that reasonable amounts of both isomers were present. Its thermal stability was such that spectra could be obtained up to 140°, where coalescence was well advanced. Moreover, the dynamics of the cis-trans isomerization of the compound had been investigated earlier by ^{1}H nmr.[90]

Carbon-13 spectra of the carbonyl and methyl regions of $Os(CO)_4(SiMe_3)_2$ between 30° and 140° are shown in Figure 12. The rate constants indicated are those which best simulate the methyl region; they lead to $\Delta H^{\dagger}$ = 16.4 ± 0.3 kcal mol^{-1}, $\Delta S^{\dagger}$ = -2.3 ± 0.8 e.u. for the cis to trans reaction, in satisfactory agreement with, although slightly smaller than, the values $\Delta H^{\dagger}$ = 17.9 ± 0.6 and 18.0 ± 0.6 kcal mol^{-1}, $\Delta S^{\dagger}$ = 1.6 ± 1.7 and 1.5 ± 1.7 e.u. obtained by ^{1}H nmr in dibromomethane,[90] and toluene-d_8, respectively.*

The rate data obtained from the methyl region were then used to calculate the spectra for the carbonyl region, under the assumption that axial-equatorial averaging occurs only *via* the trans isomer. The excellent agreement between observed and simulated spectra in the carbonyl region justifies the assumption, and must be regarded as strong evidence that this is the major, if not the only, process occurring for axial-equatorial averaging in the

---

* The ^{13}C nmr rate data were obtained over a larger temperature range (35°-110°) than ^{1}H nmr data (40°-100°). Also, the chemical shift difference between the cis and trans resonances was greater in the ^{13}C spectrum (33 Hz) than in the ^{1}H spectrum (10 Hz). Both of these factors could explain the smaller errors associated with the activation parameters derived from line-shape analysis of ^{13}C nmr spectra.[57]

cis isomer. Line-shape analysis reveals that any other process which interchanges the axial and equatorial carbonyls must have a rate less than about one tenth that for cis-trans isomerization; otherwise detectable broadening of the cis carbonyl signals would result. The upper limit of one tenth is based upon the following half width data for peaks of the cis isomer: observed at low temperature limit (-20°), 2.8 Hz; calculated at 55° based only upon cis to trans isomerization (rate 25.2 sec^{-1}), 10.8 Hz; observed at 55°, 9.0 Hz; calculated at 55° with a simultaneous axial-equatorial interchange (rate 2.5 sec^{-1}), 11.8 Hz.

Further proof for a trans intermediate in the carbonyl rearrangement of the cis isomer comes from the ^{13}C nmr studies of *cis*-$Fe(CO)_4(SnR_3)_2$ derivatives (R = Me, Et, Pr, Bu, and Ph). The weighted average of the three $Sn-^{13}CO$ coupling constants from the slow exchange spectrum is significantly higher than the value found in the fast exchange limiting spectrum. For example, in *cis*-$Fe(CO)_4$-$(SnMe_3)_2$, the weighted average of $Sn-^{13}CO$ coupling constants is 75 Hz; the observed value, at 20° and 40°, is 60 Hz. This discrepancy may be due to the presence of a small amount of *trans*-$Fe(CO)_4(SnR_3)_2$ at high temperatures. In *trans*-$Os(CO)_4(SnMe_3)_2$, $^2J(Sn-^{13}CO)$ is 31 Hz (Figure 3), smaller than any coupling constant in the cis isomer (Table VI, page 60).

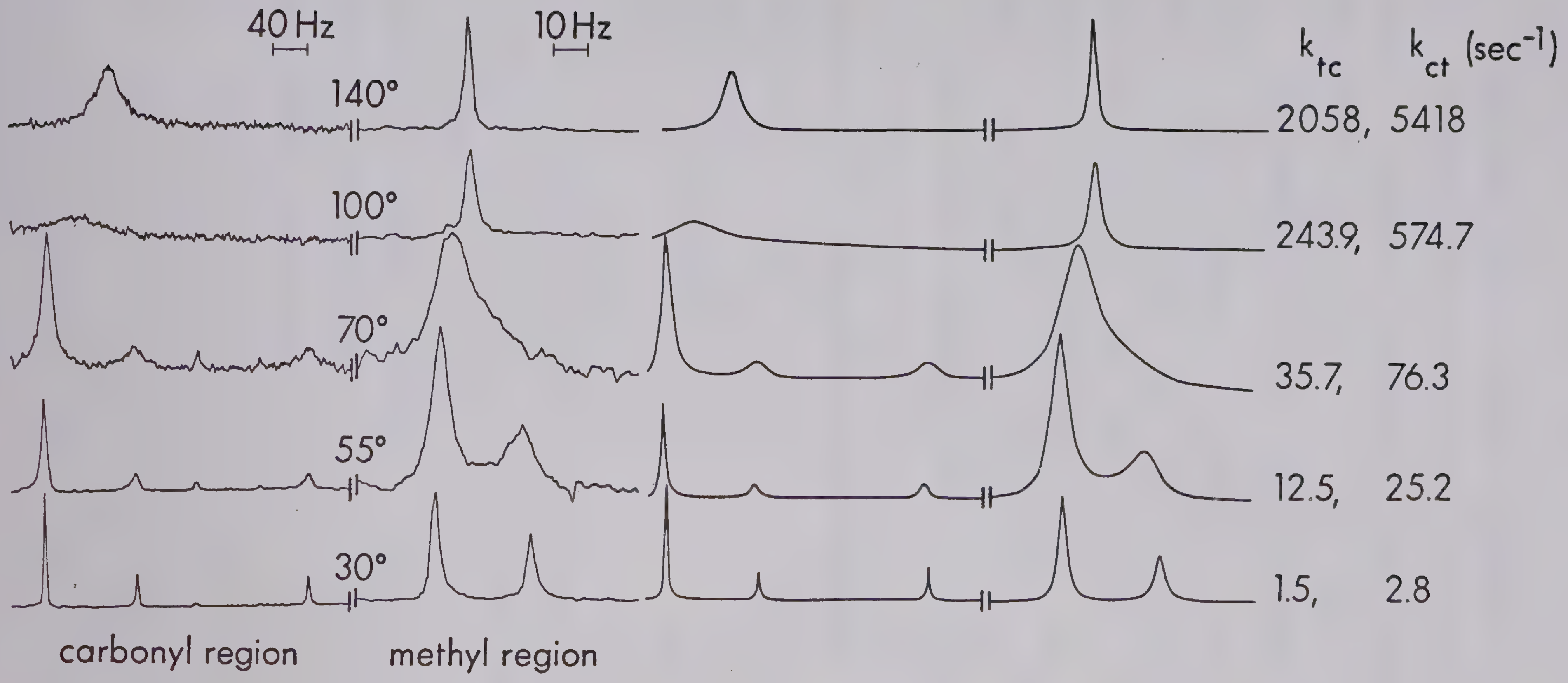

Figure 12. Variable temperature ^{13}C nmr spectra of the equilibrium mixture of *cis*- and *trans*-$Os(CO)_4(SiMe_3)_2$ in decalin, with corresponding simulated spectra at right. Sample is enriched with ^{13}CO.

The trans isomer may be obtained from the cis isomer *via* a trigonal or Bailar twist,[160-164] which is a non-bond breaking mechanism. Support for this mechanism comes from the isomerization study of *cis*-$Ru(^{13}CO)_2(CO)_2(SiCl_3)_2$.[165]

An alternative to the above mechanism is suggested by the X-ray structure of *cis*-$Fe(CO)_4(SiMe_3)_2$ (Chapter V). One way of describing the distorted structure of the molecule would be to say that the four CO groups are approximately tetrahedrally arranged, with the trimethylsilyl groups over two of the faces of the tetrahedron. A similar geometry was observed in the crystal structure of *cis*-$Fe[PhP(OEt)_2]_4H_2$,[158] with the phosphorus atoms tetrahedrally coordinated around the metal, and the hydrogens occupying two faces. The averaging of ^{31}P resonances in this molecule may occur *via* a tetrahedral jump mechanism.[156,157] A motion (or jump) of the hydrogen atoms over a tetrahedral edge would result in a distorted trans structure, which would equilibrate ^{31}P resonances by inversion. Then, of course, the hydrogens return to a cis position. This rearrangement occurs without bond rupture. A similar mechanism is possible for *cis*-$Fe(CO)_4$-$(SiMe_3)_2$, although lack of nuclear labelling precludes any definite conclusions.

2.3 Trends in Activation Energies for the Rearrangement of $M(CO)_4(ER_3)_2$ Derivatives.

The ^{13}C nmr study of *cis*-$Fe(CO)_4(SiMe_3)_2$ and *cis*-$Fe(CO)_4(SnR_3)_2$ (R = Me, Et, Pr, Bu, and Ph) presented above established that averaging of axial and equatorial ^{13}CO resonances was rapid on the nmr time scale at room temperature, and that ligand dissociation did not occur during the averaging process. A favoured averaging mechanism involved isomerization to the trans form (in which all ^{13}CO groups are equivalent) and back to the cis form.

We discuss here the variation over the family of compounds studied of the barrier to axial-equatorial averaging. In view of the foregoing, this is assumed to be equivalent to the barrier for cis to trans isomerization in all cases.

The most striking fact is that barriers are lowest for the iron compounds. All *cis*-$Fe(CO)_4(ER_3)_2$ derivatives (R = alkyl group) exhibit a single ^{13}CO resonance at room temperature. The activation parameters for *cis*-$Fe(CO)_4$-$(SiMe_3)_2$ and *cis*-$Fe(CO)_4(GeMe_3)_2$ derived from spectral simulation are $\Delta H^{\dagger} = 10.4 \pm 0.6$ and 12.5 ± 0.4 kcal mol^{-1} and $\Delta S^{\dagger} = -2.3 \pm 2.6$ and 0.6 ± 1.5 e.u., respectively. The barrier for the rearrangement of *cis*-$Fe(CO)_4(SnMe_3)_2$ is similar to that of the silicon analog (see below).

Although it was an objective of the present investigation to characterize the nonrigid behaviour of these compounds quantitatively, the quality of ^{13}C nmr spectra in the region of collapse for most derivatives was rather poor despite all reasonable efforts (see Experimental Section). Attempts at simulation were not justified in these cases. However, to permit at least a qualitative assessment of barriers, Table VIII presents values of $\Delta G^{\dagger}$ calculated at the coalescence temperature from the axial-equatorial ^{13}CO separation at the low temperature limit. As Table VIII shows, the crude $\Delta G^{\dagger}$ values so calculated are in excellent agreement with those from a complete line shape analysis where available. This is true even in the case of $Os(CO)_4(SiMe_3)_2$, where the involvement of the trans form in coalescence is ignored in the crude calculation. Thus, we consider that the $\Delta G^{\dagger}$ values of Table VIII are useful as an indication of trends.

Free energies of activation for the averaging process are 6-8 kcal higher for the ruthenium and osmium derivatives than for the corresponding iron compounds (of Table VIII). A similar trend was noted among the hydrides $M[P(OR)_3]_4H_2$ (M = Fe, Ru) insofar as the barrier to rearrangement was concerned;[157] thus $\Delta G^{\dagger}$ for $Fe[PhP(OEt)_2]_4H_2$ was 12.2 kcal mol^{-1}, while for $Ru[PhP(OEt)_2]_4H_2$ it was 17.2 kcal mol^{-1}.

An important trend arises in the series $Fe(CO)_4$-$(SiMe_{3-n}Cl_n)_2$, where the barrier increases steadily with

increasing chlorine substitution. Thus (Table VIII), $\Delta G^{\dagger}$ = 10.7 kcal for n = 0, 13.2 kcal for n = 1, 16.5 kcal for n = 2, and 17.5 kcal for n = 3. The same trend was previously noted in the osmium series $Os(CO)_4(SiMe_3)_2$, $Os(CO)_4(SiMe_2Cl)_2$, and $Os(CO)_4(SiMeCl_2)_2$,[90] but no information is available for $Os(CO)_4(SiCl_3)_2$, for which only the trans isomer is known.

For the series *cis*-$Fe(CO)_4(SnR_3)_2$ (R = Me, Et, Pr, Bu, and Ph), there is little variation in $\Delta G^{\dagger}$ values, i.e., the steric bulk of the SnR_3 groups has little influence upon the rearrangement. However, chlorine substitution increases the barrier for rearrangement, as observed for the iron-silicon complexes, and *cis*-$Fe(CO)_4(SnCl_3)_2$ is stereochemically rigid on the nmr time scale at room temperature.

There appears to be a correlation between ^{13}CO chemical shifts and stereochemical nonrigidity in these molecules: the more deshielded the carbonyl resonances, the lower the barrier to axial-equatorial rearrangement. This is illustrated below for $Fe(CO)_4(SiMe_{3-n}Cl_n)_2$ derivatives:

Compound	CO_{ax}	CO_{eq}	$\Delta G^{\dagger}$ (kcal mol^{-1}) at coalescence
cis-$Fe(CO)_4(SiMe_3)_2$	208.50	207.64	10.7
cis-$Fe(CO)_4(SiMe_2Cl)_2$	205.70	203.27	13.2
cis-$Fe(CO)_4(SiMeCl_2)_2$	202.46	200.14	16.5
cis-$Fe(CO)_4(SiCl_3)_2$	199.44	197.34	17.5

Table VIII

Coalescence Temperatures and Free Energies of Activation for Axial-Equatorial Averaging in *cis*-$M(CO)_4(ER_3)_2$ Derivatives.[a]

Compound	$\Delta\delta$ (Hz)	Coalescence Temp (°C)	$\Delta G^{\dagger}$ (kcal mol^{-1}) at coalescence
$Fe(CO)_4(SiMe_3)_2$[b]	19.5	-55	10.7 (10.9)[i]
$Fe(CO)_4(SiMe_2Cl)_2$[c]	55.0	5	13.2
$Fe(CO)_4(SiMeCl_2)_2$[c,d]	52.5	70	16.5
$Fe(CO)_4(SiCl_3)_2$[c,d]	47.5	90	17.5
$Fe(CO)_4(GeMe_3)_2$[b]	40.5	-20	12.1 (12.3)[i]
$Fe(CO)_4(SnMe_3)_2$[e]	4.7	-75	10.2
$Fe(CO)_4(SnEt_3)_2$[b]	22.0	-50	10.9
$Fe(CO)_4(SnPr_3)_2$[b]	18.0	-60	10.5
$Fe(CO)_4(SnBu_3)_2$[b]	20.7	-50	10.9
$Fe(CO)_4(SnPh_3)_2$[b]	6.1	-73	10.2
$Fe(CO)_4(SnCl_3)_2$[b]	2.4	>20	>15.8
$Ru(CO)_4(SnMe_3)_2$[f]	112.3	100	17.4
$Ru(CO)_4(SiCl_3)_2$[g]	...	...	25.7
$Os(CO)_4(SiMe_3)_2$[d,h]	199.0	100	17.0 (16.8)[i]

Footnotes to Table VIII

[a] From ^{13}C nmr spectra with the single exception noted. $\Delta\delta$ is the chemical shift difference between axial and equatorial carbonyl groups in the low temperature limiting spectrum.

[b] CD_2Cl_2 solvent

[c] Toluene-d_8 solvent

[d] Trans isomer also present (see text and Table III) the peaks of which are involved in coalescence.

[e] CD_2Cl_2:methylcyclohexane-d_{14} (1:1) solvent (see text).

[f] As neat liquid.

[g] Free energy of activation for cis to trans isomerization in *n*-octane by conventional kinetic methods as calculated from data in reference 95.

[h] Decalin solvent.

[i] Values in parenthesis are $\Delta G^{\dagger}$ calculated for coalescence temperature from $\Delta H^{\dagger}$ and $\Delta S^{\dagger}$ obtained from complete line-shape analysis treatment.

One way of explaining these results may be *via* the π-back bonding theory of chemical shifts, which was presented in Chapter II. A more shielded carbonyl resonance implies less π-back donation to the carbonyls and more to the $SiMe_{3-n}Cl_n$ groups. This in turn may be related to the barrier to cis-trans isomerization. Thus, compounds containing good π-back bonding ligands, such as $SiCl_3$, would have a higher barrier, and this indeed was observed in this work. Arguments of this kind have been used before to explain the hindered rotation of coordinated monoolefins in transition metal complexes or the rotation about single bonds or partial double bonds in organic molecules.[57]

On the other hand, it may be that a ground state geometry other than the idealized regular octahedron provides a facile path to rearrangements. For *cis*-$M(CO)_4$-$(ER_3)_2$ derivatives a considerable range of distortion is possible, from the pseudo-bicapped tetrahedral *cis*-$Fe(CO)_4$-$(SiMe_3)_2$[96] to the almost perfectly octahedral *cis*-$Ru(CO)_4$-$(GeCl_3)_2$.[166] The structure of these and of other related $M(CO)_4(ER_3)_2$ derivatives will be discussed in Chapter V.

The study of the dynamic behaviour of $M(CO)_4(ER_3)_2$ molecules by ^{13}C nmr is complicated by the large span in the barrier for cis-trans isomerization. One often has to go to very low or to very high temperatures to observe limiting spectra. Two examples will illustrate this point.

The ^{13}C nmr spectrum of *cis*-$Fe(CO)_4(SnMe_3)_2$ showed a single ^{13}CO resonance down to -80° (CD_2Cl_2) and -90° (toluene-d_8). Attempts to reach lower temperatures using methylcyclohexane-d_{14} failed because of high viscosity of the solution below -60°. Using a ^{13}CO-enriched sample in the solvent CF_2HCl:CD_2Cl_2 (4:1), a single resonance was again observed at -110°. However, all three Sn-^{13}CO couplings were observed, which established that the compound is stereochemically rigid at -110°, and that the single carbonyl resonance is due to accidental degeneracy of the axial and equatorial peaks.

In the mixed solvent methylcyclohexane-d_{14}:CD_2Cl_2 (1:1), two ^{13}CO peaks separated by 4.7 Hz were observed at -110° (Figure 11). At the end of data collection, it was noted that the solution had separated into two layers. However, we believe that there was a genuine separation of the axial and equatorial resonances since two sets of ^{13}CO-Sn couplings were observed to be centered about the peak to low field and one stronger set centered about the high field peak. The couplings were identical in magnitude to those found in the CF_2HCl/CD_2Cl_2 experiment.

Although the ^1H nmr spectrum of *cis*- and *trans*-$Os(CO)_4$-$(SiMe_3)_2$ showed coalescence at 55°, temperatures as high as 140° were required to observe a well advanced coalescence in the ^{13}C nmr spectrum. Most of the compounds studied here decompose rapidly at these high temperatures, and

although collapse of ^{13}CO resonances in $M(CO)_4(EMe_3)_2$ derivatives (M = Ru, Os; E = Si, Ge, Sn, and Pb) was observed at 90°, the coalescence temperature could be determined in but a few special cases (see Table VIII).

3. Experimental Section

The nmr instrumentation and technique has been described in Chapter II. All variable temperature ^{13}C nmr spectra were recorded on the Bruker HFX-90 spectrometer; the room temperature spectrum of ^{13}CO-enriched $Fe(CO)_4(SiMe_3)_2$ was obtained on the Varian HA-100 instrument.

The number of pulses was usually one thousand (1K), but as many as 2K to 12 K pulses were required in spectra where coalescence was occurring.

The spectrum of $Ru(CO)_4(SnMe_3)_2$ above 100° was determined using the pure liquid. The lock consisted of dimethylsulfoxide-d_6 contained in a 5 mm nmr tube fitted coaxially in the larger tube. The spectra of $Os(CO)_4(SiMe_3)_2$ were measured in a sealed tube, with freshly distilled decalin as solvent, and dimethylsulfoxide-d_6 in a sealed capillary as the lock. The sample (1.0 g) was enriched with ^{13}CO to approximately 25%. At 140° slight refluxing of solvent in the tube occurred, resulting in some loss of resolution. For this reason, spectra at higher temperatures were not attempted. No relaxation reagent was used in experiments where a line-shape analysis

was carried out.[127]

The simulation of the nmr spectra of $Fe(CO)_4(SiMe_3)_2$, $Fe(CO)_4(GeMe_3)_2$ and $Os(CO)_4(SiMe_3)_2$ was carried out using a two or six site exchange program written and supplied by Professor D. L. Rabenstein of this department. The computations were carried out on an IBM 360/67 or an Amdahl 470 V/6 computer at the University of Alberta.

The following rates were found for $Fe(CO)_4(SiMe_3)_2$: -70°, 9.09; -65°, 19.2; -60°, 26.3; -55°, 51.8; -50°, 85.5; -45°, 147.1; -40°, 344.8 sec^{-1}. The half-width used in simulation was 2.6 Hz (see page 68). From these results, activation parameters of $\Delta H^{\dagger} = 10.4 \pm 0.6$ kcal mol^{-1} and $\Delta S^{\dagger} = -2.3 \pm 2.6$ eu were calculated from a least squares fit to the Eyring equation.

The rates obtained for $Fe(CO)_4(GeMe_3)_2$ were as follows: -40°, 12.5; -30°, 35.71; -20°, 94.34; -15°, 169.5; -10°, 312.5; -5°, 476.2 sec^{-1}. The half-width used in simulation was 2.6 Hz, the value observed at -50°. These rates led to the following activation parameters: $\Delta H^{\dagger} = 12.5 \pm 0.4$ kcal mol^{-1} and $\Delta S^{\dagger} = 0.6 \pm 1.5$ eu.

The line-shape analysis of $Os(CO)_4(SiMe_3)_2$ was complicated by two factors: the chemical shift difference between the methyl peaks of the trans and cis isomers varied with temperature, and the ratio of isomers changed with temperature.

Study of the change in the methyl carbon chemical shift difference with temperature at temperatures below

the region of collapse suggested the following relationship between the chemical shift difference ($\Delta\delta$) with temperature (T°K) as established by a least squares fit:

$$\Delta\delta = -0.0844\ T + 54.08$$

From this relationship $\Delta\delta$ in the region of coalescence could be estimated.

Similarly from the ratio of isomers, as obtained by integration at temperatures below 50°, the following equation was established by least squares:

$$\log K = -185.9/T + 0.870,$$

where K is the ratio trans:cis. Thus the ratio of isomers at temperatures greater than 50° could be estimated. The equation implies that $\Delta H° = 0.85$ kcal mol^{-1} and $\Delta S° = 4$ eu for the equilibrium:

$$\textit{cis}\text{-Os(CO)}_4\text{(SiMe}_3\text{)}_2 \rightleftharpoons \textit{trans}\text{-Os(CO)}_4\text{(SiMe}_3\text{)}_2$$

These results are in good agreement with values obtained using ^{1}H nmr data (CH_2Br_2[90] or toluene-d_8 solvent).

Low temperature limiting half widths (-20°) used in spectral simulation were 2.0 Hz for trans Me, and 2.2 Hz for cis Me, leading to the following rates. The first value given after the temperature (°C) is k_{ct}, the rate of isomerization of cis and trans in sec^{-1}, and the second figure is the corresponding rate (k_{tc}) for the trans to cis process:

35°, 5.00, 2.70; 40°, 6.67, 3.52; 45°, 11.1, 5.75; 50°, 15.4, 7.81; 55°, 25.2, 12.5; 60°, 35.3, 17.2; 65°, 42.2, 20.2; 70°, 76.3, 35.7; 75°, 100, 45.5; 80°, 147, 66.7;

90°, 297, 130; 100°, 575, 244; 110°, 1220, 500.

From these results activation parameters of $\Delta H^{\dagger}_{ct} = 16.4 \pm 0.3$ kcal mol^{-1}, $\Delta S^{\dagger}_{ct} = -2.3 \pm 0.8$ eu, $\Delta H^{\dagger}_{tc} = 15.6 \pm 0.3$ kcal mol^{-1}, and $\Delta S^{\dagger}_{tc} = -6.3 \pm 0.8$ eu were calculated from a least squares fit to the Eyring equation.

In the calculation of the activation parameters only rate constants between 35° and 110°C were used since values outside this range were subject to larger experimental error; this was especially the case with the spectrum at 140°.

From the Eyring equation, rate constants at particular temperatures were calculated and used to simulate the spectra in the carbonyl region. The model used in calculating the simulated spectra assumed that the trans signal gave rise to axial or equatorial resonances in the cis molecule with equal (0.5) probability; that the axial and equatorial resonances each produced the trans resonance with unit probability; and that the probability for direct axial-equatorial carbonyl interchange was zero. Half widths of ^{13}CO resonances in the low temperature limiting spectrum (-20°) were 2.4 Hz for the trans isomer, and 2.8 Hz for both axial and equatorial signals of the cis isomer.

The small peak observed between the cis carbonyl resonances is due to an impurity, possibly $[Os(CO)_4SiMe_3]_2$.

For the rest of the compounds, where collapse of the carbonyl signals was observed, line shape analysis of the spectra was not considered worthwhile. Because of the large chemical shift difference (2-5 ppm) between the two peaks the signal in the region of collapse is spread over a large region and is therefore weak. Large errors are consequently involved in simulating such a spectrum with concomitant errors in the activation parameters. Several spectra having 8K scans each would have been necessary for a satisfactory analysis. The time required for 8K scans is approximately two hours and many of the compounds showed signs of decomposition after only one two-hour period at the temperature of collapse.

An approximate method of calculating $\Delta G^{\dagger}$ from the chemical shift separation (at slow exchange) and the collapse temperature was therefore carried out using the relationships $\tau = 1/\pi\sqrt{2}\ \ \Delta\nu$ and $1/\tau = \kappa(kT/h)\exp(-\Delta G^{\dagger}/RT)$ where τ = lifetime at temperature T, κ = transmission coefficient = 1, T = temperature of collapse, and $\Delta\nu$ = chemical shift difference in the low temperature limiting spectrum.

In cases where $\Delta G^{\dagger}$ was calculated by both this method and from the results of the line-shape analysis it was found that the two values agreed within experimental error.

The line-shape analysis of the ^{1}H nmr spectra of $Os(CO)_4(SiMe_3)_2$ in toluene-d_8 was carried out as described

above for the ^{13}C nmr spectra. The following relationships between the chemical shift difference ($\Delta\delta$) and temperature (-30 to 40°) and between the ratio of isomers (K = trans/cis) and temperature (-30 to 32°) were established by least squares fit:

$$\Delta\delta = -0.0211\ T + 9.69$$

$$\log K = -146.9/T + 0.663$$

From these relationships, $\Delta\delta$ and K in the region of coalescence could be estimated. Also, $\Delta H° = 0.7$ kcal mol^{-1} and $\Delta S° = 3.0$ eu for the equilibrium.

$$\textit{cis}\text{-Os(CO)}_4\text{(SiMe}_3\text{)}_2 \rightleftharpoons \textit{trans}\text{-Os(CO)}_4\text{(SiMe}_3\text{)}_2$$

may be calculated.

Low temperature limiting half widths (-10°) used in spectral simulation were 0.75 Hz for the trans isomer, and 0.70 Hz for the cis isomer, leading to the following rates. The first value given after the temperature (°C) is k_{ct}, the rate of isomerization of cis to trans in sec^{-1}, and the second figure is the corresponding rate (k_{tc}) for the trans to cis process:

40°, 3.91, 2.5; 50°, 10.77, 6.67; 55°, 15.64, 9.52; 60°, 24.89, 14.93; 65°, 34.54, 20.41; 70°, 47.05, 27.40; 80°, 90.57, 51.28; 90°, 287.8, 158.7; 100°, 516.5, 277.8.

From these rates the following activation parameters were calculated: $\Delta H^{\dagger}_{ct} = 18.0 \pm 0.6$ kcal mol^{-1}, $\Delta S^{\dagger}_{ct} = 1.5 \pm 1.7$ eu, $\Delta H^{\dagger}_{tc} = 17.3 \pm 0.6$ kcal mol^{-1}, and $\Delta S^{\dagger}_{tc} = -1.6 \pm 1.7$ eu.

CHAPTER V

THE STRUCTURE OF $M(CO)_4(ER_3)_2$ DERIVATIVES.

1. Introduction

The idealized polytopal isomers in the six-atom family are the octahedron, the trigonal prism,[49] and the bicapped tetrahedron.[96, 167,168] The stabilization of one polytopal isomer with respect to another will be the result of a) minimizing all non-bonded contacts, b) maximizing the metal-ligand bonding interactions, and c) maximizing bonding interactions between the atoms of the ligand itself.[169]

The octahedron is, in most cases, the most stable polytopal isomer, and consequently, most six-coordinate molecules are stereochemically rigid. However, during recent years, a growing number of six-coordinate stereochemically nonrigid molecules has been reported[57] and two non-bond breaking mechanisms have been proposed for their rearrangement: the trigonal or Bailar

twist[160-164] and the tetrahedral jump.[156,157*] The intermediates (or transition states) in these rearrangement mechanisms are the trigonal prism and the distorted trans octahedron, respectively, both of which are normally of relatively high energy.[167,169] Lowering the barrier to rearrangement can nevertheless be achieved, and two strategies suggest themselves: a) destabilizing the ground state octahedron, and b) stabilizing the intermediates or transition states. These possibilities will be considered in this chapter, where the structure of a number of *cis*- and *trans*-$M(CO)_4(ER_3)_2$ derivatives will be discussed.

2. Discussion of the Structure of *cis*-$M(CO)_4(ER_3)_2$ Derivatives.

Most six-coordinate molecules are assumed, and seldom

---

[*] Another non-bond breaking mechanism has also been proposed, the rhombic, or Ray-Dutt, twist.[170] However, this mechanism is completely identical with the Bailar twist.[164] Of course, numerous bond-breaking rearrangement mechanisms are possible, which occur *via* a five-coordinate intermediate or transition state.[171] However, these mechanisms have not been discussed here because no evidence for them, as far as the systems studied in Chapter IV are concerned, is available.

proven, to be octahedral. However, several X-ray investigations have shown that in *cis*-$M(CO)_4(ER_3)_2$ derivatives significant distortions from idealized octahedral geometry may exist. The two extremes here would be the regular octahedral geometry and the tetrahedral $M(CO)_4$ arrangement with the ER_3 ligands in two of the tetrahedral faces. The average of the observed "cis" and "trans" angles between CO groups may be taken as a measure of the distortion.[172] The limiting values of these angles would be 90° and 180° for the octahedron, and 109.5° for the tetrahedron.

The molecular structure of *cis*-$Fe(CO)_4(SiMe_3)_2$, which was obtained by Dr. R. A. Smith of this department,[96] is shown in Figure 13. The molecule exhibits great distortion from regular octahedral geometry such that it may be best described as a pseudo-bicapped tetrahedron with the trimethylsilyl groups as capping ligands.

The angle between the axial carbonyl carbons (C(3)-Fe-C(4)) is 141.2° instead of the expected 180° for a regular octahedron. The angles between the axial and equatorial carbonyl carbons (C(1)-Fe-C(3) and C(1)-Fe-C(4)) are 103.9° and 103.4°, respectively. Only the angle between the equatorial carbonyl carbons (C(1)-Fe-C(1')) at 89.5° is within 1° of its idealized octahedral value. The Si-Fe-Si' angle is 111.8°. Atoms O(3), C(3), Fe, C(4), and O(4) are coplanar. Also atoms O(1), O(1'), C(1), C(1'), Fe, Si, and Si' are coplanar.

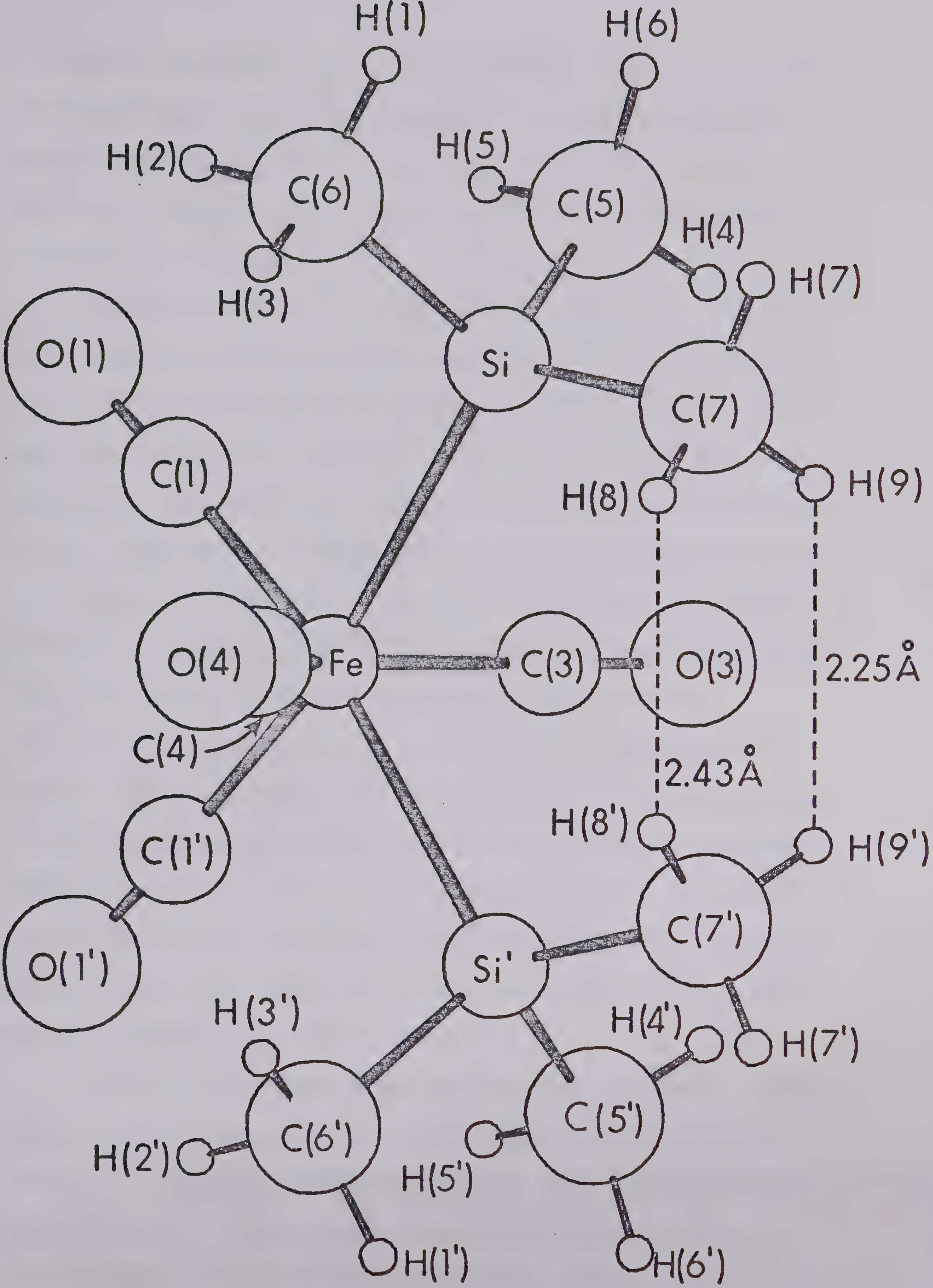

Figure 13. Molecular structure of *cis*-$Fe(CO)_4(SiMe_3)_2$.

The orientation of the $SiMe_3$ groups with respect to each other was initially surprising in that two methyl groups (C(7) and C(7')) point almost directly at one another. The C(7)-C(7') contact at 3.437(7) Å would be considered attractive.

The silicon atom is equidistant from C(1), C(3) and C(4), and all three angles between silicon-iron-and C(1), C(3), and C(4) are less than 90°. This corresponds to a very favorable cis-ligand interaction between the whole trimethylsilyl group and the three carbonyl carbons closest to it. The methyl carbons are staggered with respect to the carbonyl carbons such that C(5) is almost bisecting the C(1)-Fe-C(3) angle, C(6) bisecting the C(1)-Fe-C(4) angle, and C(7) bisecting the C(3)-Fe-C(4) angle. This "bisecting" geometry dictates the unusual arrangement of methyl groups centered on C(7) and C(7'). The distortion in this structure relieves the intramolecular repulsions C(4)-C(6) and C(3)-C(5). The hydrogen-hydrogen contacts between H(8)-H(8') and H(9)-H(9') correspond to repulsion[173] and the Si-Fe-Si' angle is consistent with net repulsion between the trimethylsilyl groups.

Although the distortion observed in *cis*-$Fe(CO)_4(SiMe_3)_2$ may be rationalized using steric arguments, explanations based on electronic reasons have been brought forward as well. Thus, it was argued, based on extended Hückel calculations, that very good σ-donors, such as the trimethylsilyl group, can stabilize the bicapped tetra-

hedron,[167] and the iron becomes an essentially d^{10} system. Recent calculations from this laboratory, carried out by Dr. A. C. Sarapu using the method of Fenske and Hall,[174] have found that much of the electron density at the metal is removed by increased back-donation to the carbonyl 2π orbitals.[96] Nevertheless, these results corroborate the above description of the electronic structure insofar as the sigma framework is concerned.

The molecular structure of *cis*-$Fe(CO)_4(SnPh_3)_2$, which was determined by Dr. H. P. Calhoun of this department,[98] is shown in Figure 14. The molecule is significantly distorted from regular octahedral geometry, although not as much as *cis*-$Fe(CO)_4(SiMe_3)_2$. Thus, the angle between the axial carbonyl carbons (C(1)-Fe-C(3)) is 159.6°, and the angle between the equatorial carbons is 92.0°. A comparison of the E-Fe-E angles (E = Si, Sn) in *cis*-$Fe(CO)_4(SiMe_3)_2$ (111.8°) and *cis*-$Fe(CO)_4(SnPh_3)_2$ (95.95°) indicates less repulsion between the ER_3 groups in the latter molecule. This is the result of a longer iron-tin bond (2.666 Å) and of the propeller-type arrangement of the phenyl groups.

While the silicon atom in *cis*-$Fe(CO)_4(SiMe_3)_2$ was equidistant from the three cis-carbonyl carbons, this was not the case with *cis*-$Fe(CO)_4(SnPh_3)_2$. In fact, in this structure for say, atom Sn(1), there is only one short contact, to C(1) at 2.94 Å. The other two distances, to C(3) and C(4), are much longer (3.06 and 3.14 Å,

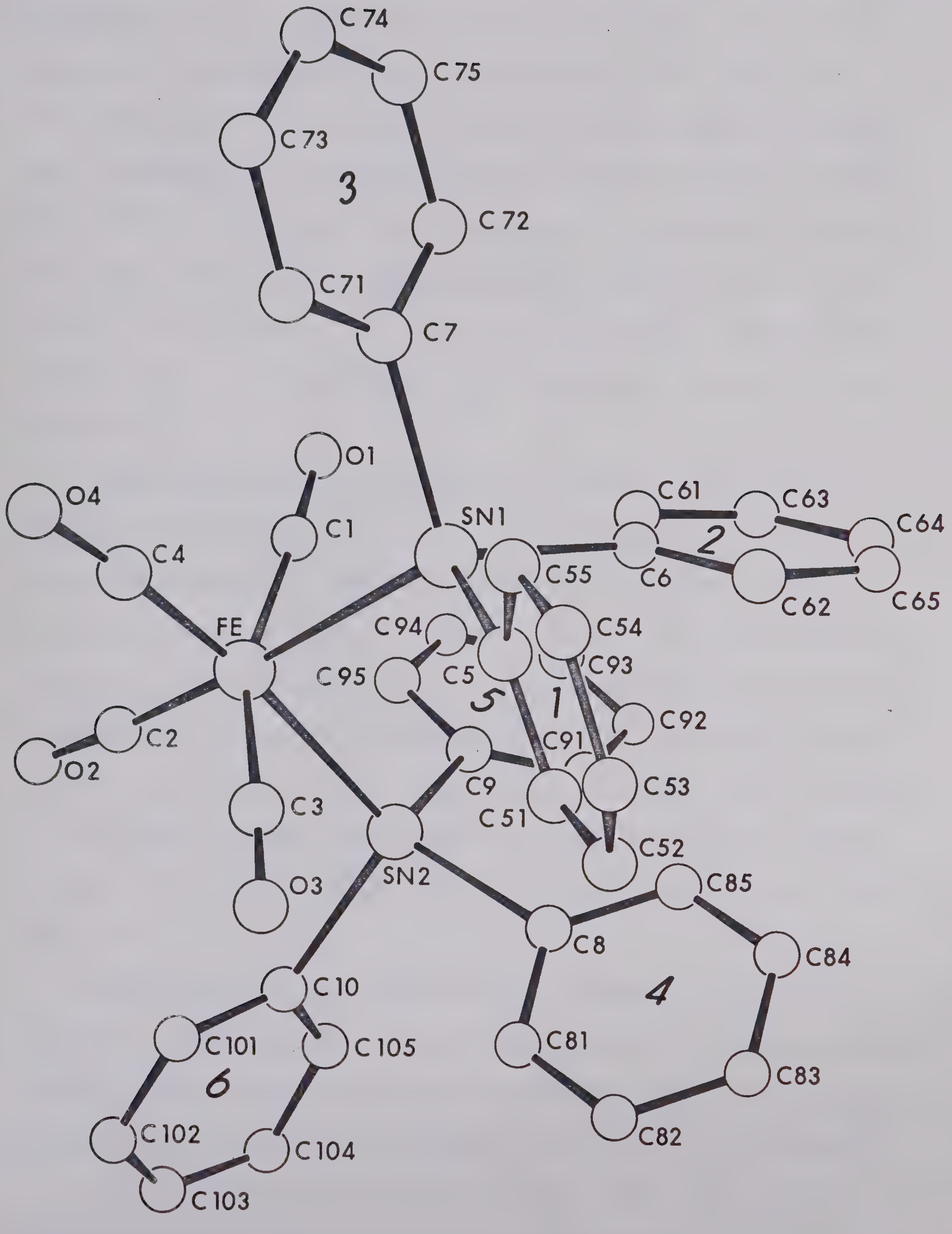

Figure 14. Molecular structure of *cis*-$Fe(CO)_4(SnPh_3)_2$.

respectively). On the other hand, Sn(2) is closest to C(3), distance 2.93 Å. Atoms O(2), C(2), Fe, C(4), O(4), Sn(1), and Sn(2) are non-coplanar; the opposite was found in *cis*-$Fe(CO)_4(SiMe_3)_2$. The carbonyls in *cis*-$Fe(CO)_4(SiMe_3)_2$ were staggered with respect to the adjacent methyl groups. By contrast, they are almost eclipsed in *cis*-$Fe(CO)_4(SnPh_3)_2$, and close contacts are observed between C(3) and C(5), at 3.47 Å, and between C(3) and C(8), at 3.49 Å. These factors could explain the less distorted geometry observed in this molecule.

The structure of the related molecule, *cis*-$Fe(CO)_4$-$HSiPh_3$, was carried out by Dr. K. A. Simpson, formerly of this department.[175] This is shown in Figure 15. The molecule exhibits marked deviation from regular octahedral geometry. The triphenylsilyl and the carbonyl groups form an idealized trigonal bipyramid with the Si-Fe-C(3) angle at 178.0°. Carbons 1, 2, and 4 are staggered with respect to the phenyl groups, and they are bent toward the $SiPh_3$ group. Thus, the silicon atom is almost equidistant from C(1), C(2), and C(4).

The angle between the "axial" carbons (C(1)-Fe-C(2)) is 149.8°, and they are displaced toward the hydrogen atom rather than the bisector of the H-Fe-Si angle. The angle between the "equatorial" carbons (C(3)-Fe-C(4)) is 96.3°.

The iron-silicon bond length was 2.415 (3), which is significantly shorter than the value observed in

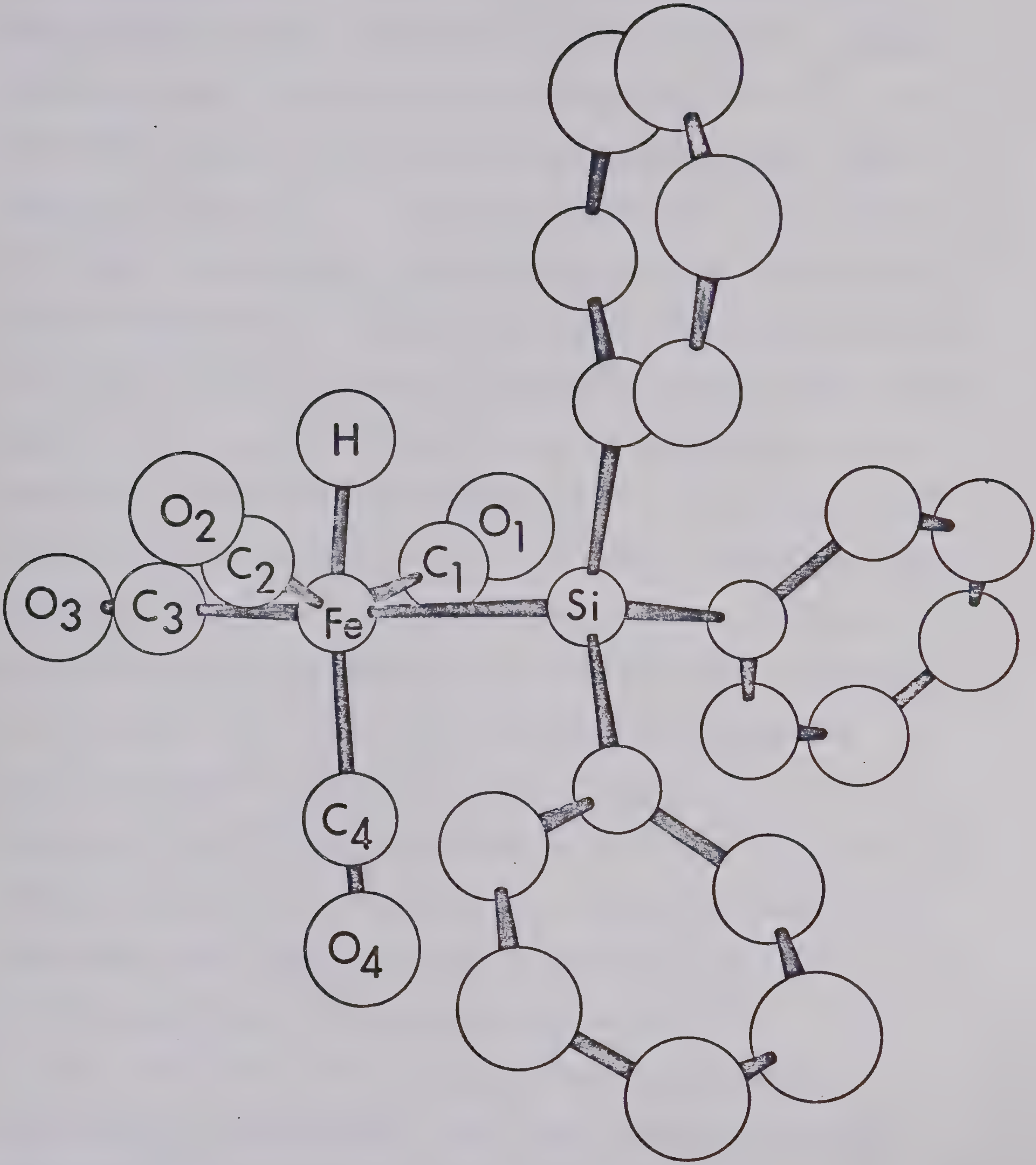

Figure 15. Molecular structure of *cis*-$Fe(CO)_4HSiPh_3$.

cis-$Fe(CO)_4(SiMe_3)_2$ (2.456(2) Å). The hydrogen atom adjacent to iron was "located" from an electron density difference map, and the Fe-H distance was 1.55 Å. The "refined" position for hydrogen afforded an Fe-H bond length of 1.64(10) Å. Other *cis*-$Fe(CO)_4X_2$ derivatives have been investigated by electron or X-ray diffraction, but the magnitude of distortion was considerably less than, say, in *cis*-$Fe(CO)_4(SiMe_3)_2$. Distortions from octahedral geometry (to angles of 156° and 165° between the axial carbonyls) have been claimed for the two independent molecules of $[Fe(CO)_4SnMe_2]_2$[176] but the reliability of this data is low due to severe disorder problems. Similar distortions were observed in the electron diffraction study of *cis*-$Fe(CO)_4H_2$,[177] or the crystal structures of $[(\eta^1\text{-}C_5H_5)_2SnFe(CO)_4]_2$,[178] $Fe(CO)_4(C_{12}H_8O)$,[179] and $Fe(CO)_4(C_8H_6O_6)$[180] where angles of 148.5, 163.6, 164.4, and 166° were observed, respectively. Smaller distortions (less than 10°) were observed in $Fe(CO)_4(HgBr)_2$,[181] $Fe(CO)_4(CF_2CF_2H)_2$,[182] or $[Fe(CO)_4SiCl_2]_2$.[183]

The multitude of X-ray diffraction studies of *cis*-$Fe(CO)_4X_2$ derivatives have demonstrated the large variation in coordination geometry about the iron atom. Distortions from regular octahedral geometry have been observed, and they seem to be the rule rather than the exception.

The crystal structure of the somewhat related *cis*-$Fe[PhP(OEt)_2]_4H_2$ showed a highly distorted geometry, with the angle between the axial phosphorous atoms at 136.7°.[158] The distortion observed in this compound was used to explain its stereochemical nonrigidity.[155-157] A similar argument seems to apply to $M(CO)_4(ER_3)_2$ derivatives as well. Thus, the most distorted complexes discussed here, *cis*-$Fe(CO)_4(SiMe_3)_2$,[96] *cis*-$Fe(CO)_4(SnPh_3)_2$,[98] and *cis*-$Fe(CO)_4HSiPh_3$[184] have been shown to be stereochemically nonrigid (see Chapter IV). Also, $[Fe(CO)_4SnBu_2]_2$ showed averaging of axial and equatorial carbonyl resonances above room temperature.[185] The structure of this compound may be related to that of the corresponding methyl analog, $[Fe(CO)_4SnMe_2]_3$, and it may show a similar distortion.

The crystal and molecular structure of *cis*-$Ru(CO)_4(GeCl_3)_2$ has been determined by Dr. R. Ball, formerly of this department, and it is shown in Figure 16.[166] The geometry of the molecule is close to regular octahedral: the angle between the axial carbonyls (C(1)-Ru-C(2)) is 173°, and the angle between the equatorial carbonyls (C(3)-Ru-C(4)) is 95°. The average of the C-Ru-C and C-Ru-Ge angles is 92.9° and 87.6°, respectively, which reflects the existence of stronger repulsive forces between the CO groups than between the CO and $GeCl_3$ ligands.[186] The angle between the $GeCl_3$ groups (Ge(1)-Ru-Ge(2)) is 91.5°, indicating little, if any, steric repulsion between

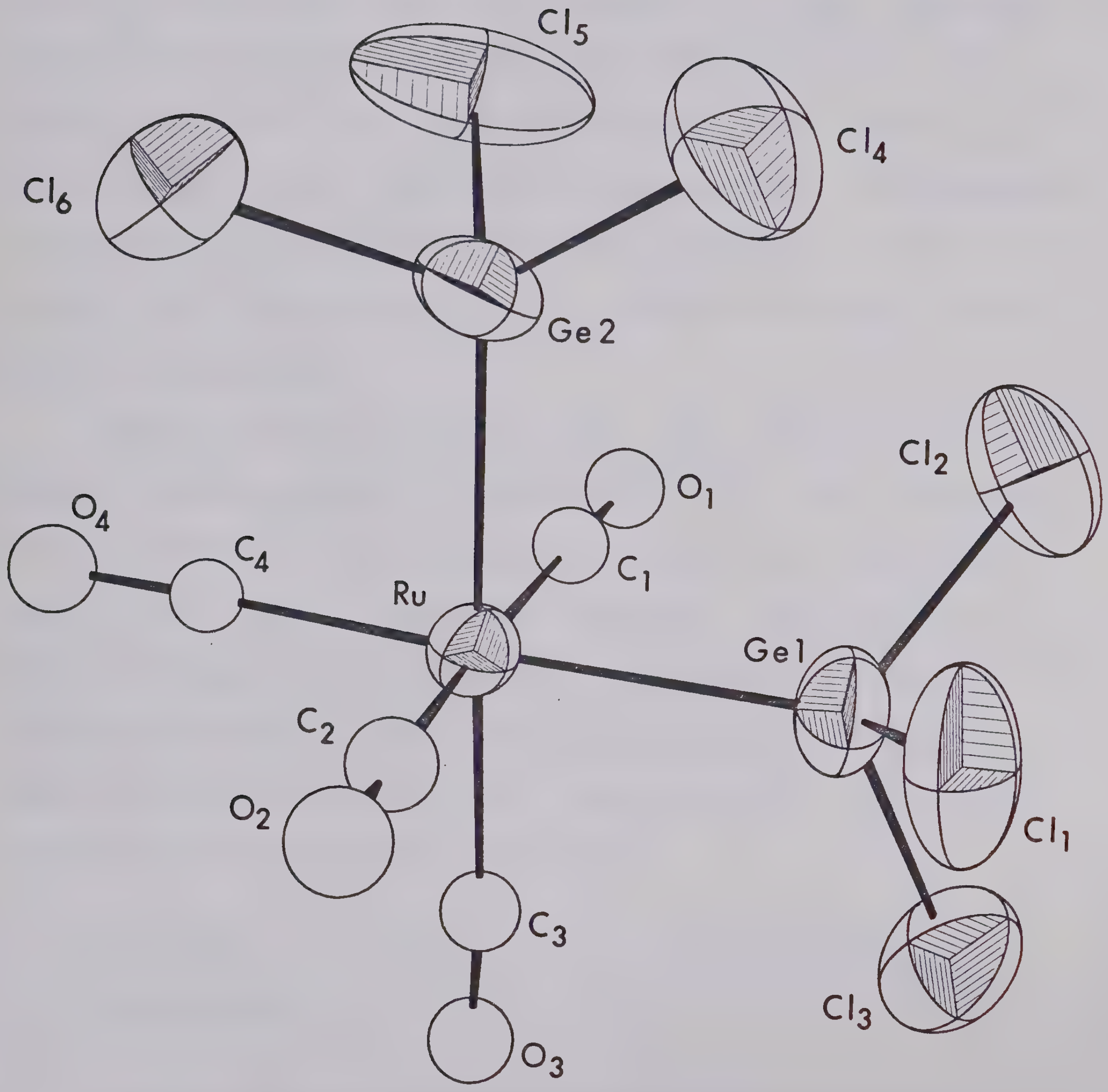

Figure 16. Molecular structure of *cis*-$Ru(CO)_4(GeCl_3)_2$.

them.

The ^{13}C nmr of *cis*-$Ru(CO)_4(GeCl_3)_2$ has not been determined. However, by analogy to all other ruthenium carbonyl derivatives whose ^{13}C nmr spectra showed stereochemical rigidity on the nmr time scale at room temperature (Chapter II and IV), it seems very likely that the same would be true for this compound as well. One could argue that the relatively high barrier for carbonyl rearrangement in ruthenium and osmium $M(CO)_4(ER_3)_2$ complexes (Chapter IV) is due to a significantly smaller distortion from regular octahedral geometry.

Infrared spectroscopy has been used extensively to study *cis*-$M(CO)_4(ER_3)_2$ in solution.[131,136] Four infrared-active carbonyl bands are predicted for such complexes, and, in most cases, four were observed. Unfortunately, the usual type of infrared study affords no information as to the distortion in these complexes, and in the above discussion, conclusions drawn from studies in the solid state were extrapolated to solution.

3. Discussion of the Structure of *trans*-$M(CO)_4(ER_3)_2$ Derivatives.

Several X-ray diffraction studies of *trans*-$M(CO)_4$-$(ER_3)_2$ derivatives have been carried out. Some structures exhibit the essentially regular octahedral geometry of D_{4h} symmetry (**10**), but distortions of two types, D_{2d} (**11**) and

C_{2h} (**12**), have also been recognized.

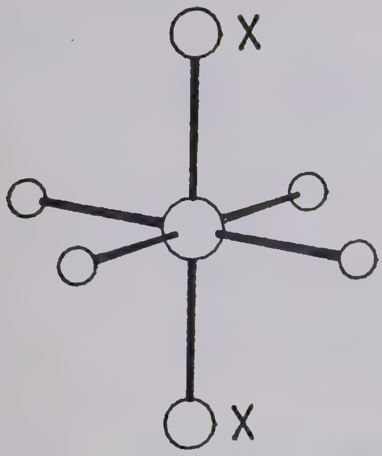

D_{4h}, 10

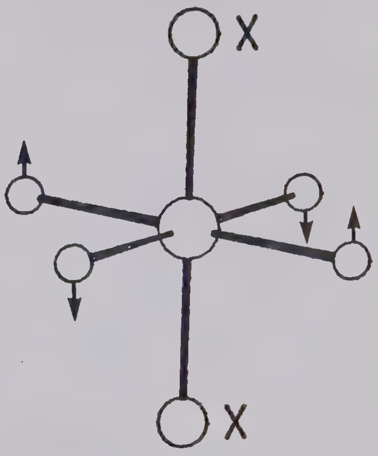

D_{2d}, 11

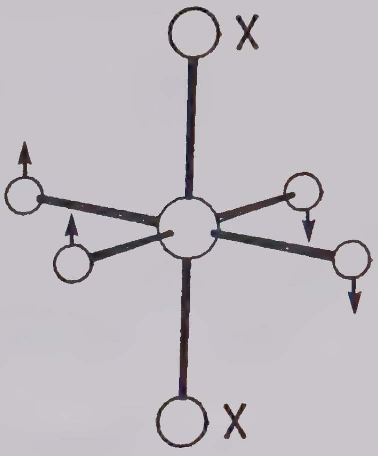

C_{2h}, 12

Infrared and Raman spectroscopy may be used to study the structure of these isomers in solution, and in certain cases, useful conclusions can be obtained. Below, a number of examples will be considered which will illustrate the power, as well as the pitfalls, of these spectroscopic techniques. Finally, the solution structures deduced for several derivatives will be compared with the solid state studies.

In Chapter IV (page 72), infrared spectroscopic evidence was presented for the existence of *trans*-$Fe(CO)_4(SiMe_3)_2$, and two infrared active bands (at 2062 and 1964 cm^{-1}) were attributed to this isomer. The other four bands in the infrared spectrum of $Fe(CO)_4(SiMe_3)_2$ (at 2069, 2006, 2000, and 1979 cm^{-1}) were assigned to the cis isomer. The selection rules for the different trans isomers, as well as for the cis isomer, of C_{2v} symmetry, are given below:

Symmetry	Infrared active	Raman active
D_{4h} (trans)	E_u	$A_{1g} + B_{1g}$
D_{2d} (trans)	$B_2 + E$	$A_1 + B_2 + E$
C_{2h} (trans)	$A_u + B_u$	$A_g + B_g$
C_{2v} (cis)	$2A_1 + B_1 + B_2$	$2A_1 + B_1 + B_2$

The infrared spectrum of *trans*-$Fe(CO)_4(SiMe_3)_2$ is consistent with both a D_{2d} and C_{2h} structure, and rules out the D_{4h} structure. However, the infrared spectrum of *trans*-$Mo(CO)_4[P(OPh)_3]_2$ showed two very weak and one strong band, while for a D_{4h} structure only one band was predicted. It was argued that the $P(OPh)_3$ groups perturb the D_{4h} symmetry and the A_{1g} and B_{1g} bands gain slight allowedness.[99] This seems unlikely for *trans*-$Fe(CO)_4(SiMe_3)_2$ as the bands attributed to it have intensity medium and strong, respectively.

According to the selection rules presented above, six Raman-active bands are expected for a mixture of cis(C_{2v}) and trans(C_{2h}) isomers and seven bands for a mixture of cis(C_{2v}) and trans(D_{2d}) isomers. The Raman spectrum of *cis*- and *trans*-$Fe(CO)_4(SiMe_3)_2$ (heptane solution) showed five bands at 2071(4.3), 2066(3.6), 2008(7.8), 2001(10), and 1984(3.6) cm^{-1} (relative intensities in parenthesis), which indicates accidental degeneracy of one (or two) bands.

One could argue, using a "gambler-type" rationale, that one accidental degeneracy is more likely than two. Therefore, the C_{2h} structure for the trans isomer would be the one to bet on.

However, the bands assigned to the trans isomer are shifted considerably in the Raman spectrum, while those assigned to the cis isomer vary little, if at all. This is a nontrivial point. For a trans isomer of D_{2d} symmetry two bands (B_2 + E) are expected to have the same position in both infrared and Raman spectra, while for a C_{2h} structure the opposite would be true. Based on the above evidence, the C_{2h} structure for *trans*-$Fe(CO)_4(SiMe_3)_2$ is favoured.

From infrared studies, D_{2d} structures were proposed for *trans*-$Fe(CO)_4I_2$ and *trans*-$Os(CO)_4I_2$.[187,188] However, as shown above, infrared spectroscopy alone cannot distinguish between a D_{2d} and a C_{2h} structure.

The infrared spectrum of $Fe(CO)_4(SiCl_3)_2$ is worthy of comment. On the basis of its infrared spectrum (four bands in heptane or in methylene chloride solution), this compound was taken to be the cis isomer.[100] The ^{13}C nmr of this compound, in CD_2Cl_2 or toluene-d_8 solution (Chapter II and IV), has shown a mixture of cis and trans isomers at room temperature. Clearly, the infrared-active band(s) of the trans isomer are accidentally degenerate with those of the cis isomer.

It was claimed that the trans isomer of $Fe(CO)_4(SiCl_3)_2$ was recognized by its infrared spectrum as a more volatile component from the reaction of $Fe_3(CO)_{12}$ and $HSiCl_3$.[189] However, in view of the low barrier for interconversion of *cis*- and *trans*-$Fe(CO)_4(SiCl_3)_2$ (page 87), all normal infrared solution measurements would involve the equilibrium cis:trans mixture. The suggestion[190] that bands attributed to *trans*-$Fe(CO)_4(SiCl_3)_2$ are due in reality to *cis*-$Fe(CO)_4$-$HSiCl_3$ is almost certainly correct.

Genuine *trans*-$Fe(CO)_4(SiCl_3)_2$ was obtained by slow sublimation, in an X-ray capillary, and its crystal structure was determined by Dr. A. Whitla of this department. The structure is shown in Figure 17. The geometry of the molecule is very close to the idealized octahedron. The C(1')-Fe-Si and C(2')-Fe-Si angles are 91.3° and 92.1°, respectively. Thus, the symmetry of the molecule could be best described as C_{2h}.

The distortion observed in this molecule may be understood in terms of the non-bonded contacts between the chlorine atoms and the carbonyl carbons. Two cis carbonyl groups are almost eclipsed with two chlorine atoms (the Cl(1)-C(2') and Cl(2)-C(1') distances are 3.31 and 3.21 Å, respectively), which is consistent with the obtuse angles at iron mentioned above.

The iron-silicon bond length is 2.326(1) Å, which is considerably shorter than the value observed in

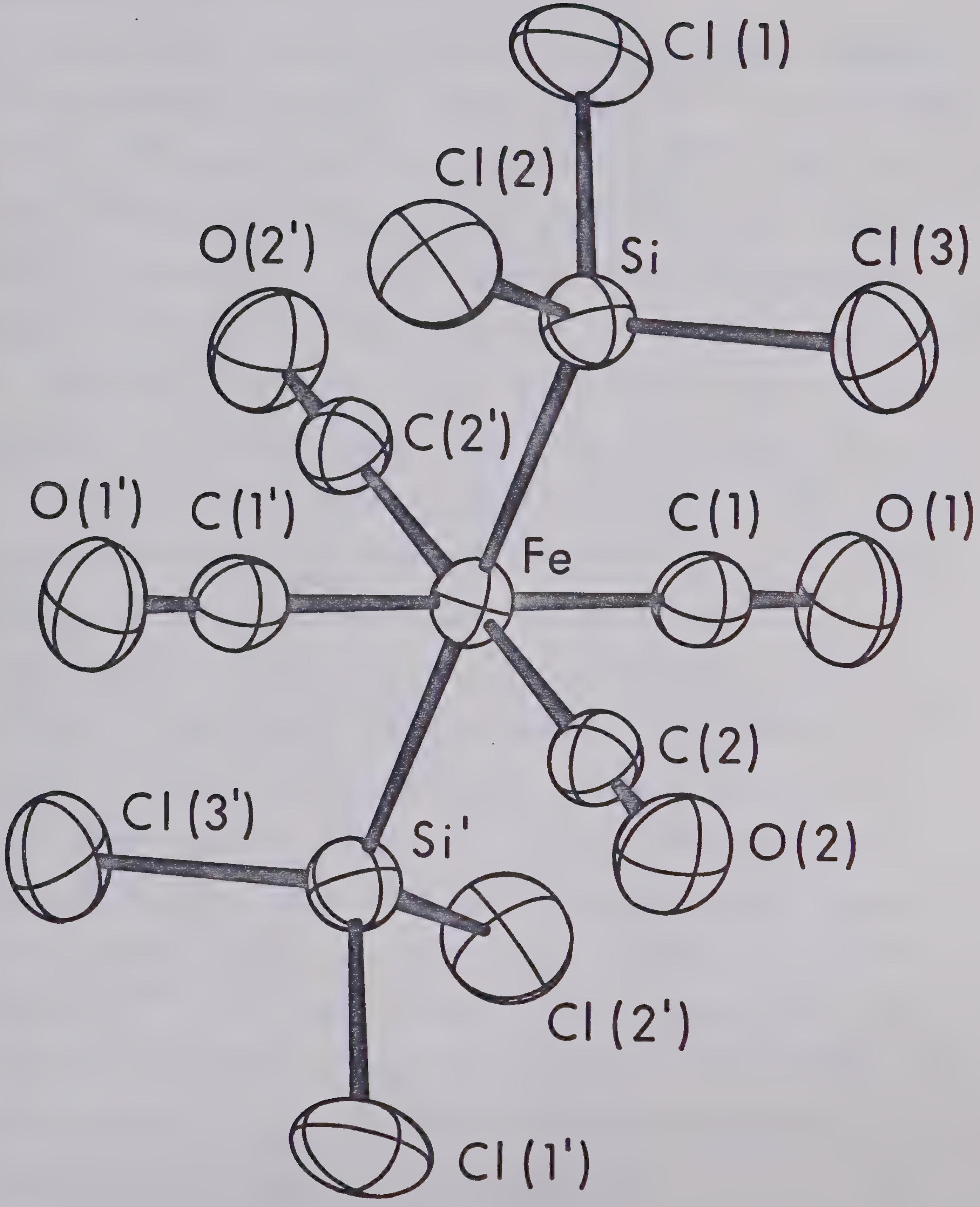

Figure 17. Molecular structure of *trans*-$Fe(CO)_4(SiCl_3)_2$.

cis-$Fe(CO)_4(SiMe_3)_2$ (2.456(2) Å) and in *cis*-$Fe(CO)_4HSiPh_3$ (2.415(3) Å). This is consistent with increased π back-donation to the $SiCl_3$ group.

A similar geometry has been observed in the solid state for *trans*-$Ru(CO)_4(GeCl_3)_2$ (Figure 18),[166,186] *trans*-$Os(CO)_4$-$(SnPh_3)_2$,[191] and *trans*-$Cr(CO)_4[P(OPh)_3]_2$.[192] Also, the X-ray diffraction study of $Mn(CO)_5Si(SiMe_3)_3$ has shown a similar distortion: two cis carbonyls eclipsed with the $SiMe_3$ groups are bent away from the $Si(SiMe_3)_3$ ligand, while the other two carbonyls, which are staggered with respect to the $SiMe_3$ groups, are bent toward the $Si(SiMe_3)_2$ ligand.[193]

Finally, two ruthenium complexes should be mentioned, *trans*-$Ru[PhP(OEt)_2]_4H_2$ and *trans*-$Ru(PHMe_2)_4Cl_2$. An X-ray diffraction study of the first derivative has shown significant distortion from regular octahedral geometry, and the six atom RuH_2P_4 polyhedron has D_{2d} symmetry. Perhaps the best single indicator of the distortion is the P-Ru-P angle of 161.4°.[159] On the other hand, an X-ray structural investigation of the second derivative, *trans*-$Ru(PHMe_2)_4Cl_2$, has shown almost regular octahedral geometry.[194] All trans angles in this molecule were 180° (the molecule has a center of symmetry). The symmetry of the molecule is C_{2h}, and deviations from octahedral geometry of 2.5° and 4.6° were observed.

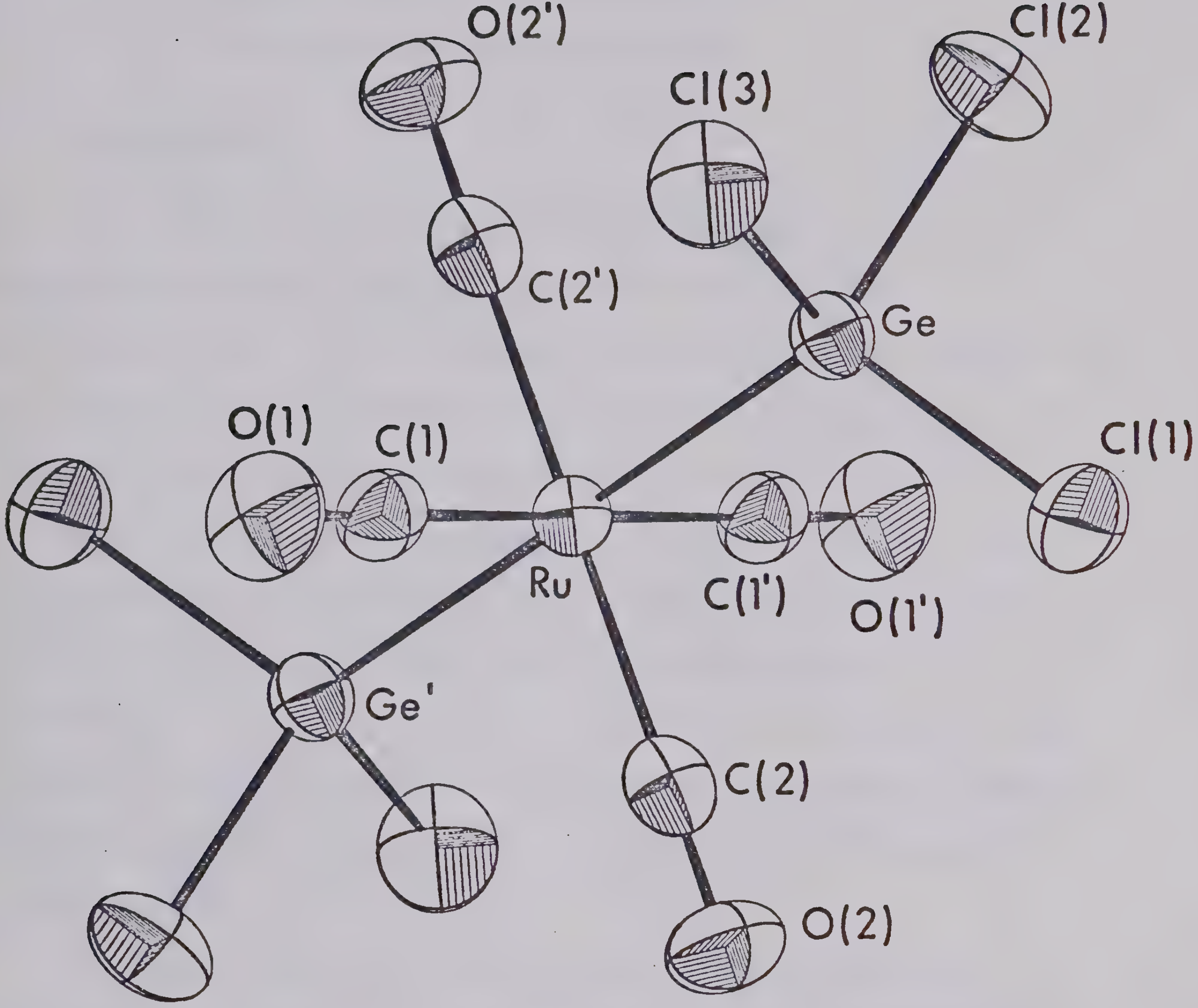

Figure 18. Molecular structure of *trans*-$Ru(CO)_4(GeCl_3)_2$.

CHAPTER VI

METAL CARBONYL DERIVATIVES OF 1,2-BIS(DIMETHYLSILYL)ETHANE

1. Introduction

The ^{13}C nmr studies of the stereochemically nonrigid behaviour of $M(CO)_4(ER_3)_2$ derivatives (M = Fe, Ru, Os; E = Si, Ge, Sn, Pb; R = organic group and halogen) described in Chapter IV have suggested the intermediacy of the trans form in the carbonyl rearrangement of the cis isomer.

To further our understanding of such systems, it was of interest to prepare analogs in which the silyl groups were linked so that they would be constrained to cis positions. In such chelated derivatives, for example, the possibility of interchange of axial and equatorial carbonyls without passing through a trans octahedral form could be investigated.

The reaction of silicon-hydrogen bonds with metal carbonyls has proven to be of great utility,[19-21,195] and it was accordingly decided to utilize the silane $HMe_2Si-CH_2-CH_2-SiMe_2H$ as a starting material. This chapter describes a convenient synthesis of this useful ligand, and its reaction with $Fe(CO)_5$, $Ru_3(CO)_{12}$, $Os_3(CO)_{12}$, and $Co_2(CO)_8$.

2. Results and Discussion

The silane starting material has been prepared in

an overall yield of 56% from commercially available organosilicon compounds using the following sequence of reactions.[92]

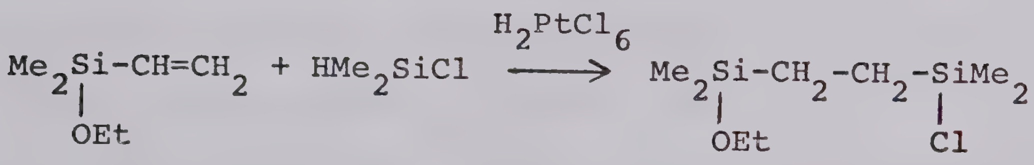

$$\underset{\mathrm{OEt}}{\mathrm{Me_2Si}}\text{-}\mathrm{CH{=}CH_2} + \mathrm{HMe_2SiCl} \xrightarrow{\mathrm{H_2PtCl_6}} \underset{\mathrm{OEt}}{\mathrm{Me_2Si}}\text{-}\mathrm{CH_2}\text{-}\mathrm{CH_2}\text{-}\underset{\mathrm{Cl}}{\mathrm{SiMe_2}} \quad (1)$$

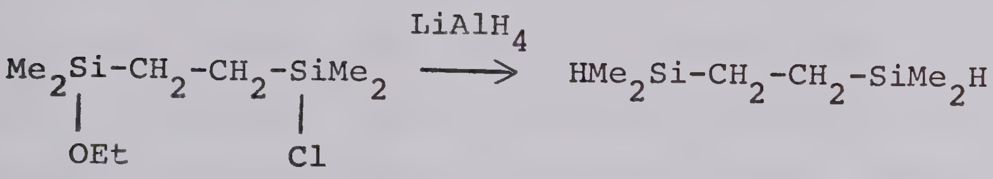

$$\underset{\mathrm{OEt}}{\mathrm{Me_2Si}}\text{-}\mathrm{CH_2}\text{-}\mathrm{CH_2}\text{-}\underset{\mathrm{Cl}}{\mathrm{SiMe_2}} \xrightarrow{\mathrm{LiAlH_4}} \mathrm{HMe_2Si}\text{-}\mathrm{CH_2}\text{-}\mathrm{CH_2}\text{-}\mathrm{SiMe_2H} \quad (2)$$

The intermediate in this preparation, 1-(dimethylethoxysilyl)-2-(dimethylchlorosilyl)ethane, was not isolated, but was reduced directly with $LiAlH_4$ to yield 1,2-bis-(dimethylsilyl)ethane. This silane has been prepared before by the $LiAlH_4$ reduction[196] of the somewhat less readily available 1,2-bis(dimethylchlorosilyl)ethane.[197-199]

In general, the silane reacted either thermally or with ultraviolet irradiation with carbonyls of the iron group to produce the anticipated chelate complexes 13, 14, and 15. These have been fully characterized by

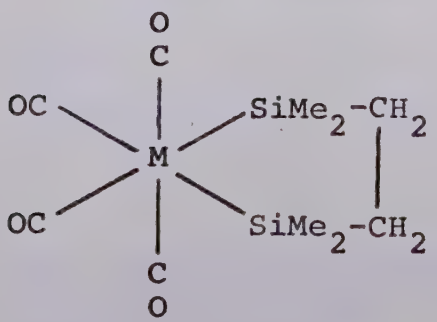

13, M = Fe

14, M = Ru

15, M = Os

analysis, mass spectrometry, infrared, and nmr spectroscopy (^1H and ^{13}C).[92]

Compound **13** was prepared by reaction of $Fe(CO)_5$ with the silane under ultraviolet irradiation; it is a yellow, air-sensitive compound, decomposing slowly in solution or on storage to form $Fe_3(CO)_{12}$ and $Fe_2(CO)_9$.

The much more stable ruthenium and osmium derivatives **14** and **15** were prepared in a nearly quantitative reaction of the silane with $M_3(CO)_{12}$ at 175° and 1000 psi of CO.* They are white waxy solids. Solutions of **14** and **15** in *n*-heptane showed no change in infrared spectra after a 24-hour exposure to the atmosphere.

Complexes **13** - **15** have C_2 symmetry, taking into account the nonplanar character of the five-membered chelate ring. Four carbonyl stretching bands are expected, and observed in **13** and **14** (cf. Table IX); three bands are observed in **15**, no doubt owing to accidental degeneracy.

Reaction of cobalt carbonyl with excess silane at room temperature produced white, crystalline $(OC)_4CoSiMe_2CH_2CH_2Me_2SiCo(CO)_4$, **16**, a rather unstable compound particularly in solution. Formation of this non-chelated compound indicates an alternative reaction pathway for the silane. The reaction presumably proceeds *via* $HSiMe_2CH_2CH_2Me_2SiCo(CO)_4$, although this intermediate

---

* The reaction of **14** with cyclooctatetraene has recently been described.[200]

was not observed; reaction of the second silicon-hydrogen bond with another molecule of $Co_2(CO)_8$ [or $HCo(CO)_4$] must then be preferred to chelation, since the latter would be expected to form a rather improbable cobalt(III) complex.

The infrared spectrum of 16 is as expected for noninteracting cobalt tetracarbonyl groups. The E mode is not split[201] since the threefold symmetry is not sufficiently perturbed by the rather similar methyl and methylene substituents on silicon. The appearance of a weak shoulder on the higher energy side of the 2089 cm^{-1} band is unusual; we can offer no explanation but believe that it is genuine.

An iron complex closely related to 16, $[(\eta^5\text{-}C_5H_5)Fe(CO)_2SiMe_2CH_2]_2$, has recently been prepared by reaction of the metal carbonyl anion with 1,2-bis(dimethylchlorosilyl)ethane.[202] The iron compound appears to be more stable.

2.1 NMR Spectra

Proton nmr spectra of all compounds (Table IX) show singlets for the methylene and methyl protons of the silane ligand. In the chelate compounds 13-15, this indicates that the expected rapid ring inversion is taking place resulting in a time-averaged C_{2v} symmetry.

Carbon-13 nmr data for compounds 13-15 are shown in Table X. The chemical shifts of the carbonyl carbons move

Table IX

Infrared and ^{1}H NMR Data of 1,2-bis(Dimethylsilyl)ethane Derivatives

Compound	Carbonyl stretching bands[a]	^{1}H nmr spectrum[c] CH_2	CH_3
13	2068(6.7), 2003(7.0), 2000(3.6),[b] 1978(10)	9.00	9.44
14	2091(4.4), 2032(6.3), 2024(8.3), 2010(10)	9.12	9.55
15	2096(2.3), 2028(4.8), 2012(10)	9.12	9.42
16	2091(4.0),[b] 2089(7.6), 2028(8.5), 1995(10)	8.87	9.38

[a] In *n*-heptane solution. Band positions in cm^{-1} with intensities in parenthesis relative to the strongest band as 10, using a percent transmission scale.

[b] Shoulder.

[c] Values on τ scale, $CDCl_3$ solution.

Table X

^{13}C NMR Data of 1,2-bis(Dimethylsilyl)ethane Derivatives[a]

Compound	Chemical shifts				
	CO_{ax}	CO_{eq}	CH_2	CH_3	$\delta_{ax} - \delta_{eq}$
13	208.89	207.86	17.54	8.37	1.03
14[b]	198.18	193.58	17.95	4.70	4.60
15	181.00	175.50	17.92	3.89	5.50

[a] Chemical shifts in toluene-d_8 on the δ scale relative to tetramethylsilane. Axial and equatorial CO groups defined so that the central metal atom and the two silicon ligands lie in the equatorial plane, as shown in text.

[b] In $CDCl_3$.

to higher field along the series Fe, Ru, Os. This trend parallels that observed in the hexacarbonyls of Cr, Mo, and W.[104] A second important trend is the increasing separation between axial and equatorial ^{13}CO shifts along the Fe, Ru, Os series. No trend of this kind seems to have been noted previously for carbonyls of any periodic group.

In Table X, the ^{13}CO resonance at lower field is assigned as axial. Previously, assignment of carbonyl resonances in *cis*-$M(CO)_4L_2$ complexes has not been possible.[66] We base our assignment on a study of *cis*-$Os(CO)_4H_2$, in which the proton-coupled ^{13}C nmr spectrum unambiguously identifies the two carbonyl resonances (see also Chapter II, section 2.1.).

The ^{13}C nmr spectra clearly establish that compounds **13**-**15** are stereochemically rigid on the nmr time scale at ambient temperature. As noted above, it was of interest to examine the possibility of axial-equatorial carbonyl exchange in these compounds, where the chelate ligand eliminates the possibility that such interchange could occur *via* a trans isomer. The compounds were therefore examined at higher temperatures (80° for **13**, 160° for **14**, and 90° for **15**), and found to be rigid at these temperatures also. Higher temperatures resulted in decomposition. This finding enables a very crude lower limit of about 20 kcal mol^{-1} to be assigned to the free energy of activation

for the exchange process.* Actually, one would expect the barrier for such an exchange in an octahedral complex to be a great deal higher.[53,57]

The usual problem in an nmr study of fluxional or nonrigid processes is to obtain the low temperature limiting spectra; the large chemical shift differences characteristic of ^{13}C nmr will aid in the solution of this problem. However, in the present case, where the barrier to exchange is expected to be reasonably high, large shift differences are disadvantageous since higher temperatures will then be required for coalescence.

The ^{13}C nmr spectra of a number of tetracarbonylmolybdenum glyoxal bis(arylimines), 17, have shown axial-equatorial carbonyl interchange,

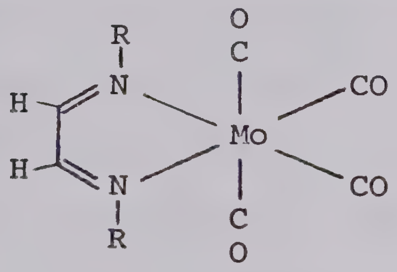

17

R = *p*-tolyl, *o*-tolyl, 2,6-dimethylphenyl, and
2,4,6-triisopropylphenyl[203]

and the free energies of activation for this process varied between 10 and 13 kcal mol^{-1}.[203] It was argued, although not

---

* Given the low temperature limiting axial-equatorial ^{13}CO shift difference of 104 Hz for compound 14, the value of $\Delta G^{\dagger}$ quoted here is that which would result in coalescence at 160°.

conclusively proved, that the rearrangement process was intramolecular and that it occurred *via* a trigonal-prismatic transition state.[203]

3. Experimental Section

Reactions were carried out under an atmosphere of dry, oxygen-free nitrogen. Solvents were distilled from $LiAlH_4$ and saturated with nitrogen. Carbonyls of ruthenium[128] and osmium[129] were prepared by literature methods. All other starting materials were commercially available, and were used as received except for $Co_2(CO)_8$, which was sublimed.

Infrared spectra in the carbonyl region were scanned at 39 cm^{-1} min^{-1} using a Perkin Elmer Model 337 grating spectrometer fitted with an external recorder. Spectra were referenced with gaseous CO, and reported bands are considered accurate to ± 1 cm^{-1}.

Mass spectra were taken with Associated Electrical Industries MS-9 or modified MS-2 instruments. Samples were introduced by direct evaporation or sublimation, at temperatures just sufficient to produce the spectrum. All compounds showed the expected molecular ions (Table XI) with consecutive loss of CO and CH_3 as the dominant feature.

Proton nmr spectra were measured on Varian A-60 and HA-100 spectrometers. Natural abundance ^{13}C nmr spectra were recorded on a Bruker HFX-90 spectrometer as described in Chapter II. Toluene-d_8 or $CDCl_3$ solutions were employed

to obtain spectra at temperatures below 100°; a spectrum of **14** at 160° was measured in *o*-dichlorobenzene. Spectra were assigned using the off-resonance technique. The ^{13}C chemical shifts were converted to the external TMS scale using as reference $CDCl_3$ or the quaternary carbon from toluene-d_8, whose chemical shifts, on the TMS scale, were taken as 77.09 and 137.46 ppm, respectively. The error in chemical shifts is believed to be ± 0.06 ppm.

The melting points (Table XI) were determined on a Unimelt Thomas Hoover apparatus or with a Kofler hot-stage.

Microanalyses were performed by Alfred Bernhardt Microanalytische Laboratorium, Bonn, West Germany, and by the microanalytical laboratory of this department. See Table XI for analytical data.

Preparation of 1,2-bis(dimethylsilyl)ethane

A mixture of 110.6 g (0.85 moles) dimethylvinylethoxysilane and 2 drops of hexachloroplatinic acid in isopropanol (0.1 *M*), was heated at 75° and 88.5 g (0.94 moles) of dimethylchlorosilane was added in dropwise fashion with stirring. The rate of addition was adjusted so that the temperature of the reaction mixture did not exceed 90°. After the addition was complete, the mixture was refluxed for 3 hr. The resulting 1-(dimethylethoxysilyl)-2-(dimethylchlorosilyl)ethane was added dropwise to a slurry of 90 g (2.37 moles) of $LiAlH_4$ in 1000 ml anhydrous ether and refluxed for 8 hr. The ether was then replaced by 1.5 l.

Table XI

Elemental Analysis, Melting Points, and Molecular Weights[a] of 1,2-bis(Dimethylsilyl)ethane Derivatives

Compound	Calculated			Found			mp
	mol. wt.	C	H	mol. wt.	C	H	
13	312	38.47	5.16	312	37.54	5.41	58-60°
14	358	33.60	4.51	358	33.20	4.79	91-92°
15	448	26.89	3.61	448	26.49	3.82	98-100°
16	486	34.58	3.32	486	34.37	3.56	128-30° (dec)

---

[a] Determined by mass spectrometer. Values quoted refer to the most intense peak of the isotopic multiplet due to the particular ion.

of Skelly B (petroleum ether bp 50-80°) and the $LiAlH_4$ residue removed by filtration. The mixture was fractionally distilled, affording 69.4 g of 1,2-bis(dimethylsilyl)-ethane (bp 115 - 20/704 mm, yield 55.8%).

Preparation of 1,2-bis(dimethylsilyl)ethane tetracarbonyliron, **13**.

A mixture of 2.01 g (10.3 mmoles) $Fe(CO)_5$ and 1.815 g (12.4 mmoles) of the silane in 215 ml Skelly B was irradiated with a 450 watt ultraviolet lamp for 45 min. The solvent was evaporated in vacuum (10 mm). An infrared spectrum showed bands of an impurity, presumably a hydrido species, in addition to the main product. Room temperature sublimation of the resulting black oil yielded 1.64 g (51.2%) of the product as a waxy yellow solid. No further sublimation took place, but the residue underwent extensive decomposition to $Fe_3(CO)_{12}$ and $Fe_2(CO)_9$.

Preparation of 1,2-bis(dimethylsilyl)ethane tetracarbonylruthenium, **14**.

A sample of $Ru_3(CO)_{12}$ (1.400 g, 2.2 mmoles), the silane (1.45 g, 9.9 mmoles), and Skelly B (30 ml) were placed in a 200-ml Parr autoclave which was pressurized with CO to 1000 psi. The autoclave was heated, with stirring, at 175° for 20 hr, cooled, and the gases were vented. The solvent was evaporated at reduced pressure (10 mm) and the remaining solid material was sublimed

onto a water cooled probe at 0.005 mm Hg and room temperature, to give 2.085 g (88.8%) of colorless waxy solid.

Preparation of 1,2-bis(dimethylsilyl)ethane tetracarbonylosmium, **15**.

Triosmium dodecacarbonyl (0.50 g, 0.55 mmoles) and the silane (0.637 g, 4.35 mmoles) were brought to reaction and worked up exactly as just described. Sublimation afforded 0.66 g (89.3%) of colorless waxy product.

Preparation of 1,2-tetracarbonylcobaltdimethylsilyl)ethane, **16**.

A sample of $Co_2(CO)_8$ (1.95 g, 5.7 mmoles) and 1,2-bis(dimethylsilyl)ethane (2.5 g, 17.1 mmoles) were placed in a Schlenk tube, and stirred under nitrogen for 1.5 hr. A vigorous evolution of hydrogen was observed during the first 15 min. of reaction. Addition of *n*-pentane (20 ml) to the brown paste precipitated the product as a white, crystalline material. Filtration at 0° gave 1.0 g of **16**, yield 36.1%. The analytical sample was recrystallized from CH_2Cl_2. Compound **16** can be handled in air for short periods, but decomposes rapidly in solution to give $Co_2(CO)_8$.

CHAPTER VII

CARBON-13 NMR STUDIES OF IRON, RUTHENIUM, OSMIUM, MANGANESE, AND RHENIUM CARBONYL HYDRIDES AND IODIDES.

1. Introduction

Over the last six years there have been an increasing number of reports on the stereochemically nonrigid behavior of six-coordinate complexes in solution. Undoubtedly, the most studied were compounds of the type ML_4H_2, where M = Fe, Ru; L = phosphine and phosphite.[155-157,204,205] The presence of the hydride ligands seemed to confer dynamic properties to these molecules.

On the other hand, recent reports from this laboratory have provided a new class of stereochemically nonrigid six-coordinate molecules. These are compounds of the type $M(CO)_4(ER_3)_2$, where M = Fe, Ru, Os; E = Si, Ge, Sn, Pb; E = organic group and halogen, and they have been investigated by ^1H nmr,[90] and especially by ^{13}C nmr (see Chapter IV).[96-98]

We have extended our ^{13}C nmr investigations to $M(CO)_4X_2$ and $M'(CO)_5X$ derivatives (M = Fe, Ru, Os; M' = Mn, Re; X = H, I) and the results of this study are presented here. Without doubt, the favourite of this chapter is $Fe(CO)_4H_2$, the first,[206,207] and the most celebrated (infrared,[208,209] Raman,[210] ^1H nmr,[211,212] Mossbauer,[208,213] and electron diffraction[177] studies) of all transition

metal carbonyl hydrides. A new and improved (although slightly unconventional) way of preparing this hydride is described here as well under the generic name of "Polar Night Synthesis." New high yield preparative methods for $M(CO)_4I_2$ (M = Ru, Os) and $M'(CO)_5I$ (M' = Mn, Re) are also given.

2. Results and Discussion

Compounds of the type $M(CO)_4X_2$ may exist in solution as cis, trans, or as a mixture of cis and trans isomers. Infrared spectroscopy has most often been used to distinguish among these possibilities on the basis that four infrared active bands are expected for a cis isomer of C_{2v} symmetry, and one for a trans isomer of D_{4h} symmetry. However, accidental degeneracy of the single band for the trans isomer with one of the four cis bands renders this method unreliable.[97]

Carbon-13 nmr has become a powerful tool in the study of such derivatives. For a *cis*-$M(CO)_4X_2$ derivative two ^{13}CO resonances of equal intensity are expected, while for a *trans*-$M(CO)_4X_2$ derivative only one ^{13}CO resonance of twice the intensity of cis resonances is expected. This indeed was observed for the *cis*-$M(CO)_4X_2$ derivatives (M = Fe, Ru, Os; X = H, I) studied here with the single exception $Fe(CO)_4H_2$ noted below. The ^{13}C chemical shift values are given in Table XII, and will be discussed below.

2.1 Assignment of ^{13}CO Resonances

The two ^{13}CO resonances of *cis*-$M(CO)_4H_2$ (M = Ru, Os) may be unambiguously assigned from the proton-coupled ^{13}C nmr spectra which show an A_2X pattern at lower field for the axial carbonyls and an AA'X pattern for the equatorial carbonyls at higher field (page 140). This is in agreement with previous findings in the *cis*-$M(CO)_4(ER_3)_2$ series (Chapter II), where, for the great majority of cases, the ^{13}C resonance of the carbonyl trans to the one-electron donor ligand was at higher field.

The coupling constant method of assigning ^{13}CO resonances failed for *cis*-$Os(CO)_4Me_2$ because the $^3J(^1H-^{13}CO)$ coupling was too small to be resolved. Attempts to assign ^{13}CO resonances using 34% ^{13}C-enriched *cis*-$Os(CO)_4(^{13}CH_3)_2$ were also unsuccessful for similar reasons.

The assignment of ^{13}CO resonances in *cis*-$M(CO)_4I_2$ derivatives (M = Fe, Ru, Os) was assumed to be the same as for the hydrido species.

On the other hand, for $M'(CO)_5X$ derivatives, the assignment seems straightforward as two ^{13}CO resonances of relative intensity 4:1, due to the radial and axial carbonyls, are expected. This indeed was observed for $Re(CO)_5H$ (Table XII). However, the ^{13}C nmr spectra of $Mn(CO)_5H$, $Mn(CO)_5I$, and $Re(CO)_5I$ showed only one broad peak at room temperature. This is due to the quadrupole moment of the ^{55}Mn, ^{185}Re, and ^{187}Re isotopes, which can potentially broaden the

signals of carbon atoms bound directly to them.[102] The radial and axial ^{13}CO resonances can nevertheless be resolved by "thermal decoupling," a method long known in ^{11}B nmr,[214] but only recently applied to ^{13}C nmr.[102] Thus, Figure 19 shows the variable temperature ^{13}C nmr spectra of ^{13}CO-enriched $Re(CO)_5I$ (20° spectrum in toluene-d_8; -30° and -50° spectra in toluene-d_8 : CD_2Cl_2 (1:1)). At room temperature the half width of the single ^{13}CO resonance is 7 Hz. Lowering the temperature causes a dramatic narrowing of this resonance, to 3.6 Hz at -50°, such that the ^{13}CO signal due to the axial carbonyl may be clearly resolved.

We would like to stress, however, that "cooling down" a sample is not necessarily sufficient to observe "thermal" decoupling.* For example, we determined the ^{13}C nmr spectrum of $Mn(CO)_5H$ in CD_2Cl_2 at -70°, which was no better (as far as the half width of the carbonyl resonance was concerned) than the spectrum of the same compound at -30° in toluene-d_8 (half width 20 Hz). It seems that the viscosity of the solvent may be more important than the temperature factor in "thermal" decoupling. The resonances due to the radial and axial carbonyls of $Mn(CO)_5H$ were resolved at -80° in toluene-d_8 : CD_2Cl_2 (3:1). The sample was ^{13}CO-enriched. The half width of the resonances due to the radial carbonyls was 6.2 Hz.

---

* Helpful discussions with Dr. J. Takats on this point are greatfully acknowledged.

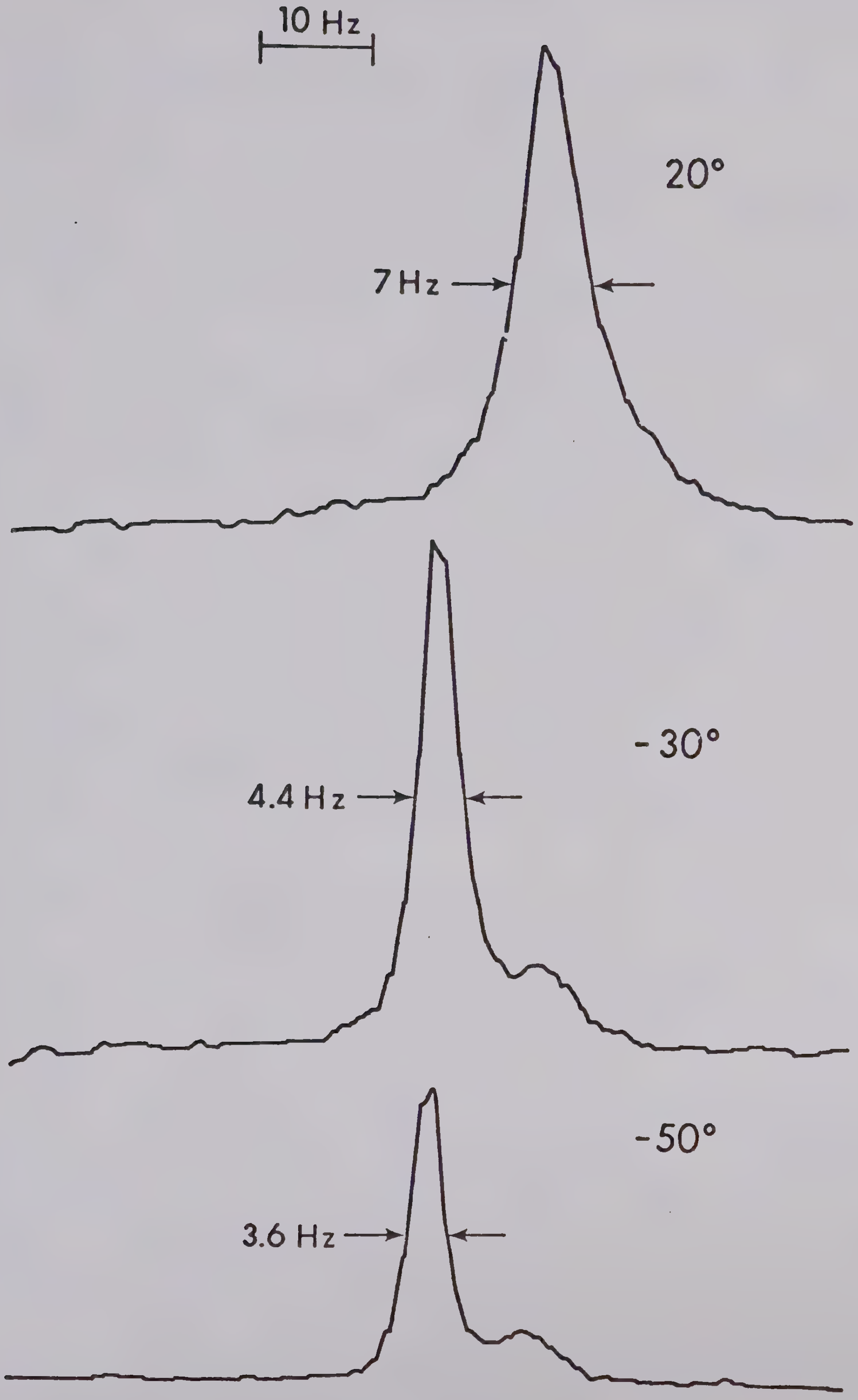

Figure 19. Variable temperature ^{13}C nmr spectra (carbonyl portion) of $Re(CO)_5I$ in toluene-d_8 (top spectrum) and toluene-d_8 : CD_2Cl_2 (1:1).

In all $M'(CO)_5X$ derivatives studied here, the ^{13}C resonance of the axial carbonyl (in trans to the one-electron donor) is at higher field than the ^{13}C resonance of the radial carbonyls. This was found to be true for other pentacarbonylmanganese and pentacarbonylrhenium derivatives which have been investigated.[60,101,102]

The axial ^{13}CO resonance of $Mn(CO)_5I$ was not observed despite a careful search. Only one ^{13}CO peak was observed in toluene-d_8 at -90° (half width 6.7 Hz) or in CF_2HCl at -110° (half width 1.5 Hz). It may be that the axial and radial carbonyl resonances are accidentally degenerate in this compound. The chemical shift difference between radial and axial ^{13}CO resonances decreases on going from $Re(CO)_5H$ to $Re(CO)_5I$ (Table XII), and the same may also apply to $Mn(CO)_5H$ and $Mn(CO)_5I$.

The ^{13}C nmr spectrum of $Mn(CO)_5I$ was run using a ^{13}CO-enriched sample. Although slight preferences in the ^{13}CO exchange of $Mn(CO)_5Br$ have been noted,[215] our exchange time ensured enrichment in both radial and axial positions. Therefore, another possibility could be ^{13}C - ^{13}C coupling between radial and axial carbonyl carbons which could broaden considerably the axial signal.

2.2 Carbon-13 Chemical Shifts

The ^{13}C chemical shift values are given in Table XII. The ^{13}C nmr of $Fe(CO)_4H_2$ at -80° shows only one resonance rather than the expected two resonances. This aspect will be fully discussed below.

The ^{13}CO resonances are shifted upfield on descending a group of the periodic table or on going to the right of a given period. Thus, the order of shielding is Fe < Ru < Os, Mn < Re, Mn < Fe, and Re < Os. This was also observed in Chapter II, and it may be rationalized using the π back-bonding theory of ^{13}C chemical shifts (page 43).

Substitution of the group X has a marked effect on ^{13}CO chemical shifts. For example, in *cis*-$Os(CO)_4Me_2$, the ^{13}CO resonances are shifted upfield by 9 and 16 ppm as compared to $Os(CO)_5$.* The corresponding upfield shift in *cis*-$Os(CO)_4H_2$ is 13 and 15 ppm. In *cis*-$Os(CO)_4I_2$, the upfield shift is even more pronounced, 27 and 30 ppm with regard to $Os(CO)_5$!

The dramatic shielding effect of iodine has long been known, although it has not been satisfactorily explained.

---

* The ^{13}C nmr of $Os(CO)_5$ in toluene-d_8 shows one resonance at 182.67 ppm down to -70°. Presumably, the molecule is stereochemically nonrigid

Table XII

^{13}C Chemical Shifts and ^{13}C-^{1}H Coupling Constants in *cis*-$M(CO)_4X_2$ and $M'(CO)_5X$ Derivatives.[a]

Compound	CO_{ax}	CO_{eq}	Coupling Constants[b]			Temp °K
$Fe(CO)_4H_2$	205.27			9[c]		193[d]
$Ru(CO)_4H_2$	192.54	190.11				223
	192.64	190.43	7	7	19	223[e]
$Os(CO)_4H_2$	173.55	171.55	8	7	13	300
$Fe(CO)_4I_2$	204.57	198.47				298
	204.46	197.82				303[f]
$Ru(CO)_4I_2$	178.24	177.75				303[f]
$Os(CO)_4I_2$	159.60	156.39				303[f]
$Os(CO)_4Me_2$[g]	177.70	170.58				303
$Mn(CO)_5H$	210.82	211.36	7		14	193[h]
$Mn(CO)_5I$	...[i]	205.37				183
$Re(CO)_5H$	182.67	183.21	8		7	293
$Re(CO)_5I$	176.13	176.51				223[j]

Footnotes to Table XII

[a] Chemical shifts in ppm downfield from TMS; coupling constants in Hz. Solvent is toluene-d_8 except as noted. For *cis*-$M(CO)_4X_2$ derivatives, axial and equatorial groups defined so that the central metal atom and the two X ligands lie in the equatorial plane. For $M'(CO)_5X$ derivatives, the axial CO is the one in trans to X.

[b] The three coupling constants given for *cis*-$M(CO)_4H_2$ derivatives represent $^2J(^1H-^{13}CO_{ax})$, $^2J(^1H_{cis}-^{13}CO_{eq})$, and $^2J(^1H_{trans}-^{13}CO_{eq})$, respectively. The two coupling constants given for $M'(CO)_5H$ represent $^2J(^1H-^{13}CO_{ax})$ and $^2J(^1H-^{13}CO_{eq})$, respectively.

[c] Average value of the three coupling constants (see text). Solvent methylcyclohexane-d_{14}, temperature 223° K.

[d] CD_2Cl_2 : CF_2HCl (3:1) solvent.

[e] Methylcyclohexane-d_{14} solvent.

[f] CD_2Cl_2 solvent

[g] Chemical shift of $^{13}CH_3$ -7.60 ppm; $^1J(^1H-^{13}CH_3) = 131$ Hz.

[h] Toluene-d_8 : CD_2Cl_2 (3:1) solvent.

[i] Resonance not observed, see text.

[j] Toluene-d_8 : CD_2Cl_2 (1:1) solvent.

For example, the ^{13}C chemical shifts of CH_4, CH_3I, CH_2I_2, CHI_3, and CI_4 are -2.1,[216] -20.5, -53.8, -139.7,[217] and -292.3[218] ppm, respectively. The last value represents the most shielded carbon nucleus yet recorded in a diamagnetic compound. The shielding of carbon atoms by the adjacent iodine atom(s) is often referred to, by organic chemists, as the "heavy atom effect." It was suggested that the pronounced upfield shifts exhibited by iodo derivatives may be due to differences in the spin-pairing features associated with electron delocalization.[217]

The upfield shifts observed on replacing a hydrogen by iodine in ruthenium and osmium derivatives were between 12-15 ppm. This effect was less marked for iron, manganese, and rhenium derivatives, where the upfield shift was 5-7 ppm.

It is interesting to note that the chemical shift difference between axial and equatorial ^{13}CO resonances in the iron, ruthenium, and osmium derivatives varied from 0.5 to 6 ppm. However, the corresponding difference between radial and axial ^{13}CO resonances in manganese and rhenium derivatives was considerably smaller (0.4-0.5 ppm).

The ^{13}C nmr of $Mn(CO)_5H$ has been determined before,[219] and two very broad resonances (width of approximately 75 Hz) at 0.1 (intensity 1) and -17.7 ppm (intensity 4) with respect to carbon disulfide were reported. On the TMS

scale,* these values would correspond to 192.7 and 210.5 ppm, respectively. Although the chemical shift of the radial carbonyl resonance is fairly close to the value given in Table XII, we believe that the chemical shift of the axial carbonyl, as reported by these authors,[219] is in error. The half width of our radial ^{13}CO resonance at -80° was 6.2 Hz (page 133), just sufficient to resolve the axial ^{13}CO resonance. Also, the $^2J(^1H-^{13}CO)$ coupling constants determined by us from the proton-coupled ^{13}C nmr spectrum (Table XII) were identical with the values obtained by ^1H nmr of ^{13}CO-enriched $Mn(CO)_5H$.[220]

2.3 Carbon-13 Coupling Constants

The $^1H-^{13}C$ coupling constants observed in *cis*-$M(CO)_4H_2$ and $M'(CO)_5H$ derivatives (M = Fe, Ru, Os; M' = Mn, Re) are given in Table XII. As described previously, the proton-coupled ^{13}C nmr spectrum of a *cis*-$M(CO)_4H_2$ derivative is expected to show an A_2X system for the axial carbonyls and an AA'X system for the equatorial carbonyls. This indeed was observed for *cis*-$Ru(CO)_4H_2$ and *cis*-$Os(CO)_4H_2$ (Figure 20), although of the six lines expected for the X part of the AA'X system,[222,223] only the four strong intensity lines were resolved. Thus the equatorial carbonyl resonance appeared as a doublet of doublets. The AA' part of the

---

* The ^{13}C chemical shift of CS_2, on the TMS scale, is 192.8 ppm.[221]

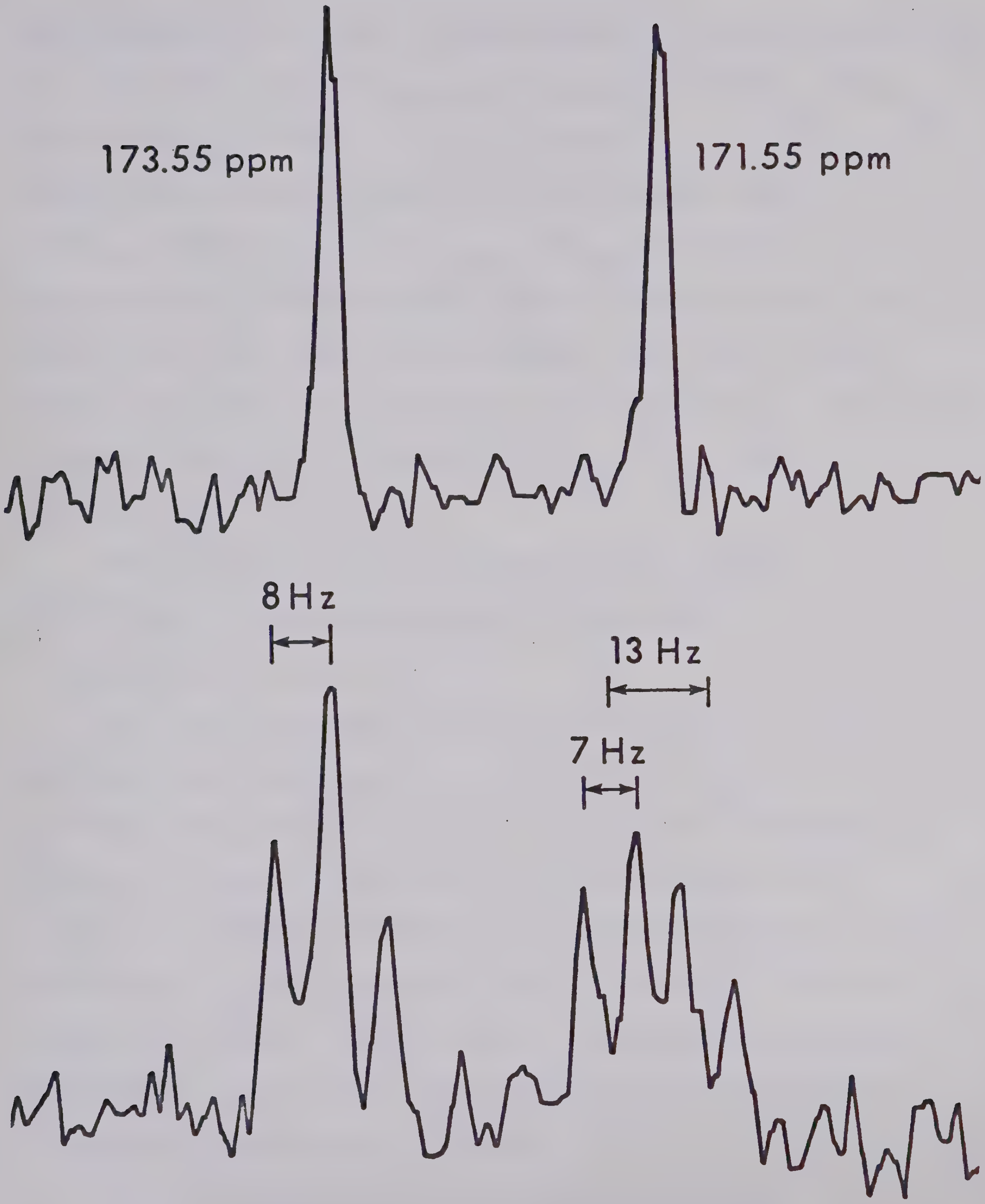

Figure 20. Proton-decoupled (top) and -coupled ^{13}C nmr spectra of *cis*-Os(CO)$_4$H$_2$ in toluene-d$_8$.

AA'X system, i.e., the ^{13}C satellites in the ^{1}H nmr spectrum, was also difficult to analyse. Therefore, $^{2}J(^{1}H_{cis}-^{13}CO_{eq})$ and $^{2}J(^{1}H_{trans}-^{13}CO_{eq})$ values in Table XII are approximate only, having been obtained by a first-order analysis. The $^{2}J(^{1}H_{cis}-^{13}CO_{eq})$ and $^{2}J(^{1}H_{trans}-^{13}CO_{eq})$ could not be experimentally distinguished, and it was assumed that the larger was due to the trans coupling. The value of the trans coupling in *cis*-Ru$(CO)_4H_2$ and *cis*-Os$(CO)_4H_2$ was larger than the other two couplings, $^{2}J(^{1}H_{cis}-CO_{eq})$ and $^{2}J(^{1}H-CO_{ax})$.

For *cis*-Os$(CO)_4H_2$, it was possible to observe $^{1}J(^{189}Os-^{1}H) = 40.5$ Hz from the ^{1}H nmr spectrum in toluene-d_8.

The axial and equatorial ^{13}CO resonances of Fe$(CO)_4H_2$ were not resolved even at very low temperatures (see below), and the proton-coupled ^{13}C nmr spectrum at -50° showed a binomial triplet indicating equivalent carbonyls and protons at this temperature. The observed coupling constant (Table XII) would correspond to the average of the three coupling constants expected for a cis molecule, or to the weighted average of the coupling constants expected for a mixture of cis and trans isomers.

For M'$(CO)_5H$ derivatives, the cis and trans $^{2}J(^{1}H-^{13}CO)$ coupling constants were readily observed in the proton-coupled ^{13}C nmr spectrum of Re$(CO)_5H$, although very low temperature and ^{13}C enrichment were required to resolve

these couplings in $Mn(CO)_5H$. The ^1H-^{13}CO coupling constants for $Mn(CO)_5H$ were reported previously from the ^1H nmr spectrum,[220] and we confirm these values. As noted earlier,[220] the cis coupling in $Mn(CO)_5H$ was larger than the trans coupling. However, the situation reverses for $Re(CO)_5H$, and the trans coupling is slightly larger than the cis coupling.

2.4 Stereochemical Nonrigidity

From the dynamic nuclear magnetic viewpoint, molecules are divided into two main classes: stereochemically nonrigid molecules, which exhibit internal rotations, conformational flips, "ring whizzing," proton transfers, or polytopal rearrangements on the nmr time scale, and "other" types of molecules, which show none of these phenomena on the nmr time scale, and have recently been referred to as "the dog in the night-time."57

Of all compounds described in this chapter, only one, $Fe(CO)_4H_2$ was found to be stereochemically nonrigid. The infrared[208,209] and Raman[210] spectrum of $Fe(CO)_4H_2$ indicate cis geometry in solution. However, the proton-decoupled ^{13}C nmr of this compound in CD_2Cl_2 : CF_2HCl (3:1) showed a single ^{13}CO resonance at -80°, with a width at half height ($W_{1/2}$) of 3 Hz. At -100°, the spectrum showed a very broad, flat peak, with $W_{1/2}$ = 16 Hz, which could be

due to the two resonances of *cis*-Fe(CO)$_4$H$_2$.* This is shown in Figure 21. Spectra at lower temperature could not be obtained because of the reduced solubility of the compound.

The proton-coupled ^{13}C nmr spectrum of Fe(CO)$_4$H$_2$ in methylcyclohexane-d$_{14}$ showed a binomial triplet at -50°, thus proving the intramolecular nature of the rearrangement process. Presumably, the carbonyl rearrangement process in *cis*-Fe(CO)$_4$H$_2$ occurs *via* the trans isomer, as indicated in Chapter IV for M(CO)$_4$(ER$_3$)$_2$ derivatives.

The ^{13}C nmr of *cis*-Ru(CO)$_4$H$_2$ showed stereochemical rigidity on the nmr time scale at -50° and -20°. Higher temperatures were not attempted because of the low thermal stability of this compound. Similarly, *cis*-Os(CO)$_4$H$_2$ and *cis*-Os(CO)$_4$Me$_2$ were rigid at room temperature and at 90°.

The room temperature ^{13}C nmr spectra of *cis*-Fe(CO)$_4$I$_2$ in toluene-d$_8$ or CD$_2$Cl$_2$ showed two resonances due to the axial and equatorial carbonyl groups. However, when the ^{13}C nmr spectrum of *cis*-Fe(CO)$_4$I$_2$ was determined in a mixture of toluene-d$_8$ and CHCl$_3$ and no precaution was taken against exposing the sample to the light, a peak at 199.76 ppm was observed in addition to the two resonances mentioned above. It is interesting to speculate that this resonance is due to the trans isomer of this species.

---

* The $\Delta G^{\dagger}$ value for the carbonyl rearrangement in this molecule, assuming a chemical shift difference of 10 Hz, and a coalescence temperature of -100°, is 8.6 kcal mol^{-1}.

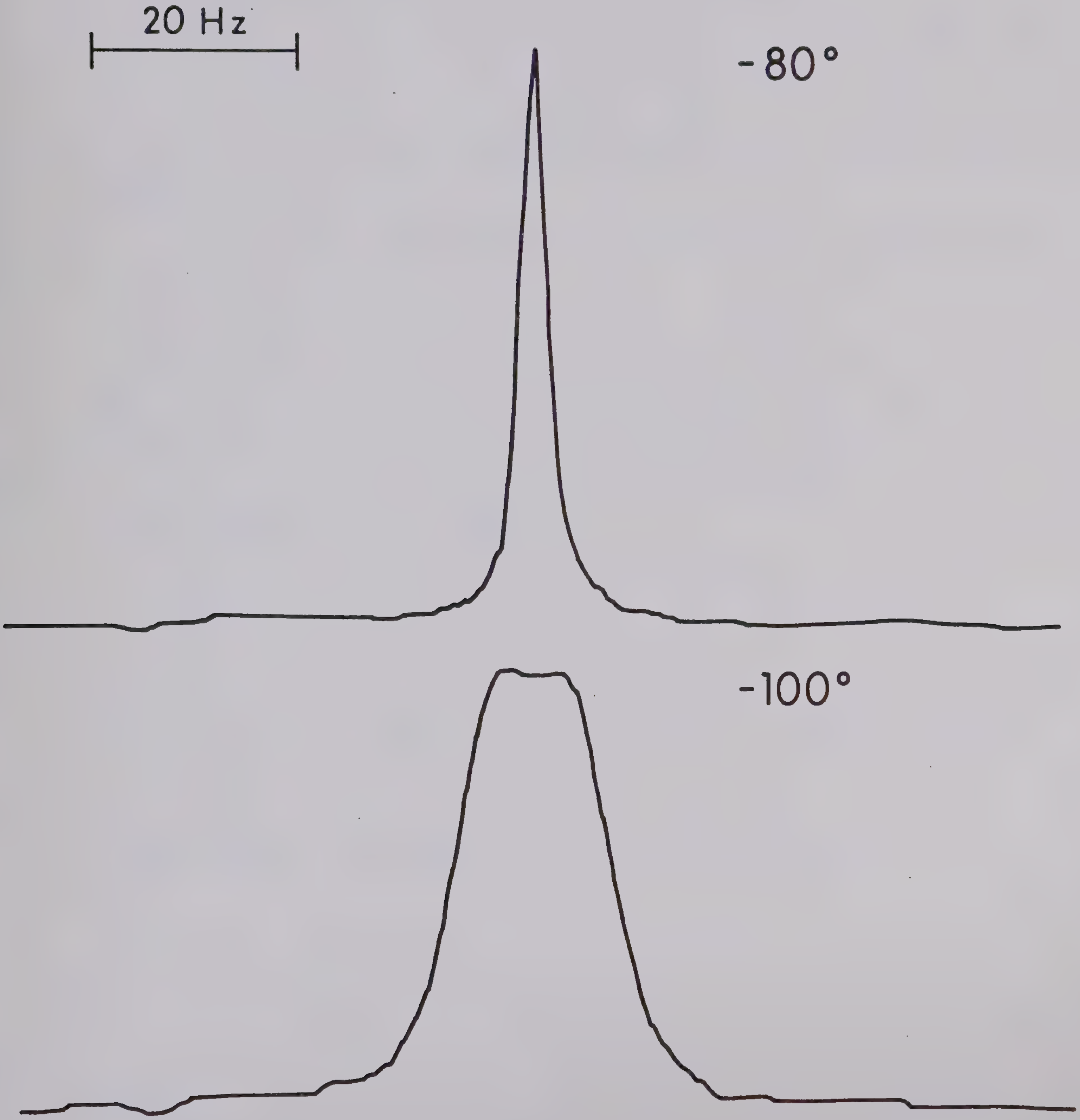

Figure 21. Variable temperature ^{13}C nmr spectra of *cis*-$Fe(CO)_4H_2$ in CD_2Cl_2 : CF_2HCl (3:1).

The conversion of *cis*-$Fe(CO)_4I_2$ to the trans isomer, in light, was much investigated earlier.[187] An attempt has been made to determine the ^{13}C nmr spectrum of *cis*-$Fe(CO)_4I_2$ (^{13}CO enriched sample in toluene-d_8 solution, degassed and sealed under vacuum) above room temperature. However, the compound decomposed rapidly as the probe was heated to 80°.

An electron diffraction study[177] of *cis*-$Fe(CO)_4H_2$ showed significant distortion from a regular octahedron such that the geometry of this compound could be best described as pseudo-bicapped tetrahedral (page 106). Perhaps this could explain the low barrier for carbonyl rearrangement in this complex.

On the other hand, the X-ray structure of *cis*-$Ru(CO)_4I_2$,[224] and the neutron and X-ray diffraction study of $Mn(CO)_5H$[225] showed considerably smaller deviations from regular octahedral geometry. Both of these compounds were found to be stereochemically rigid on the nmr time scale, under the conditions stated in Table XII.

3. Experimental Section

NMR instrumentation and technique has been described in Chapter II. The proton-coupled ^{13}C nmr spectrum of *cis*-$Os(CO)_4H_2$ has been determined using gated decoupling.

Reactions were carried out under an atmosphere of dry, oxygen-free nitrogen or argon. Solvents were distilled from $LiAlH_4$ and saturated with nitrogen. Nmr solvents were dried over $CaCl_2$.

Carbonyls of ruthenium[128] and osmium[129] were obtained by literature methods. All other starting materials were commercially available and were used as received.

Preparation of *cis*-$Ru(CO)_4H_2$,[226] *cis*-$Os(CO)_4H_2$,[227] $Mn(CO)_5H$,[228] $Re(CO)_5H$,[229] *cis*-$Fe(CO)_4I_2$,[230] and *cis*-$Os(CO)_4Me_2$[139] was carried out according to published procedures.

"Polar Night Synthesis": Preparation of *cis*-$Fe(CO)_4H_2$

Although the preparation of this compound has been described recently,[208] we give here a modification of the above procedure which reduces significantly the reaction time from about five days to 16 hr.

To potassium hydroxide (10 g) and barium hydroxide (13 g) were added water (60 ml) and iron pentacarbonyl (10 ml), under nitrogen. The mixture was degassed by several freeze-thaw cycles at -196°, and was shaken, at room temperature and in the dark, for 12 hr. The resulting slurry was filtered to yield an orange solution. The

solution was concentrated to half its original volume under vacuum.

From this point on, all operations were carried out outside, in the middle of a mild Alberta winter night, when temperatures were around -10° to -20° C.

A standard high-vacuum line equipped with a water-cooled mercury diffusion pump was taken outside (see Frontispiece*). Apiezon L grease was used on all stopcocks; turning the stopcocks at these temperatures was facilitated by warming them with a heat gun.

The flask with the orange solution containing $Fe(CO)_4H^-K^+$ was attached to the high-vacuum line, and concentrated H_2SO_4 (15 ml) was added dropwise, over 2 hr. The volatile materials were fractionated under vacuum using two -63° traps and a -196° trap. The *cis*-$Fe(CO)_4H_2$ was collected in the -196° trap. The hydride and the solvent were distilled into the nmr tube, and the tube was sealed under vacuum.

The hydride *cis*-$Fe(CO)_4H_2$ has been stored in the dark at -196°, in a tube sealed under vacuum, for up to six months. However, this compound decomposes rapidly above -20°. Also, exposure of a tube containing *cis*-$Fe(CO)_4H_2$ at -196° to laboratory fluorescent light brought about decomposition presumably to red $H_2Fe_3(CO)_{12}$[231] in less

---

* The picture was taken with a Canon FT/QL 55mm f1.2 camera equipped with a Mecablitz 185 flash unit.

than 15 sec.

The preparation of *cis*-$Ru(CO)_4H_2$ may be carried out very conveniently using the conditions just described for the iron analog.

Preparation of *cis*-$Os(CO)_4I_2$

Triosmium dodecacarbonyl (0.5 g, 0.55 mmol), iodine (0.42 g, 1.65 mmol) and benzene (15 ml) were placed in a 200-ml Parr autoclave which was pressurized with CO to 600 psi. The autoclave was heated, with stirring, at 160° for 13 hr, cooled to room temperature, and then the gases were vented. Yellow crystals of *cis*-$Os(CO)_4I_2$ separated out, which were removed by filtration and were washed with pentane (15 ml) to yield 0.8 g (87%) of product.

The infrared spectrum of *cis*-$Os(CO)_4I_2$ was similar to that reported by others,[232] and it showed bands at 2163(1.8), 2100(10.0), 2085(7.3), and 2050(7.5) cm^{-1} in heptane.

The ruthenium analog, *cis*-$Ru(CO)_4I_2$, has been prepared similarly by Dr. R. K. Pomeroy in over 90% yield. The reaction temperature was 100°. The preparation of this derivative has been described previously,[233] however, attempts to repeat this synthesis in this laboratory were unsuccessful.

Preparation of $Mn(CO)_5I$

Dimanganese decacarbonyl (1.5 g, 3.85 mmol), iodine (0.976 g, 3.85 mmol) and benzene (15 ml) were placed in a 200-ml Parr autoclave which was pressurized with CO to 550 psi. The autoclave was heated, with stirring, at 130° for 6 hr, cooled to room temperature, and then the gases were vented.

Filtration yielded 0.76 g of ruby-red $Mn(CO)_5I$, which was washed with pentane (15 ml). The residue was evaporated at reduced pressure (10 mm) and sublimation (room temperature and 0.005 mm Hg) afforded an additional 1.11 g of product. The infrared spectrum of $Mn(CO)_5I$[234] showed no impurities. Total yield 76%.

Earlier this compound was prepared by direct reaction of $Mn_2(CO)_{10}$ with iodine in a sealed Carius tube at 130-140°,[235] or 90°.[236] The reported yields were lower (50%),[236] and the product was contaminated with $Mn_2(CO)_{10}$.

Preparation of $Re(CO)_5I$

Dirhenium decacarbonyl (1.304 g, 2 mmol), iodine (0.508 g, 2 mmol) and benzene (15 ml) were placed in a 200-ml Parr autoclave which was pressurized with CO to 1000 psi. The autoclave was heated, with stirring, at 150° for 21 hr, cooled to room temperature, and then the gases were vented. Filtration afforded 1.38 g of pale-

yellow $Re(CO)_5I$, which was washed with pentane (15 ml). The infrared spectrum[234] of the product showed no impurities. The residue was evaporated at reduced pressure (10 mm) and sublimation (room temperature and 0.005 mm Hg) yielded 0.17 g of product, which contained a small amount of $Re_2(CO)_{10}$. Total yield 86%.

Enrichment with ^{13}CO

The following compounds were enriched with ^{13}CO: *cis*-$Fe(CO)_4I_2$,[237] *cis*-$Ru(CO)_4I_2$,[238] $Mn(CO)_5H$,[220] $Mn(CO)_5I$, and $Re(CO)_5I$. The enrichment of the last two compounds was carried out as described in Chapter II, under ultraviolet irradiation, and the solvent was cyclohexane. The irradiation time (140 watt Engelhard-Hanovia Inc. lamp, at 10 cm from the flask) was 30 min. and 17 hr, respectively.

REFERENCES

1. L. Mond, C. Langer, and F. Quincke, *J. Chem. Soc.*, **57**, 749 (1890).
2. M. I. Bruce, *Adv. Organometal. Chem.*, **10**, 273 (1972).
3. E. W. Abel and F. G. A. Stone, *Quart. Rev.*, **23**, 325 (1969).
4. E. W. Abel and F. G. A. Stone, *Quart. Rev.*, **24**, 498 (1970).
5. M. J. Mays, ed., "M. T. P. Int. Rev. Sci.," Inorg. Chem., Ser. One, vol. 6, Butterworths, London, 1972.
6. E. W. Abel and F. G. A. Stone, "Organometallic Chemistry," vol. 2, The Chemical Society, London, 1973.
7. M. B. Hall and R. F. Fenske, *Inorg. Chem.*, **11**, 1619 (1972).
8. F. A. Cotton, *Chem. Rev.*, **55**, 551 (1955).
9. J. Chatt and B. L. Shaw, *J. Chem. Soc.*, **1959**, 705.
10. G. Wilkinson, *Pure Appl. Chem.*, **30**, 627 (1972).
11. P. S. Braterman and R. J. Cross, *J. Chem. Soc. Dalton Trans.*, **1972**, 657.
12. G. Yagupsky, W. Mowat, A. Shortland, and G. Wilkinson, *J. C. S. Chem. Comm.*, **1970**, 1369.
13. B. K. Bower and H. G. Tennent, *J. Amer. Chem. Soc.*, **94**, 2512 (1972).
14. J. Bredt, H. Thoulet, and J. Schmit, *Ann.*, **437**, 1 (1924).

15. J. R. Wiseman and W. A. Pletcher, *J. Amer. Chem. Soc.*, **92**, 956 (1970).

16. J. A. Marshall and H. Faubl, *J. Amer. Chem. Soc.*, **92**, 948 (1970).

17. L. Galyer, K. Mertis, and G. Wilkinson, *J. Organometal. Chem.*, **85**, C37 (1975).

18. K. Mertis, L. Galyer, and G. Wilkinson, *J. Organometal. Chem.*, **97**, C65 (1975).

19. E. H. Brooks and R. J. Cross, *Organometal. Chem. Rev. A*, **6**, 227 (1970).

20. H. G. Ang and P. T. Lau, *Organometal. Chem. Rev. A*, **8**, 235 (1972).

21. F. Glockling and S. R. Stobart, ref. 5, chapter 3.

22. C. Windus, S. Sujishi, and W. P. Giering, *J. Organometal. Chem.*, **101**, 279 (1975).

23. G. E. Coates, M. L. H. Green, and K. Wade, "Organometallic Compounds," vol. II, Methuen & Co. Ltd., London, 1968, p. 1.

24. C. A. Tolman, *Chem. Soc. Rev.*, **1**, 337 (1972).

25. F. A. Cotton and J. M. Troup, *J. Amer. Chem. Soc.*, **96**, 5070 (1974).

26. L. Mond and F. Quincke, *Chem. News*, **63**, 301 (1891); M. Berthelot, *Compt. Rend.*, **112**, 1343 (1891).

27. B. Beagley, D. W. J. Cruickshank, P. M. Pinder, A. G. Robiette, and G. M. Sheldrick, *Acta Cryst.*, **25B**, 737 (1969).

28. J. Donohue and A. Caron, *Acta Cryst.*, **17**, 663 (1964).

29. M. B. Smith and R. Bau, *J. Amer. Chem. Soc.*, **95**, 2388 (1973).

30. F. A. Cotton and J. M. Troup, *J. Amer. Chem. Soc.*, **96**, 3438 (1974).

31. B. T. Kilbourn, K. N. Raeburn, and D. T. Thompson, *J. Chem. Soc. A*, **1969**, 1906.

32. H. B. Chin, M. B. Smith, R. D. Wilson, and R. Bau, *J. Amer. Chem. Soc.*, **96**, 5285 (1974).

33. B. A. Frenz and J. A. Ibers, *Inorg. Chem.*, **11**, 1109 (1972).

34. B. A. Frenz, J. H. Enemark, and J. A. Ibers, *Inorg. Chem.*, **8**, 1288 (1969).

35. F. Calderazzo and F. L'Eplattenier, *Inorg. Chem.*, **6**, 1220 (1967).

36. J. Dewar and H. O. Jones, *Proc. Roy. Soc. (London)*, **A76**, 558 (1905).

37. H. M. Powell and R. V. G. Ewens, *J. Chem. Soc.*, **1939**, 286.

38. F. A. Cotton and J. M. Troup, *J. Chem Soc., Dalton Trans.*, **1974**, 800.

39. J. R. Moss and W. A. G. Graham, *Chem. Comm.*, **1970**, 835.

40. A. S. Foust, J. K. Hoyano, and W. A. G. Graham, *J. Organometal. Chem.*, **32**, C65 (1971).

41. J. Dewar and H. O. Jones, *Proc. Roy. Soc. (London)*, **A79**, 66 (1906).

42. C. H. Wei and L. F. Dahl, *J. Amer. Chem. Soc.*, 91, 1351 (1969).

43. F. A. Cotton and J. M. Troup, *J. Amer. Chem. Soc.*, 96, 4155 (1974).

44. F. A. Cotton and D. L. Hunter, *Inorg. Chim. Acta*, 11, L9 (1974).

45. E. R. Corey and L. F. Dahl, *J. Amer. Chem. Soc.*, 83, 2203 (1961).

46. R. Mason and A. I. M. Rae, *J. Chem. Soc. A*, 1968, 778.

47. E. R. Corey and L. F. Dahl, *Inorg. Chem.*, 1, 521 (1962).

48. D. K. Huggins, N. Flitcroft, and H. D. Kaesz, *Inorg. Chem.*, 4, 166 (1965).

49. E. L. Muetterties, *J. Amer. Chem. Soc.*, 91, 1636 (1969).

50. K. F. Kuhlmann and D. M. Grant, *J. Amer. Chem. Soc.*, 90, 7355 (1968).

51. T. C. Farrar and E. D. Becker, "Pulse and Fourier Transform NMR," Academic Press, 1971.

52. F. A. Cotton, *Acc. Chem. Res.*, 1, 257 (1968).

53. E. L. Muetterties, *Acc. Chem. Res.*, 3, 266 (1970).

54. K. Vrieze and P. W. N. M. van Leeuwen, *Prog. Inorg. Chem.*, 14, 1 (1971).

55. P. Gillespie, P. Hoffman, H. Klusacek, D. Marquarting, S. Pfohl, F. Ramirez, E. A. Tsolis, and I. Ugi, *Angew. Chem. Int. Ed.*, 10, 687 (1971).

56. E. L. Muetterties, "M. T. P. Int. Rev. Sci.," Inorg. Chem., Ser. One, vol. 9, Butterworths, London, 1972, p. 39.

57. L. M. Jackman and F. A. Cotton, ed., "Dynamic Nuclear Magnetic Resonance Spectroscopy," Academic Press, New York, San Francisco, London, 1975.

58. F. A. Cotton, *J. Organometal. Chem.*, **100**, 29 (1975).

59. J. B. Stothers, "Carbon-13 NMR Spectroscopy," Academic Press, New York, 1972.

60. L. J. Todd and J. R. Wilkinson, *J. Organometal. Chem.*, **77**, 1 (1974).

61. B. E. Mann, *Adv. Organometal. Chem.*, **12**, 245 (1974).

62. F. A. Cotton, A. Danti, J. S. Waugh, and R. W. Fessenden, *J. Chem. Phys.*, **29**, 1427 (1958).

63. R. Bramley, B. N. Figgis, and R. S. Nyholm, *Trans. Faraday Soc.*, **58**, 1893 (1962).

64. J. B. Stothers and P. C. Lauterbur, *Can. J. Chem.*, **42**, 1563 (1964).

65. R. A. Friedel and H. L. Retcofsky, and W. G. Schneider, unpublished results, quoted in ref. 64.

66. P. C. Lauterbur and R. B. King, *J. Amer. Chem. Soc.*, **87**, 3266 (1965).

67. B. E. Mann, *J. C. S. Chem. Comm.*, **1971**, 1173.

68. O. A. Gansow, A. R. Burke, and G. N. LaMar, *J. C. S. Chem. Comm.*, **1972**, 456.

69. O. A. Gansow, A. R. Burke, and W. D. Vernon, *J. Amer. Chem. Soc.*, **94**, 2550 (1972).

70. F. A. L. Anet, unpublished results, quoted in ref. 59.

71. J. P. Jesson and P. Meakin, *J. Amer. Chem. Soc.*, **95**, 1344 (1973).

72. H. Mahnke, R. J. Clark, R. Rosanske, and R. K. Sheline, *J. Chem. Phys.*, **60**, 2997 (1974).

73. L. Kruczynski and J. Takats, private communication.

74. E. L. Muetterties and J. W. Rathke, *J. C. S. Chem. Comm.*, **1974**, 850.

75. P. R. Hoffman and K. G. Caulton, *J. Amer. Chem. Soc.*, **97**, 4221 (1975).

76. P. Meakin and J. P. Jesson, *J. Amer. Chem. Soc.*, **95**, 7272 (1973).

77. J. P. Jesson and P. Meakin, *Inorg. Nucl. Chem. Letters*, **9**, 1221 (1973).

78. J. P. Jesson and P. Meakin, *J. Amer. Chem. Soc.*, **96**, 5760 (1974).

79. J. S. Miller and K. G. Caulton, *Inorg. Chem.*, **14**, 2296 (1975).

80. R. S. Berry, *J. Chem. Phys.*, **32**, 933 (1960).

81. L. Kruczynski, L. K. K. LiShingMan, and J. Takats, *J. Amer. Chem. Soc.*, **96**, 4006 (1974).

82. S. T. Wilson, N. J. Coville, J. R. Shapely, and J. A. Osborn, *J. Amer. Chem. Soc.*, **96**, 4038 (1974).

83. L. Kruczynski and J. Takats, *J. Amer. Chem. Soc.*, **96**, 932 (1974).

84. C. G. Kreiter, S. Stüber, and L. Wackerle, *J. Organometal. Chem.*, **66**, C49 (1974).

85. L. Kruczynski and J. Takats, *Inorg. Chem.*, in press.

86. L. Kruczynski, J. L. Martin, and J. Takats, *J. Organometal. Chem.*, **80**, C9 (1974).

87. L. Kruczynski, J. L. Martin, and J. Takats, *J. Organometal. Chem.*, **85**, C53 (1975).

88. A. Forster, B. F. G. Johnson, J. Lewis, T. W. Matheson, B. H. Robinson, and W. G. Jackson, *J. C. S. Chem. Comm.*, **1974**, 1042.

89. L. Milone, S. Aime, E. W. Randall, and E. Rosenberg, *J. C. S. Chem. Comm.*, **1975**, 452; S. Aime,O. Gambino, L. Milone, E. Sappa, and E. Rosenberg, *Inorg. Chim. Acta*, **15**, 53 (1975).

90. R. K. Pomeroy and W. A. G. Graham, *J. Amer. Chem. Soc.*, **94**, 274 (1972).

91. P. C. Lauterbur, *J. Chem. Phys.*, **26**, 217 (1957).

92. L. Vancea and W. A. G. Graham, *Inorg. Chem.*, **13**, 511 (1974).

93. B. F. G. Johnson and J. A. Segal, *J. C. S. Chem. Soc.*, **1972**, 1312.

94. D. F. Gill, B. E. Mann, and B. L. Shaw, *J. Chem. Soc., Dalton Trans.*, **1973**, 311.

95. R. K. Pomeroy, R. S. Gay, G. O. Evans, and W. A. G. Graham, *J. Amer. Chem. Soc.*, **94**, 272 (1972).

96. M. J. Bennett, W. A. G. Graham, C. E. Jones, A. C. Sarapu, R. A. Smith, and L. Vancea, *Inorg. Chem.*, submitted.

97. L. Vancea, R. K. Pomeroy, and W. A. G. Graham, *J. Amer. Chem. Soc.*, **98**, 1407 (1976).

98. R. K. Pomeroy, H. P. Calhoun, L. Vancea, and W. A. G. Graham, manuscript in preparation.

99. M. Y. Darensbourg and D. J. Darensbourg, *J. Chem. Ed.*, **47**, 33 (1970).

100. W. Jetz and W. A. G. Graham, *J. Amer. Chem. Soc.*, **89**, 2773 (1967).

101. M. J. Webb and W. A. G. Graham, *J. Organometal. Chem.*, **93**, 119 (1975).

102. L. J. Todd and J. R. Wilkinson, *J. Organometal. Chem.*, **80**, C31 (1974).

103. F. A. Cotton and C. S. Kraihanzel, *J. Amer. Chem. Soc.*, **84**, 4432 (1962).

104. O. A. Gansow, B. Y. Kimura, G. R. Dobson, and R. A. Brown, *J. Amer. Chem. Soc.*, **93**, 5922 (1971).

105. O. A. Gansow, D. A. Schexnayder, and B. Y. Kimura, *J. Amer. Chem. Soc.*, **94**, 3406 (1972).

106. P. S. Braterman, D. W. Milne, E. W. Randall, and E. Rosenberg, *J. Chem. Soc., Dalton Trans.*, **1973**, 1027.

107. B. E. Mann, *J. Chem. Soc., Dalton Trans.*, **1973**, 2012.

108. G. M. Bancroft, K. D. Butler, L. E. Manzer, A. Shaver, and J. E. H. Ward, *Can. J. Chem.*, **52**, 782 (1974).

109. G. M. Bodner, S. B. Kahl, K. Bork, B. N. Storhoff, J. E. Wuller, and L. J. Todd, *Inorg. Chem.*, **12**, 1071 (1973).

110. G. M. Bodner and L. J. Todd, *Inorg. Chem.*, **13**, 1335 (1974).

111. G. M. Bodner, *Inorg. Chem.*, **13**, 2563 (1974).

112. G. M. Bodner, *Inorg. Chem.*, **14**, 1932 (1975).

113. G. M. Bodner, *Inorg. Chem.*, **14**, 2694 (1975).

114. A. N. Nesmeyanov, L. A. Fedorov, N. P. Avakyan, P. V. Petrovskii, E. I. Fedin, E. V. Arshavskaya, and I. I. Kristskaya, *J. Organometal. Chem.*, **101**, 121 (1975).

115. D. J. Darensbourg and M. Y. Darensbourg, *Inorg. Chem.*, **9**, 1691 (1970).

116. J. I. Musher, *Adv. Magn. Res.*, **2**, 177 (1966).

117. M. Karplus and J. A. Pople, *J. Chem. Phys.*, **38**, 2803 (1963).

118. J. A. Pople, *Mol. Phys.*, **7**, 301 (1964).

119. G. E. Maciel, *J. Chem. Phys.*, **42**, 2746 (1965).

120. H. Mahnke, R. K. Sheline, and H. W. Spiess, *J. Chem. Phys.*, **61**, 55 (1974).

121. F. A. Cotton, W. T. Edwards, F. C. Rauch, M. A. Graham, R. N. Perutz, and J. J. Turner, *J. Coord. Chem.*, **2**, 247 (1973).

122. W. E. Lamb, Jr., *Phys. Rev.*, **60**, 817 (1941).

123. W. H. Flygare and J. Goodisman, *J. Chem. Phys.*, **49**, 3122 (1968).

124. J. Evans and J. R. Norton, *Inorg. Chem.*, **13**, 3042 (1974).

125. G. M. Bodner, manuscript submitted. Personal communication to W. A. G. Graham, March 1975.

126. R. Ditchfield and P. D. Ellis, "Topics in Carbon-13 NMR Spectroscopy," G. C. Levy, ed., John Wiley and Sons, 1974.

127. F. A. Cotton, D. L. Hunter, and A. J. White, *Inorg. Chem.*, **14**, 703 (1975).

128. M. I. Bruce and F. G. A. Stone, *J. Chem. Soc. A*, **1967**, 1238.

129. B. F. G. Johnson, J. Lewis, and P. A. Kilty, *J. Chem. Soc. A*, **1968**, 2859.

130. W. Jetz and W. A. G. Graham, *J. Organometal. Chem.*, **69**, 383 (1974).

131. W. Jetz, Ph. D. Thesis, University of Alberta, 1970.

132. J. D. Cotton, S. A. R. Knox, I. Paul, and F. G. A. Stone, *J. Chem. Soc. A*, **1967**, 264.

133. F. Hein and W. Jehn, *Ann.*, **684**, 4 (1965).

134. R. Kummer and W. A. G. Graham, *Inorg. Chem.*, **7**, 1208 (1968).

135. S. A. R. Knox and F. G. A. Stone, *J. Chem. Soc. A*, **1969**, 2559.

136. R. K. Pomeroy, Ph. D. Thesis, University of Alberta, 1972.

137. S. A. R. Knox and F. G. A. Stone, *J. Chem. Soc. A*, **1971**, 2874.

138. J. D. Cotton, S. A. R. Knox, and F. G. A. Stone, *J. Chem. Soc. A*, **1968**, 2758.

139. R. D. George, S. A. R. Knox, and F. G. A. Stone, *J. Chem. Soc., Dalton Trans.*, **1973**, 972.

140. S. A. R. Knox and F. G. A. Stone, *J. Chem Soc. A*, **1970**, 3147.

141. R. K. Pomeroy and W. A. G. Graham, to be submitted for publication.

142. K. Noack and H. Ruch, *J. Organometal. Chem.*, **17**, 309 (1969).

143. W. McFarlane, *J. C. S. Chem. Comm.*, **1971**, 609.

144. C. W. Haigh, J. Hilton, L. H. Sutcliffe, and G. J. T. Tiddy, *J. Magn. Res.*, **18**, 241 (1975).

145. J. Hilton and L. H. Sutcliffe, *Progress NMR Spectroscopy*, **10**, 27 (1975).

146. W. McFarlane, *J. Chem. Soc. A*, **1967**, 528.

147. H. Dreeskamp and G. Stegmeier, *Z. Naturforsch.*, **22a**, 1458 (1967).

148. F. J. Weigert and J. D. Roberts, *J. Amer. Chem. Soc.*, **91**, 4940 (1969).

149. N. F. Ramsey, *Phys. Rev.*, **91**, 303 (1953).

150. J. A. Pople and D. P. Santry, *Mol. Phys.*, **9**, 1 (1964).

151. C. J. Jameson and H. S. Gutowsky, *J. Chem. Phys.*, **51**, 2790 (1969).

152. G. W. Smith, *J. Chem. Phys.*, **39**, 2031 (1963).

153. G. W. Smith, *J. Chem. Phys.*, **40**, 2037 (1963).

154. H. A. Bent, *J. Chem. Ed.*, **37**, 616 (1960).

155. F. N. Tebbe, P. Meakin, J. P. Jesson, and E. L. Muetterties, *J. Amer. Chem. Soc.*, **92**, 1068 (1970).

156. P. Meakin, E. L. Muetterties, F. N. Tebbe, and J. P. Jesson, *J. Amer. Chem. Soc.*, **93**, 4701 (1971).

157. P. Meakin, E. L. Muetterties, and J. P. Jesson, *J. Amer. Chem. Soc.*, **95**, 75 (1973).

158. L. J. Guggenberger, D. D. Titus, M. T. Flood, R. E. Marsh, A. A. Orio, and H. B. Gray, *J. Amer. Chem. Soc.*, **94**, 1135 (1972).

159. L. J. Guggenberger, *Inorg. Chem.*, **12**, 1317 (1973).

160. W. G. Gehman, Ph. D. Thesis, Pennsylvania State University, 1954.

161. L. Seiden, Ph. D. Thesis, Northwestern University, 1957.

162. J. C. Bailar, Jr., *J. Inorg. Nucl. Chem.*, **8**, 165 (1958).

163. C. S. Springer, Jr. and R. E. Sievers, *Inorg. Chem.*, **6**, 852 (1967).

164. J. E. Brady, *Inorg. Chem.*, **8**, 1208 (1969).

165. R. K. Pomeroy, T. W. Ng, and W. A. G. Graham, in preparation.

166. R. Ball and M. J. Bennett, *Inorg. Chem.*, **11**, 1806 (1972).

167. R. Hoffmann, J. M. Howell, and A. R. Rossi, *Inorg. Chem.*, in press.

168. J. K. Burdett, *Inorg. Chem.*, **15**, 212 (1976).

169. R. A. D. Wentworth, *Coord. Chem. Rev.*, **9**, 171 (1972).

170. P. Ray and N. K. Dutt, *J. Ind. Chem. Soc.*, **20**, 81 (1943).

171. C. S. Springer, Jr., *J. Amer. Chem. Soc.*, **95**, 1459 (1973).

172. B. A. Frenz and J. A. Ibers, "Transition Metal Hydrides," E. L. Muetterties, ed., M. Dekker, Inc., New York, 1971, p. 33.

173. N. A. Bailey and R. Mason, *Acta Cryst.*, **21**, 652 (1966).

174. M. B. Hall and R. F. Fenske, *Inorg. Chem.*, **11**, 768 (1972).

175. K. A. Simpson, Ph. D. Thesis, University of Alberta, 1973.

176. C. J. Gilmore and P. Woodward, *J. Chem. Soc., Dalton Trans.*, **1972**, 1387.

177. E. A. McNeill, Ph. D. Thesis, Cornell University, 1975.

178. P. G. Harrison, T. J. King, and J. A. Richards, *J. Chem. Soc., Dalton Trans.*, **1975**, 2097.

179. F. A. Cotton, J. M. Troup, W. E. Billups, L. P. Lin, and C. V. Smith, *J. Organometal. Chem.*, **102**, 345 (1975).

180. R. C. Pettersen, J. L. Cihonski, F. R. Young, and R. A. Levenson, *J. C. S. Chem. Comm.*, **1975**, 370.

181. H. W. Baird and L. F. Dahl, *J. Organometal. Chem.*, **7**, 503 (1967).

182. M. R. Churchill, *Inorg. Chem.*, **6**, 185 (1967).

183. P. W. Codding and W. A. G. Graham, private communication.

184. C. E. Jones and W. A. G. Graham, private communication.

185. T. J. Marks and G. W. Grynkewich, *J. Organometal. Chem.*, **91**, C9 (1975).

186. R. D. Ball, Ph. D. Thesis, University of Alberta, 1970.

187. M. Pankowski and M. Bigorgne, *J. Organometal. Chem.*, **19**, 393 (1969).

188. M. Bigorgne, R. Poilblanc, and M. Pankowski, *Spectrochim. Acta*, **26A**, 1217 (1970).

189. O. Kahn and M. Bigorgne, *J. Organometal. Chem.*, **10**, 137 (1967).

190. W. Jetz and W. A. G. Graham, *Inorg. Chem.*, **10**, 4 (1971).

191. J. P. Collman, D. W. Murphy, E. B. Fleicher, and D. Swift, *Inorg. Chem.*, **13**, 1 (1974).

192. H. S. Preston, J. M. Stewart, H. J. Plastas, and S. O. Grim, *Inorg. Chem.*, **11**, 161 (1972).

193. B. K. Nicholson, J. Simpson, and W. T. Robinson, *J. Organometal. Chem.*, **47**, 403 (1973).

194. F. A. Cotton, B. A. Frenz, and D. L. Hunter, *Inorg. Chim. Acta*, **16**, 203 (1976).

195. C. S. Cundy, B. M. Kingston, and M. F. Lappert, *Adv. Organometal. Chem.*, **11**, 253 (1973).

196. V. F. Mironov, V. P. Kozyukov, and V. D. Sheludyakov, *Dokl. Akad. Nauk SSSR*, **179**, 600 (1968); *Proc. Acad. Sci. USSR, Chem. Sect. (Engl. Transl.)*, **179**, 261 (1968).

197. W. A. Piccoli, G. G. Haberland, and R. L. Merker, *J. Amer. Chem. Soc.*, **82**, 1883 (1960).

198. H. Sakurai, K. Tominaga, T. Watanabe, and M. Kumada, *Tetrahedron Lett.*, **1966**, 5493.

199. M. Ishikawa, M. Kumada, and H. Sakurai, *J. Organometal. Chem.*, **23**, 63 (1970).

200. J. D. Edwards, R. Goddard, S. A. R. Knox, R. J. McKinney, F. G. A. Stone, and P. Woodward, *J. C. S. Chem. Soc.*, **1975**, 828.

201. D. J. Patmore and W. A. G. Graham, *Inorg. Chem.*, **6**, 981 (1967).

202. R. B. King, K. H. Pannell, C. R. Bennett, and M. Ishaq, *J. Organometal. Chem.*, **19**, 327 (1969).

203. W. Majunke, D. Leibfritz, T. Mack, and H. tom Dieck, *Chem. Ber.*, **108**, 3025 (1975).

204. P. Meakin, L. J. Guggenberger, J. P. Jesson, D. H. Gerlach, F. N. Tebbe, W. G. Peet, and E. L. Muetterties, *J. Amer. Chem. Soc.*, **92**, 3482 (1970).

205. T. Kruck and R. Kobelt, *Chem. Ber.*, **105**, 3772 (1972).

206. W. Hieber, *Naturwiss.*, **19**, 360 (1931).

207. W. Hieber and F. Leutert, *Ber. Deutsch. Chem. Gess.*, **64**, 2832 (1931).

208. K. Farmery and M. Kilner, *J. Chem. Soc. A*, **1970**, 634.

209. S. R. Stobart, *J. Chem. Soc., Dalton Trans.*, **1972**, 2442.

210. G. F. Bradley and S. R. Stobart, *J. C. S. Chem. Comm.*, **1975**, 325.

211. F. A. Cotton and G. Wilkinson, *Chem. Ind. (London)*, **1956**, 1305.

212. E. O. Bishop, J. L. Down, P. R. Emtage, R. E. Richards, and G. Wilkinson, *J. Chem. Soc.*, **1959**, 2484.

213. G. M. Bancroft, M. J. Mays, and B. E. Prater, *J. Chem. Soc. A*, **1970**, 956.

214. H. Beall, C. H. Bushweller, W. J. Dewkett, and M. Grace, *J. Amer. Chem. Soc.*, **92**, 3484 (1970).

215. J. D. Atwood and T. L. Brown, *J. Amer. Chem. Soc.*, **97**, 3380 (1975).

216. H. Spiesecke and W. G. Schneider, *J. Chem. Phys.*, **35**, 722 (1961).

217. W. M. Litchman and D. M. Grant, *J. Amer. Chem. Soc.*, **90**, 1400 (1968).

218. O. W. Howarth and R. J. Lynch, *Mol. Phys.*, **15**, 431 (1968).

219. F. J. Weigert and J. D. Roberts, unpublished results, quoted in ref. 220.

220. G. M. Whitesides and G. Maglio, *J. Amer. Chem. Soc.*, **91**, 4980 (1969).

221. G. C. Levy and J. D. Cargioli, *J. Magn. Res.*, **6**, 143 (1972).

222. T. Schaefer, *Can. J. Chem.*, **40**, 1678 (1962).

223. E. W. Garbisch, *J. Chem. Ed.*, **45**, 402 (1968).

224. L. F. Dahl and D. L. Wampler, *Acta Cryst.*, **15**, 946 (1962).

225. S. J. LaPlaca, W. C. Hamilton, J. A. Ibers, and A. Davidson, *Inorg. Chem.*, **8**, 1928 (1969).

226. J. D. Cotton, M. I. Bruce, and F. G. A. Stone, *J. Chem. Soc. A*, **1968**, 2162.

227. F. L'Eplattenier and F. Calderazzo, *Inorg. Chem.*, **6**, 2092 (1967).

228. R. B. King, *Organometal. Syn.*, **1**, 158 (1965).

229. W. Beck, W. Hieber, and G. Braun, *Z. Anorg. Allg. Chem.*, **308**, 23 (1961).

230. W. Hieber and G. Bader, *Chem. Ber.*, **61**, 1717 (1928).

231. W. Hieber and H. Vetter, *Z. Anorg. Allg. Chem.*, **212**, 145 (1933).

232. L. A. W. Hales and R. J. Irving, *J. Chem. Soc. A*, **1967**, 1389.

233. B. F. G. Johnson, R. D. Johnston, and J. Lewis, *J. Chem. Soc. A*, **1969**, 792.

234. H. D. Kaesz, R. Bau, D. Hendrickson, and J. M. Smith, *J. Amer. Chem. Soc.*, **89**, 2844 (1967).

235. E. O. Brimm, M. A. Lynch, Jr., and W. J. Sesny, *J. Amer. Chem. Soc.*, **76**, 3831 (1954).

236. K. J. Reimer and A. Shaver, *J. Organometal. Chem.*, **93**, 239 (1975).

237. I. S. Butler and H. K. Spendjian, *J. Organometal. Chem.*, **18**, 145 (1969).

238. R. S. Gay, Ph. D. Thesis, University of Alberta, 1970.

B30149